(NASA-CR-152239) THRUST AND MASS FLOW CHARACTERISTICS OF FOUR 36 INCH DIAMETER TIP TURBINE FAN THRUST VECTORING SYSTEMS IN AND OUT OF GROUND EFFECT (McDonnell Aircraft Co.) 105 p HC A06/MF A01 CSCL 21E G3/07

N79-26056

Unclas 28379

MCDONNELL DOUGLAS CORPORATION

NASA CR 152239
COPY NO. 4 REPORT MDC A5704 • JUNE 1979

THRUST AND MASS FLOW CHARACTERISTICS OF FOUR 36 INCH DIAMETER TIP TURBINE FAN THRUST VECTORING SYSTEMS IN AND OUT OF GROUND EFFECT

Contract No NAS 2-9690

PREPARED BY
D W Esker
H A Roddiger

MCDONNELL AIRCPAFT COMPANY

Box 516, Saint Louis, Missouri 63166 – Tel. (314)232–0232

MCDONNELL DOUGLAS

TABLE OF CONTENTS

LIST OF PAGES

SUMMARY

Operation of V/STOL aircraft in close ground proximity can induce significant changes in both aerodynamic lift and the performance level of the aircraft propulsion system. Determination of induced lift effects by means of powered models is a commonly used experimental method, however calibration of the model propulsion units both in and out of ground effect must be included so that propulsion forces can be separated from the measured forces.

This report describes the calibration tests carried out on the propulsion system components of a 70 percent scale, powered model of a NASA 3-fan V/STOL aircraft configuration. The three X376B/T58 turbotip fan units used in the large scale powered model were tested on an isolated basis over a range of ground heights from H/D of 1.02 to ∞. A higher pressure ratio LF336/J85 fan unit was tested over a range of ground heights from 1.55 to ∞. The results of the test program demonstrated that: (1) the thrust and mass flow performance of the X376B/T58 nose lift unit is essentially constant for H/D variations down to 1.55. At H/D equal to 1.02 back pressurization of the fan exit occurs and is accompanied by an increase in thrust of five percent, (2) a change in nose fan exit hub shape from flat plate to hemispherical produces no significant difference in louvered lift nozzle performance for height variations from H/D = 1.02 to ∞, (3) operation of the nose lift nozzle at the higher fan pressure ratio generated by the LF336/J85 fan system causes no significant change in ground proximity performance down to an H/D of 1.55, the lowest height tested with this unit, and (4) the performance of the left and right X376B/T58 lift/cruise units in the vertical lift mode remains unchanged, within $\pm$ two percent for the range of ground heights from H/D = 1.02 to ∞.

LIST OF FIGURES

LIST OF FIGURES (continued)

LIST OF FIGURES (continued)

NOMENCLATURE

A(i) - Load Cell (i) Axial Load; i = 1 through 3

A_{BG} - Gas Generator Bellmouth Area

A_{FANE} - Annulus Area @ Fan Exit Rake

A_N - Calibration Nozzle Exit Area

A_{TE} - Tip Turbine Exit Area

C_{DG} - Gas Generator Bellmouth Discharge Coefficient

CAF - Fan Massflow Coefficient

CAT - Turbine Massflow Coefficient

CF - Thrust Coefficient

C_P - Specific Heat @ Constant Pressure

C_V - Specific Heat @ Constant Volume

D - Nozzle Exit Diameter = .99 m (3.25 ft)

d - Thrust Moment Arm (About R.C.)

F_G - Gross Thrust

F_{GFI} - Fan Ideal Gross Thrust

F_{GTI} - Tip Turbine Ideal Gross Thrust

F_G/δ - Corrected Gross Thrust

F_{hub}/δ - Corrected Hub Force

g - Gravitational Constant

H - Height Above Ground Plane

H/D - Height of Nozzle Exit Above Ground Plane Ratioed to Nozzle Exit Diameter

M_P - Pitching Moment

M_Y - Yawing Moment

N(i) - Load Cell (i) Normal Load; i = 1 through 3

N_F - Fan Speed

$N_F/\sqrt{\theta}$ - Corrected Fan Speed

NOMENCLATURE (Cont'd)

P	- Static Pressure
P_{BG}	- Gas Generator Bellmouth Static Pressure
P_0	- Freestream Ambient Pressure
P_{SFE}	- Static Pressure @ Fan Exit (Arithmetic Avg.)
P_{STE}	- Static Pressure @ Tip Turbine Exit (Arithmetic Avg.)
P_{STD}	- Standard Pressure
P_{TO}	- Freestream Total Pressure
P_{TFE}	- Total Pressure @ Fan Exit (Area Weighted Avg.)
P_{TTE}	- Total Pressure @ Tip Turbine Exit (Arithmetic Avg.)
P_{TFE}/P_0	- Fan Pressure Ratio
P_{TTE}/P_0	- Turbine Discharge Pressure Ratio
R	- Gas Constant
R.C.	- Reference Center
S(i)	- Load Cell (i) Side Load; i = 1 through 3
T	- Temperature
T_B	- Fan Bellmouth Airflow Temperature
T_{G1}	- Gas Generator Bellmouth Airflow Temperature
T_{STD}	- Standard Temperature
T_{TFE}	- Total Temperature @ Fan Exit (Area Weighted Avg.)
T_{TTE}	- Total Temperature @ Tip Turbine Exit (Arithmetic Avg.)
W	- Airflow
W_F	- Fan Airflow
W_T	- Tip Turbine Airflow
W_{TOT}	- Total Airflow, $(W_F + W_T)$
$W\sqrt{\theta}/\delta$	- Corrected Airflow
γ	- C_P/C_V

NOMENCLATURE (Cont'd)

δ	- Standard Pressure Correction Factor, P_0/P_{STD}
δ_{LC}	- Lift/Cruise Nozzle Geometric Deflection Angle
δ_{NL}	- Nose Nozzle Louver Angle
δ_Y	- Yaw Vane Vector Angle
θ	- Standard Temperature Correction Factor, T/T_{STD}
τ	- Thrust Vector Angle

SYMBOLS

⊙	- Test Data for 5485 cm^2 Calibration Nozzle
⊡	- Test Data for 5935 cm^2 Calibration Nozzle
◇	- Test Data for 6285 cm^2 Calibration Nozzle
▱	- Test Data for 6730 cm^2 Calibration Nozzle
▽	- Test Data for H/D = ∞ (No Ground Plane)
⬡	- Test Data for H/D = 6.45
◇	- Test Data for H/D = 2.55
⊖	- Test Data for H/D = 2.0
⬠	- Test Data for H/D = 1.55
△	- Test Data for H/D = 1.02

NOTE: Open Symbols Represent Data Taken During Increasing Fan Speed; Closed Symbols During Decreasing Fan Speed

EQUATIONS

FLOW RATES

FAN

- MEASURED

W_F from calibrated fan bellmouth data

- RAKE COMPUTED

$$W_F = P_{SFE}[\gamma g/R]^{1/2}\left[(2.0\left(\frac{P_{TFE}}{P_{SFE}}\right)^{\frac{\gamma-1}{\gamma}} - 2.0)/(\gamma-1)\right]^{1/2}\left(\frac{P_{TFE}}{P_{SFE}}\right)^{\frac{\gamma-1}{2\gamma}}(A_{FANE})/(T_{TFE})^{1/2}$$

- CORRECTED

$$W_F\sqrt{\Theta}/\delta = W_F\sqrt{T_B/T_{STD}}\;/\;(P_0/P_{STD})$$

TIP TURBINE

- MEASURED

$$W_T = P_{BG}(A_{BG})(C_{DG})\left[\frac{2.0(g)}{R\left(\frac{\gamma-1}{\gamma}\right)T_{TO}}\left(\frac{P_{TO}}{P_{BG}}\right)^{\frac{\gamma-1}{\gamma}}\left[\left(\frac{P_{TO}}{P_{BG}}\right)^{\frac{\gamma-1}{\gamma}} - 1\right]\right]^{1/2}$$

- RAKE COMPUTED

$$W_T = P_{STE}[\gamma g/R]^{1/2}\left[(2.0\left(\frac{P_{TTE}}{P_{STE}}\right)^{\frac{\gamma-1}{\gamma}} - 2.0)/(\gamma-1)\right]^{1/2}\left(\frac{P_{TTE}}{P_{STE}}\right)^{\frac{\gamma-1}{2\gamma}}(A_{TE})/(T_{TTE})^{1/2}$$

- CORRECTED

$$W_T\sqrt{\Theta}/\delta = W_T\sqrt{T_{G1}/T_{STD}}/(P_0/P_{STD})$$

THRUSTS

FAN

- RAKE COMPUTED IDEAL

$$F_{GFI} = W_F\left[\frac{(2.0\left(\frac{P_{TFE}}{P_0}\right)^{\frac{\gamma-1}{\gamma}} - 2.0)}{(\gamma-1)}(\gamma g R)\left(\frac{P_0}{P_{TFE}}\right)^{\frac{\gamma-1}{\gamma}}(T_{TFE})\right]^{1/2}$$

- CORRECTED

$$F_{CFI}/\delta = F_{GFI}/(P_0/P_{STD})$$

EQUATIONS (continued)

TIP TURBINE

- RAKE COMPUTED IDEAL

$$F_{GTI} = W_T \left[\frac{\left(2.0 \left(\frac{P_{TTE}}{P_0}\right)^{\frac{\gamma-1}{\gamma}} - 2.0\right)}{(\gamma-1)} (\gamma g R) \left(\frac{P_0}{P_{TTE}}\right)^{\frac{\gamma-1}{\gamma}} (T_{TTE}) \right]^{1/2}$$

- CORRECTED

$$F_{GTI}/\delta = F_{GTI}/(P_0/\ P_{STD})$$

COEFFICIENTS

THRUST

$$CF = \frac{\text{Measured Thrust}}{\text{Total Rake Computed Ideal Thrust}}$$

FAN MASS FLOW

$$CAF = \frac{\text{Measured Flow Via Fan Bellmouth}}{\text{Rake Computed Fan Flow}}$$

TURBINE MASS FLOW

$$CAT = \frac{\text{Measured Flow Via Gas Generator Bellmouth}}{\text{Rake Computed Turbine Flow}}$$

CORRECTED FAN SPEED

$$N_F/\sqrt{\theta} = N_F/\sqrt{T_B/\ T_{STD}}$$

PERCENTAGE CORRECTED FAN SPEED

X376B

$$(N_F/\sqrt{\theta})\ \% = \frac{N_F/\sqrt{T_B/\ T_{STD}}}{4074}\ (100)$$

LF336

$$(N_F/\sqrt{\theta})\ \% = \frac{N_F/\sqrt{T_B/\ T_{STD}}}{6047}(100)$$

EQUATIONS (continued)

THRUST VECTOR ANGLE

NOSE

$$\tau = TAN^{-1} \left(\frac{\sum_{i=1}^{3} S(i)}{\sum_{I=1}^{3} A(i)} \right)$$

LIFT/CRUISE

$$\tau = TAN^{-1} \left(\frac{\sum_{i=1}^{3} N(i)}{\sum_{i=1}^{3} A(i)} \right)$$

THRUST MOMENT ARM

NOSE

$$d = \frac{M_Y}{F_G}$$

LIFT/CRUISE

$$d = \frac{M_P}{F_G}$$

1. INTRODUCTION

Evaluation of exhaust jet induced aerodynamics for Vertical/Short Takeoff and Landing (V/STOL) aircraft in ground effect is most often established experimentally. This is a result of the sensitivity of induced lift effects to aircraft geometry, the propulsion system arrangement, and the difficulty in analyzing the complex impingement flow field formed beneath the aircraft.

Induced effects are those forces and moments imposed on the airframe exclusive of the direct propulsion system thrust forces, and, thus, a means to separate the direct and induced forces must be included in the experimental technique. Operation of powered test models is one approach used commonly for determination of ground effect characteristics, (References 1-4). Powered models offer an advantage over other techniques in that both inlet and nozzle exit flows are simulated, however, calibration of the propulsive units on an isolated basis both in and out of ground effect is required. Thrust calibration of the power units provides the means to separate the direct propulsion forces from the total model forces and thereby establish the jet induced effects.

Large scale powered model (LSPM) investigationsof a three fan V/STOL aircraft were initiated at NASA-Ames in 1976. Figure 1-1 is a schematic of the 70 percent scale aircraft model which is a subsonic, low wing, multimission design. The propulsion system arrangement consists of a nose mounted lift fan and two lift/cruise fans located over the wing. This model was built by NASA under a contracted program with the McDonnell Aircraft Company (MCAIR) and underwent low speed tests in the 40 x 80 ft wind tunnel and static ground effects tests on the static test facility at NASA-Ames. Ground proximity calibrations of the powered model propulsion units were not included in the initial 1976 test phase due to program scope limitations.

The results of the initial static tests in ground effect indicated only a slight variation of total lift with ground heights, (Reference 4). This characteristic was at variance with subsequent test data obtained on a similar small scale, flat plate, jet effects model at MCAIR, (Reference 5). The large scale tests also indicated an improvement in thrust performance on the nose mounted fan in ground proximity, and this was attributed to base pressurization of the large hub area on the nose fan unit.

Questions concerning the LSPM induced lift characteristics provided the impetus for further investigations of the model, including calibrations of each of the turbotip fan propulsion units. The second ground effects test program was carried out at NASA-Ames between 4 June and 28 July 1978; the results of which are reported in Reference 6. Following completion of the 70 percent model tests, the individual X376B/T58 turbotip fan and exhaust nozzle systems were removed from the LSPM, installed and tested on an isolated thrust stand.

The objectives of the isolated fan calibration test program were:

- o Establish thrust and mass flow performance of each LSPM propulsion unit in and out of ground effects
- o Establish fan performance maps
- o Evaluate the effect of higher fan pressure ratio on the LSPM nose nozzle installation

FIGURE 1-1
LARGE SCALE POWERED MODEL

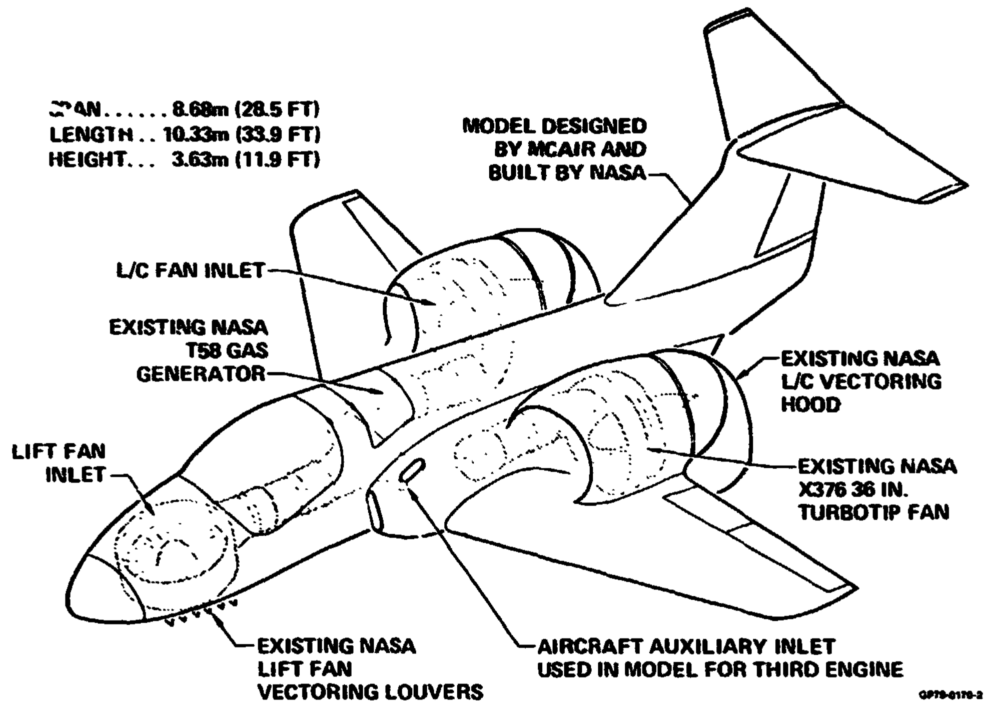

o Determine the effect of an alternate nose fan exit hub shape on nose unit performance.

The experimental approach used to meet these objectives involved installation of each fan and gas generator combination on a thrust measurement rig with bellmouth inlets, associated fan exit instrumentation, and exhaust nozzle hardware. Tests of the propulsion unit with a large plate located at various distances from the nozzle exit provided performance in ground proximity. Comparison of thrust and mass flow measurements with fan exit rake computed values established calibration coefficients for the fan exit instrumentation. The rake coefficient data was then utilized in the reduction of the 70 percent scale, powered model test data to establish installed thrust performance.

The overall program was conducted under Contract NAS 2-9690. Mr. L. Stewart Rolls and Mr. Bruno Gambucci of NASA-Ames Research Center served successively as Technical Monitor. MCAIR established the design of the thrust stand rig and associated test apparatus. Fabrication and assembly of the test hardware was performed at NASA-Ames. The experimental tests were carried out by NASA-Ames personnel with MCAIR support during the period 18 August to 29 September 1978. Data reduction and analysis were performed by MCAIR and are documented in this report.

A description of the test hardware used in this program is given in Section 2. The test results and discussion are presented in Section 3 and the conclusions in Section 4. The schedule of test runs carried out at NASA-Ames is given in Appendix A. Appendix B is a listing of the primary test data. Appendix C lists the data used to construct the thrust and massflow coefficient curves presented in Section 3.

2. TEST APPARATUS

The apparatus used during this test program consisted of the three X376B/T58 turbotip fan propulsion units used in the LSPM, the LF336/J85 turbotip fan system, fan calibration hardware including bellmouth inlets and calibration nozzles, and the thrust stand rig used to support the bellmouth, fan, gas generator, and nozzle assemblies. A description of the test configurations is given below.

2.1 LF336/J85 TURBOTIP LIFT FAN SYSTEM

The LF336/J85 lift fan system used in the test program was designed and built by General Electric for NASA under Contract NAS 2-4130. The LF336 fan, shown schematically in Figure 2-1, is a single stage, turbotip, fan-in-wing design with a fan diameter of 91.44 cm (36 in.) and an aerodynamic design pressure ratio cf 1.3. The LF336 fan flow is 98.88 kg/sec (218 lb/sec) when operating at a 100 percent design speed of 6047 rpm. The LF336 tip turbine is an axial flow, impulse turbine fed by a 360-degree double entry scroll. The turbine is designed to accept the full exhaust flow of a J85-GE-5 General Electric turbojet engine at military power setting. Figure 2-2 summarizes the LF336/J85 system performance.

2.2 X376B/T58 TURBOTIP LIFT FAN SYSTEM

The X376B/T58 lift fan systems used in the test program were supplied by the Large Scale Aerodynamics Branch of NASA-Ames. The X376B fan, shown in Figure 2-3, is a single stage, turbotip fan-in-wing design with a fan diameter of 91.44 cm (36 in.) and an aerodynamic design pressure ratio of 1.08. The X376B fan flow is 69.4 kg/sec (153 lb/sec) when operating at 100 percent design speed of 4074 rpm. The X376B tip turbine is an axial flow, impulse turbine fed by a 180-degree entry scroll. The turbine accepts the full exhaust flow of a T58-GE-8 General Electric turbojet engine at military power setting. Figure 2-3 summarizes the design characteristics of the gas generator and fan.

2.3 TEST NOZZLES

2.3.1 CALIBRATION NOZZLES - Calibration of the lift fan systems with a near ideal thrust performance nozzle was performed with four different nozzle exit areas to establish corrected flow characteristics of the test propulsion system and to establish baseline thrust performance levels. The thrust calibration nozzle was designed by MCAIR and fabricated at NASA-Ames.

Figure 2-4 presents a schematic of the thrust calibration nozzle which consists of a cylindrical outer duct and sinusoidal shaped (tapered cone) hub centerbody which transitions the exhaust flow from an annular cross section at the nozzle entrance station to a circular cross section at the nozzle exit station. At the nozzle entrance station, the outer wall diameter is 107.2 cm (42.2 in.). Two separate tapered cone hub centerbodies were used for the LF336 and X376B fans, respectively. The characteristic dimension of diameter and length for these hubs may be found on Figure 2-4. The hub centerbody is aligned with the fan aft hub and is supported off the outer wall by means of two struts which span the annular flow passage. The struts incorporate a chord length of 12.55 cm (4.94 in.), a thickness to chord ratio of 0.10, and a double circular arc cross section.

The nozzle exit area was varied by means of removable nozzle aft cones. A total

FIGURE 2-1
GENERAL ELECTRIC LF336 TURBOTIP FAN

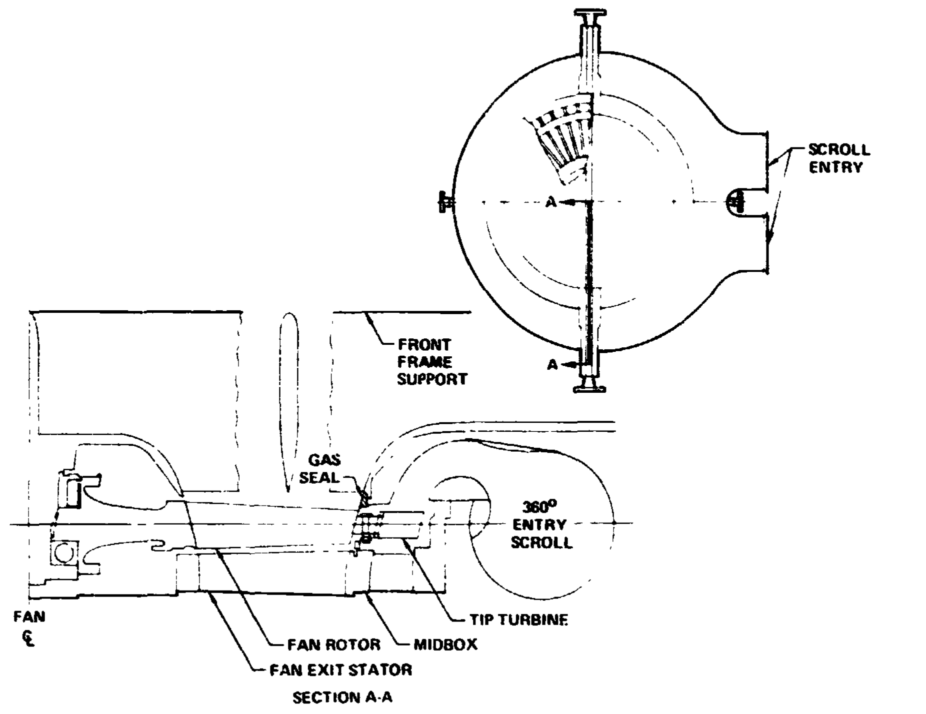

FIGURE 2-2
LF336/J85 DESIGN PERFORMANCE SUMMARY

FAN FLOW, KG/SEC, (LB/SEC)	98.88 (218)
FAN PRESSURE RATIO	1.3
BYPASS RATIO	5.0
RPM	6,047
FAN TIP SPEED, M/SEC (FT/SEC)	29.56 (970)
FAN DIAMETER, CM, (IN.)	91.44 (36)
RADIUS RATIO	0.475
TURBINE INLET FLOW, KG/SEC (LB/SEC)	20.01 (44.12)
TURBINE INLET PRESSURE, N/CM^2 (PSIA)	21.95 (31.84)
TURBINE INLET TEMPERATURE, °K, (R°)	950.6 (1,711)
TURBINE DISCHARGE PRESSURE RATIO	1.118
TURBINE DISCHARGE TEMPERATURE, °K (R°)	833 (1,500)
FAN THRUST, N, (LB)	19,688 (4,426)
TURBINE THRUST, N, (LB)	4,982 (1,120)
TOTAL THRUST, N, (LB)	24,670 (5,546)

GP76 0867 30

FIGURE 2-3
GAS GENERATOR AND TURBOTIP FAN DESIGN CHARACTERISTICS

T58-GE-8B Gas Generator

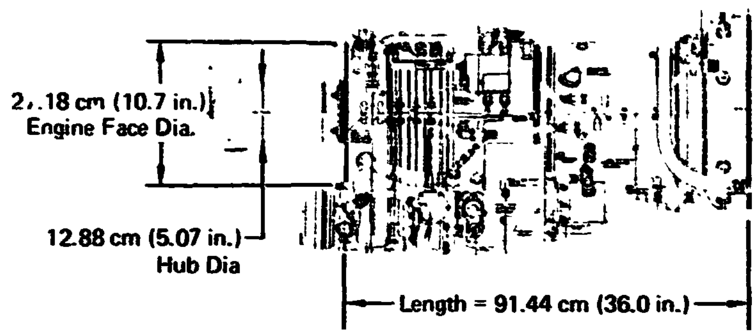

Design Point Performance (Intermediate Power)

Air Flow	5.62 kg/sec
Compressor Pressure Ratio	8.0:1
Turbine Inlet Temperature	932°C
Exhaust Gas Temperature	677°C
Engine Speed	19,500 rpm

GE-X376B Turbotip Fan

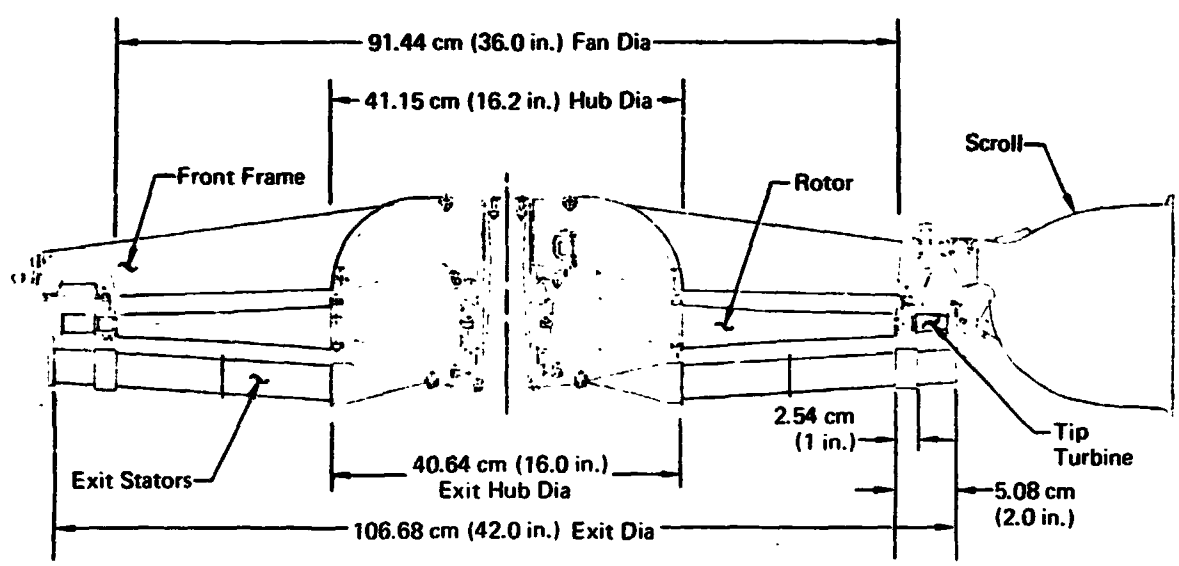

Design Point Performance (100% Speed)

Air Flow	69.4 kg/sec
Fan Pressure Ratio	1.08
Admission Arc	180°
Fan Speed (100%)	4074 rpm

GP79-0064-4

FIGURE 2-4
THRUST CALIBRATION TEST NOZZLE

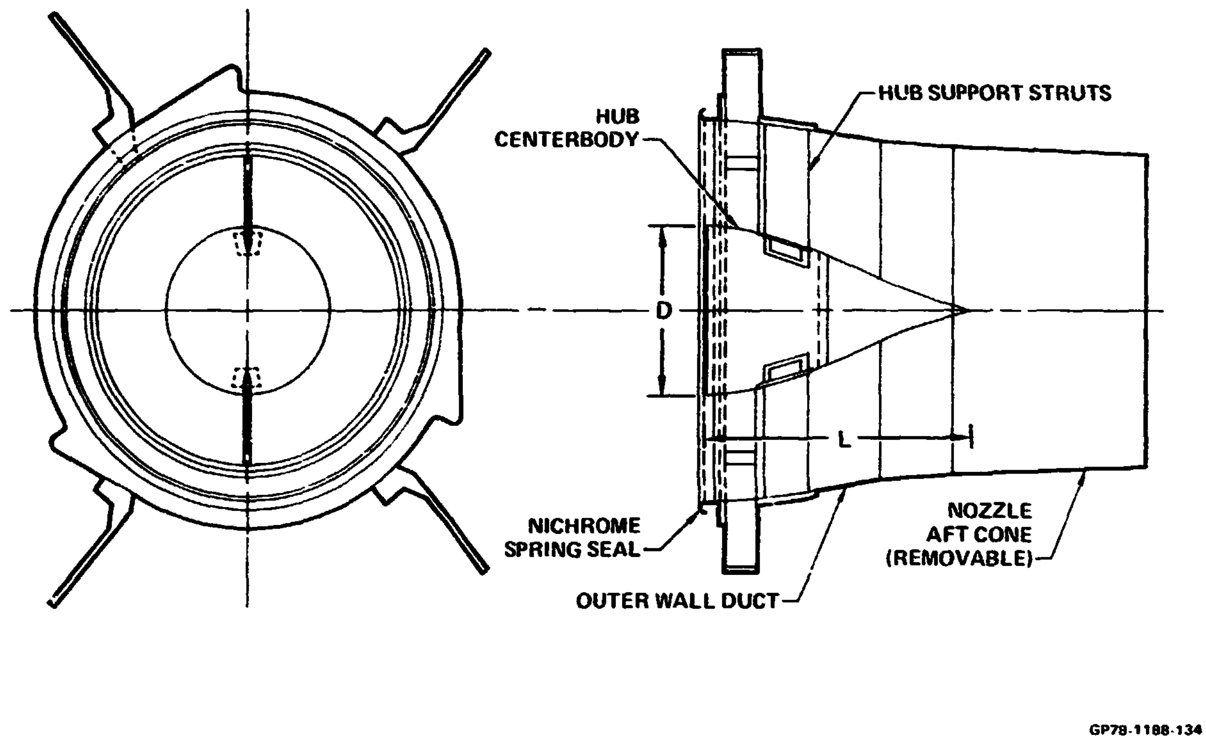

Hub Centerbody Characteristic Dimensions

LF336		X376B	
D cm (in.)	L cm (in.)	D cm (in.)	L cm (in.)
47.75 (18.8)	76.83 (30.2)	41.15 (16.2)	65.52 (25.8)

of four aft cone sections were fabricated to provide nozzle exit areas of 6730, 6285, 5935, and 5485 cm^2 (1043, 974, 920, and 850 in^2).

The entire thrust calibration assembly was mounted to a supporting framework by means of a series of struts and brackets which prevented transfer of nozzle loads to the fan. A series of nichrome leaf seals was attached to the outer duct element at the entrance station to minimize gas leakage at the fan/nozzle interface.

2.3.2 NOSE NOZZLE AND HUB - The nose lift unit thrust vectoring nozzle system utilized a remotely activated louver and drive system. Fourteen low camber louvers, each with a thickness ratio of 10 percent, provide thrust vectoring over a range from 105 to 30 degrees (δ_{NL}). Two 10 percent thick, manually positioned, articulated yaw vanes located beneath the louvers provide yaw vectoring of 0, ± 6, and ± 12 degrees (δ_Y). The yaw vanes were of the same design as those on the lift/cruise units and were detachable from the model. Details of the nose lift unit vectoring system, as installed in the LSPM, are presented in the sketch of Figure 2-5. The nose unit was tested with two fan exit hubs: hemispherical and flat plate.

2.3.3 LIFT/CRUISE NOZZLE - The lift/cruise nozzle consisted of thrust vectoring hood segments and a nozzle exit cone, as shown, installed in the LSPM, on Figure 2-6. Thrust vectoring was achieved with the fixed diameter, detachable angular hood segments, so arranged as to provide geometric deflection angles (δ_{LC}) of 0, 2[illegible], 38, 56, 71 and 95 degrees. The thrust vectoring hood segments were constant diameter with a turning radius ratio of 0.54 R/D. The nozzle exit cone was detachable and was equipped with two 10 percent thick, manually positioned, articulated yaw vanes. These vanes provide lateral vectoring of 0, ± 6, and ± 12 degrees (δ_Y) to produce yawing moments. The nozzle cone had a fixed nozzle exit area of 0.7677 m^2 (1190 $in.^2$) with an exit contraction ratio (A_{HOOD}/A_{NOZ}) of 1.16.

2.4 THRUST STAND RIG

The thrust stand rig consisted of a steel framework designed to support the fan assembly consisting of fan and gas generator, bellmouth inlets and exhaust nozzle system. The entire assembly was supported by means of three load cells located under the rig. For ground effect testing a large steel plate was used to simulate ground proximity. This ground plane was 3.67 m (12.0 ft) square providing 13.38 m^2 (144 ft^2) of simulated ground area.

Several configurations of thrust stand rig and ground plane were required to carry out the fan tests with the calibration nozzles, nose louvered lift nozzle and the lift/cruise deflector nozzles. Each of these test arrangements are described below.

2.4.1 CALIBRATION NOZZLE TEST ARRANGEMENT - Mapping of two X376B/T58 fan units, (nose and left lift/cruise) and the LF336/J85 system was carried out with the calibration nozzles installed. Figure 2-7 is a schematic of the thrust stand assembly for the mapping tests of the LF336/J85 fan. The fan bellmouth inlet used to measure fan flow was a GE-4 unit supplied by NASA and had a throat diameter of 152.4 cm. Bellmouths were also installed on the J85 and T58 gas generators for determination of gas generator inlet flow. Three load cells were positioned under the thrust stand rig and were oriented with the normal force elements parallel with the vertical direction and the axial force elements parallel with the horizontal direction. The load cell arrangement for both the LF336/J85 and X376B/T58 tests is shown in Figure 2-8. Photographs of the fan calibration test setup are shown in Figure 2-9.

FIGURE 2-5
NOSE LIFT UNIT VECTORING SYSTEM GEOMETRY

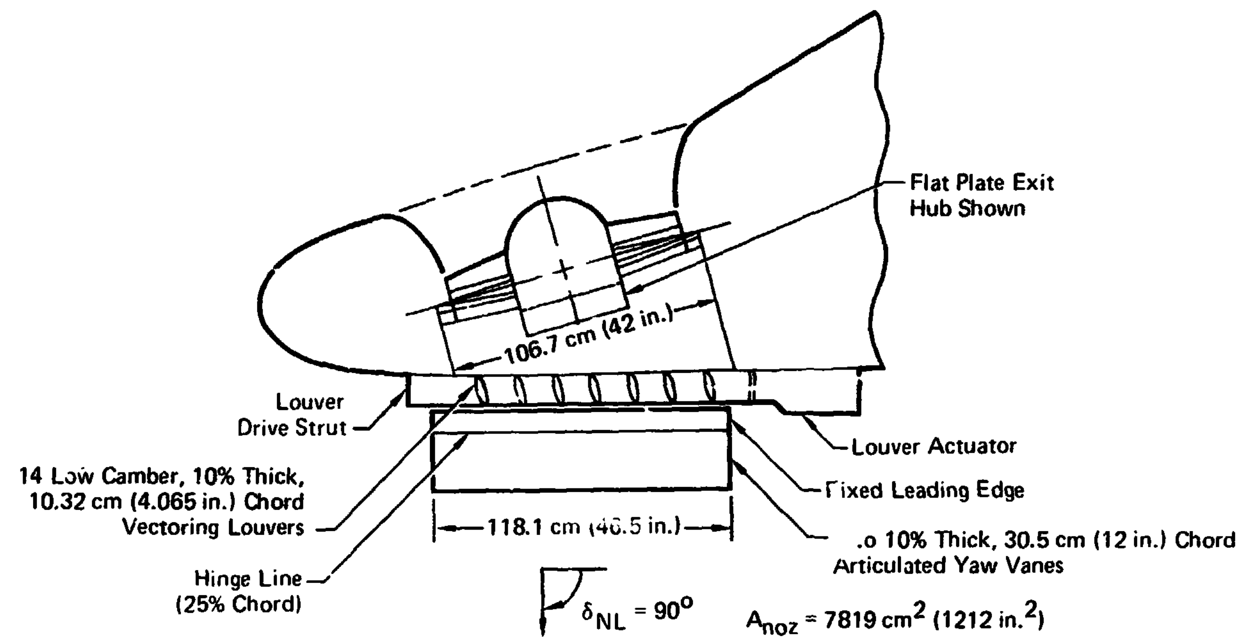

FIGURE 2-6
LIFT/CRUISE UNIT VECTORING SYSTEM GEOMETRY

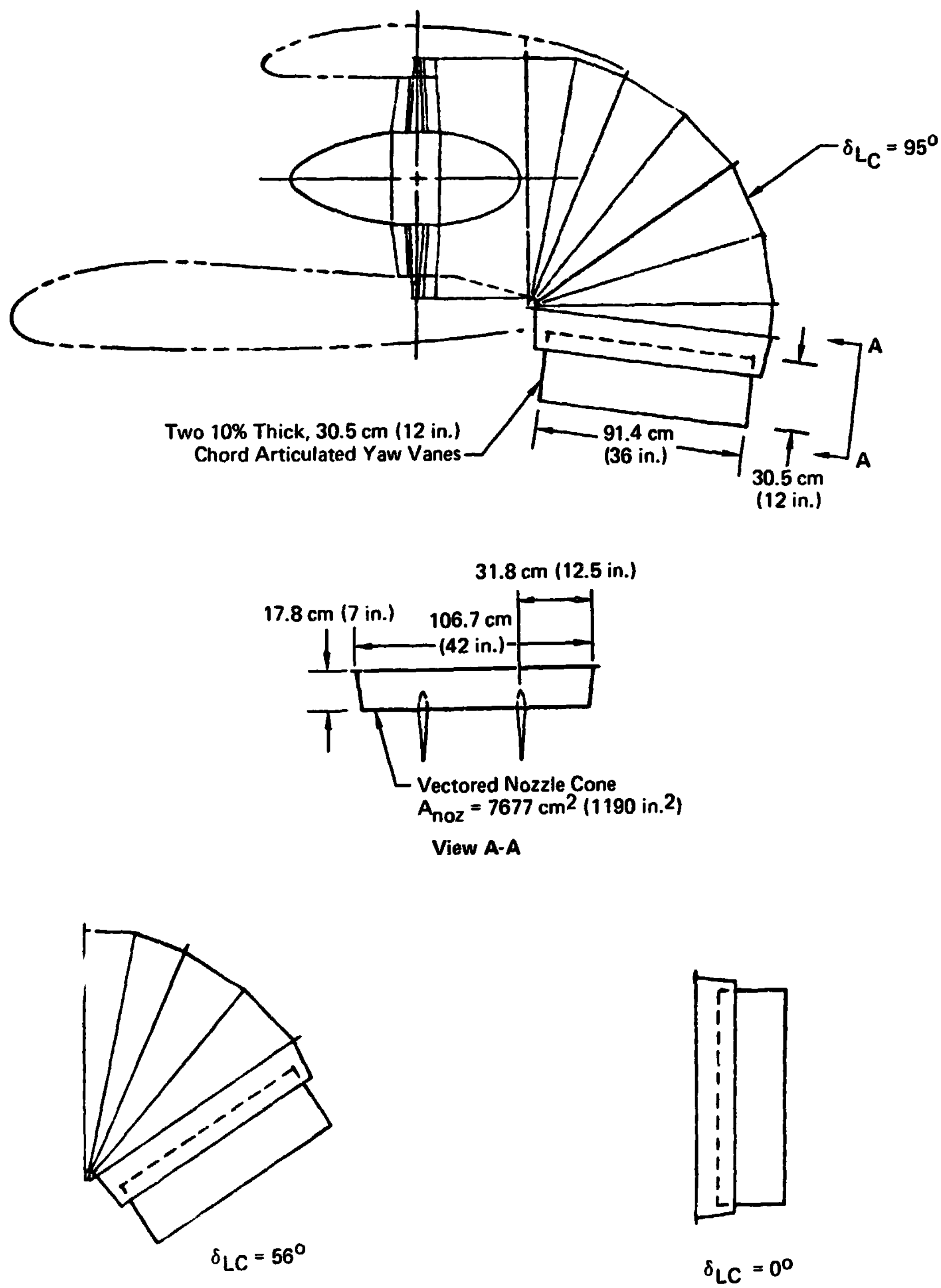

GP78-1188-149

FIGURE 2-7
LF336/J85 FAN CALIBRATION
Thrust Stand Assembly

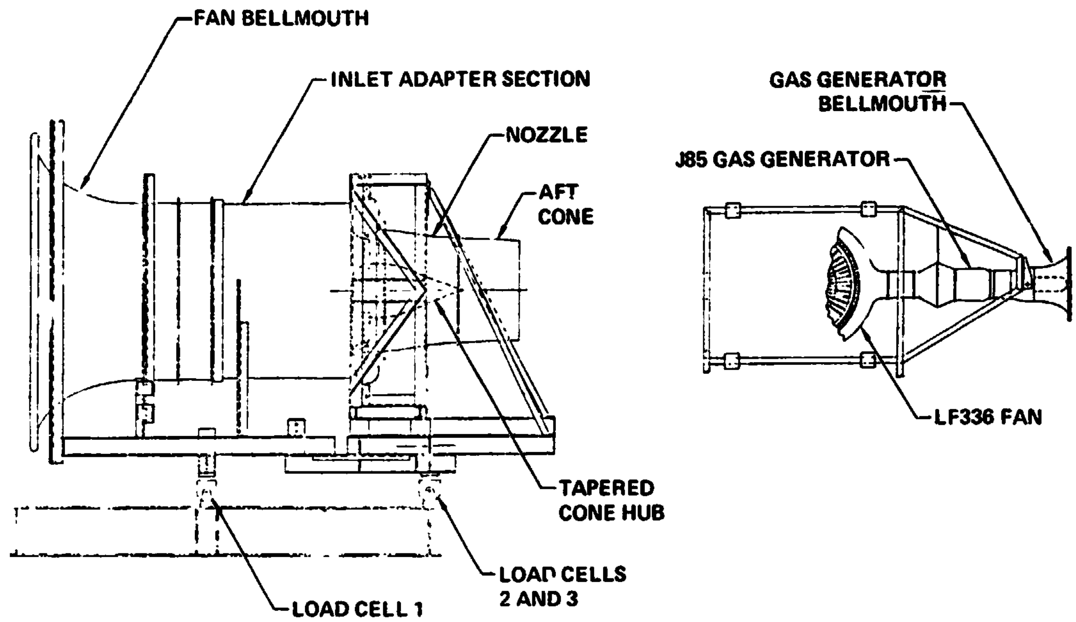

FIGURE 2-8
LOAD CELL LOCATIONS

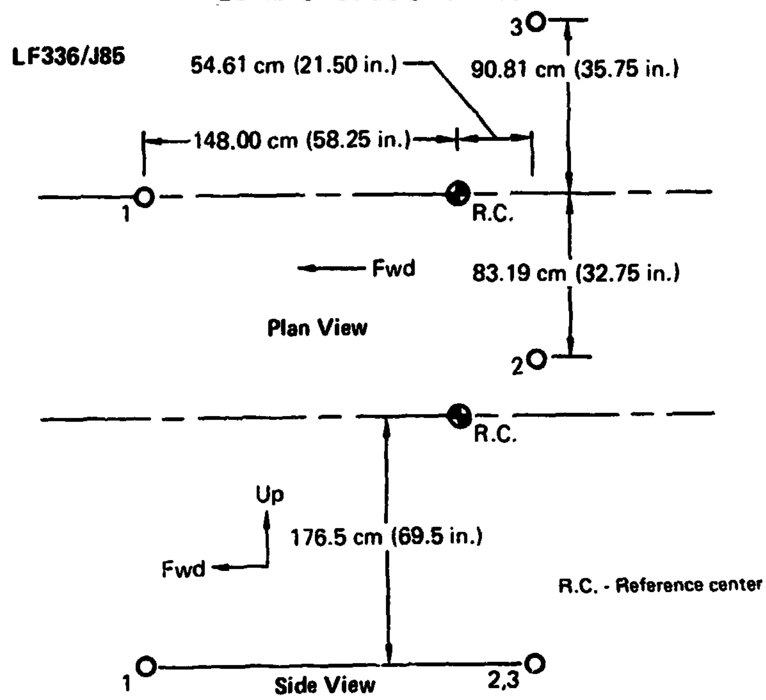

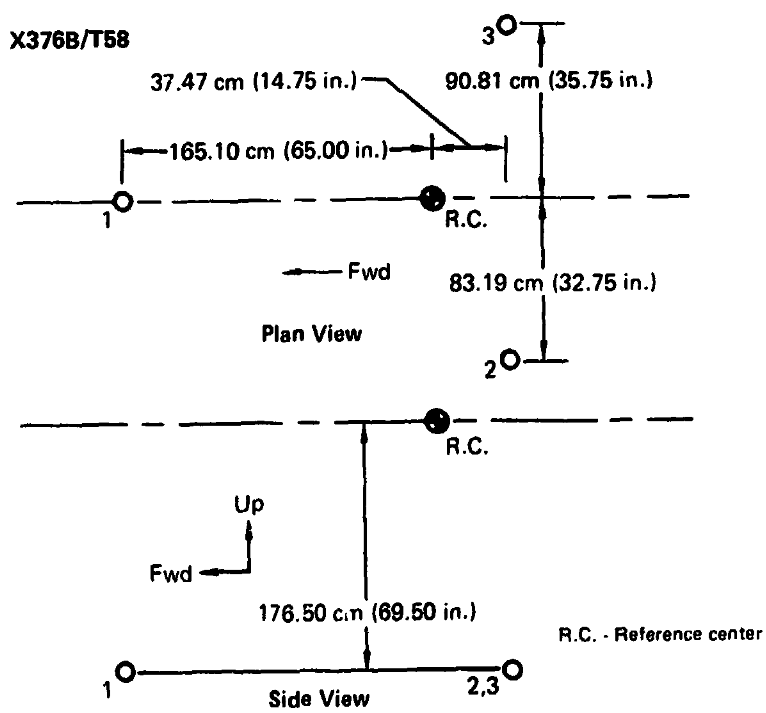

GP78-1188-112

FIGURE 2-9
LF336/J85 FAN CALIBRATION TEST SET-UP

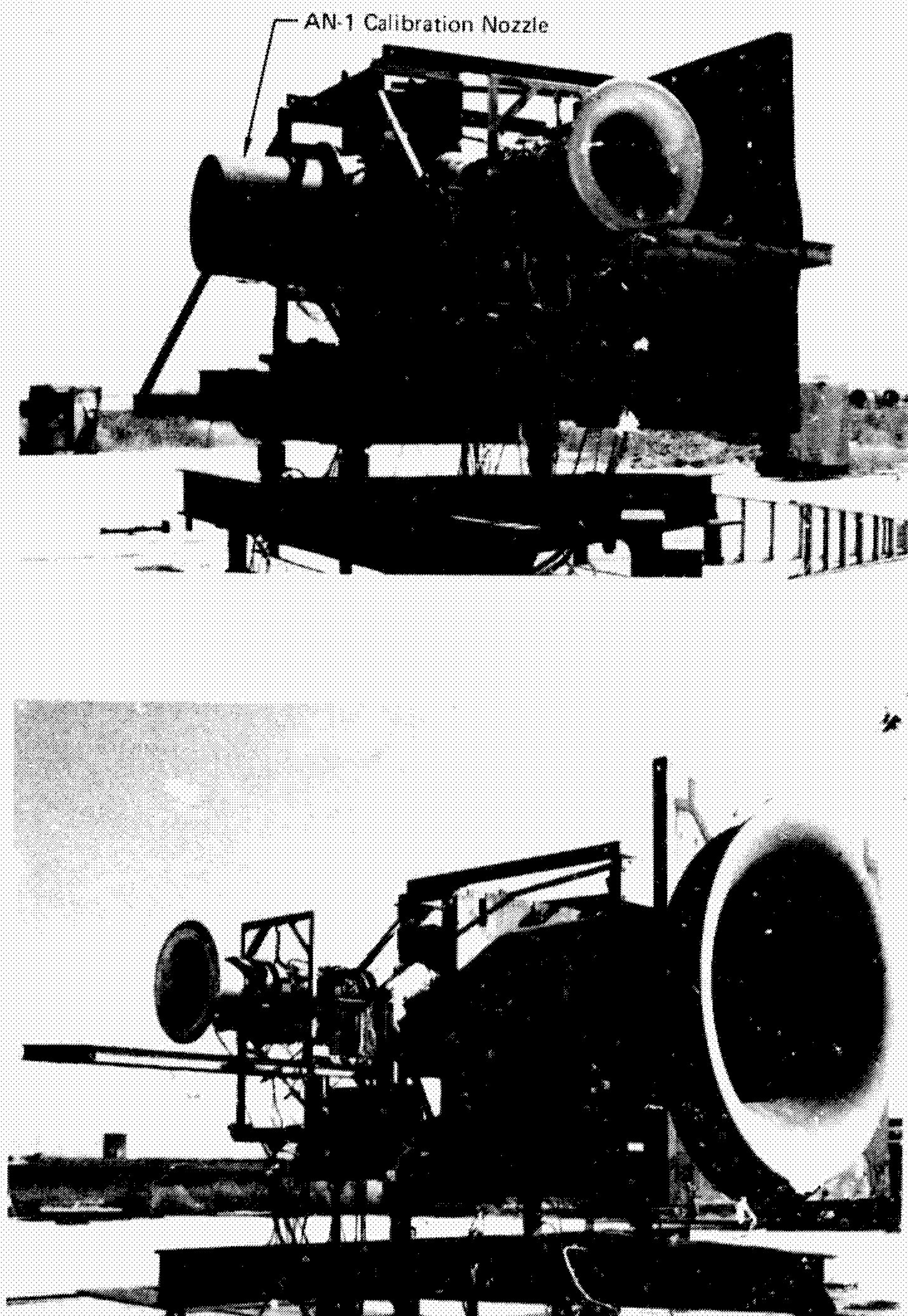

GP78 1188 140

2.4.2 NOSE LIFT NOZZLE TEST ARRANGEMENT - The experimental apparatus used for tests of the nose lift nozzle units is shown schematically in Figure 2-10. The exhaust flow of the nozzle was directed in the horizontal p'-'e for these tests. Ground effect testing was accomplished by positioning the ound plane downstream of the nozzle exit plane and normal to the thrust vector. A deflector was attached to one side of the ground plane such that the impingement flow could be directed away from the bellmouth inlets and thereby eliminate ingestion of the exhaust flow. Figures 2-11 and 2-12 show a series of photographs of the nose lift nozzle test apparatus for both the LF336/J85 and X376B/T58 units.

2.4.3 LIFT/CRUISE NOZZLE TEST ARRANGEMENT - The setup for the lift/cruise nozzle tests is shown schematically in Figure 2-13 and in the photographs of Figure 2-14. The deflected exhaust flow was directed upwards, again to prevent ingestion of the exhaust flow.

2.5 INSTRUMENTATION

The bellmouths, turbotip fans, gas generators, test nozzles and thrust stand rig were instrumented for the determination of fan and nozzle performance. The primary experimental measurements were fan speed, total gross thrust and direction, and fan and tip turbine inlet and exit pressures and temperatures. The instrumentation utilized is described below.

2.5.1 BELLMOUTH INLETS - Each bellmouth inlet (fan and gas generator) incorporated static pressure ports to provide a static differential pressure read-out. The gas generator used a single port for the differential pressure read-out, while the fan bellmouth incorporated four static ports manifolded to provide a single read-out.

The fan bellmouth static differential pressure was teed to a $2.069 \times 10^3 \frac{n}{m^2}$ (0.3 psid) transducer for recording on the digital data acquisition system and to a water manometer for hand recording. The manometer became the primary means for determining fan bellmouth airflows. Differential pressures in the fan bellmouth ranged from 2.1 to 10.8 cm.H_2O (.030 to .154 psi) for the LF336 fan and from 1.1 to 5.9 cm.H_2O (.016 to .084 psi) for the X376B fan. The water manometer was inherently more accurate than the $2.069 \times 10^3 \frac{n}{m^2}$ transducer at these low differential pressures. Accordingly, all fan bellmouth air flowrates presented in this report were calculated using the hand recorded water manometer data.

The gas generator bellmouth static differential pressure was measured using a $1.724 \times 10^2 \frac{n}{m^2}$ (2.5 psid) transducer.

Fan airflow temperature was measured using four thermocouples located 90 degrees apart on the lip of the bellmouth inlet. Gas generator airflow temperature was determined by means of a single thermocouple located on the lip of the bellmouth inlet.

2.5.2 LF336/J85 FAN AND TIP TURBINE EXIT - The fan and tip turbine exit instrumentation consisted of fixed rakes comprising 38 total pressure and 17 total temperature probes. Figure 2-15 presents the geometry of this rake, showing at the fan exit a 6 leg, 30 probe total pressure rake, a 3 leg, 9 probe total temperature rake, and at the tip turbine exit, 8 total pressure probes and 8 total temperature probes. Fan exit static pressure was measured by four taps on the hub during fan calibration test runs and six taps on the spacer between the fan exit face and hemispherical hub during g... effects test runs. Tip turbine exit static pressure was measured

FIGURE 2-10
LF336/J85 NOSE FAN IN GROUND EFFECT
Thrust Calibration Stand Assembly

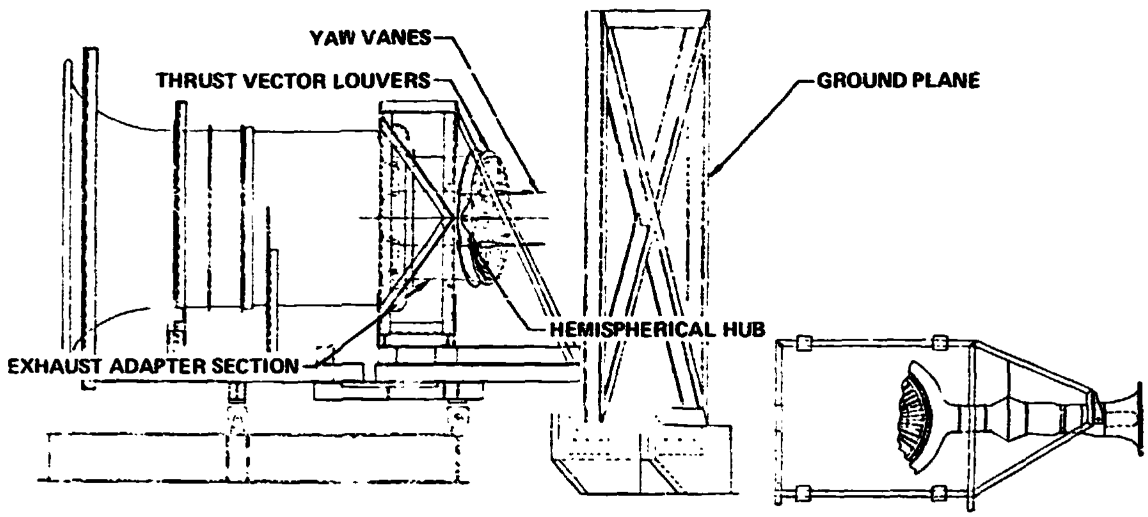

FIGURE 2-11
LF336/J85 NOSE IN GROUND EFFECT TEST SET-UP

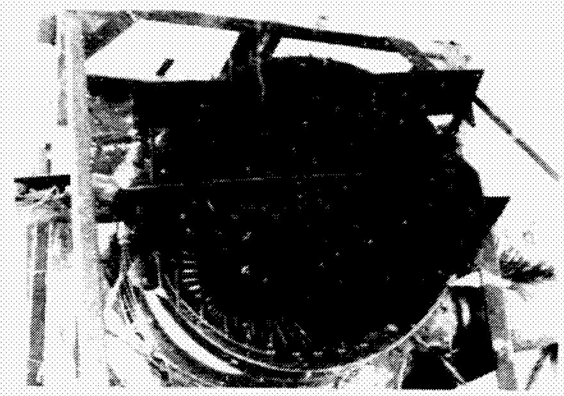

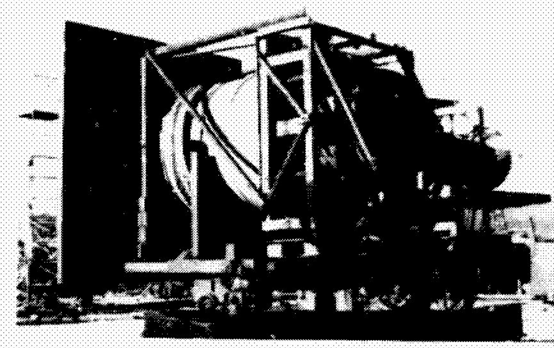

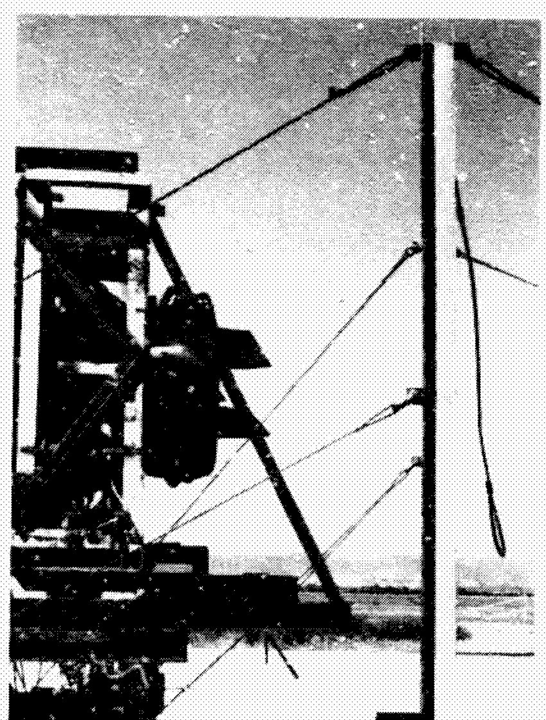

H/D = 1.55

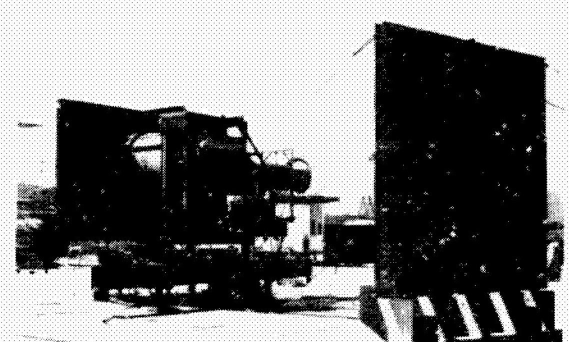

H/D = 6.45

GP78-1188-141

FIGURE 2-12
X376B/T58 NOSE IN GROUND EFFECT TEST SET-UP

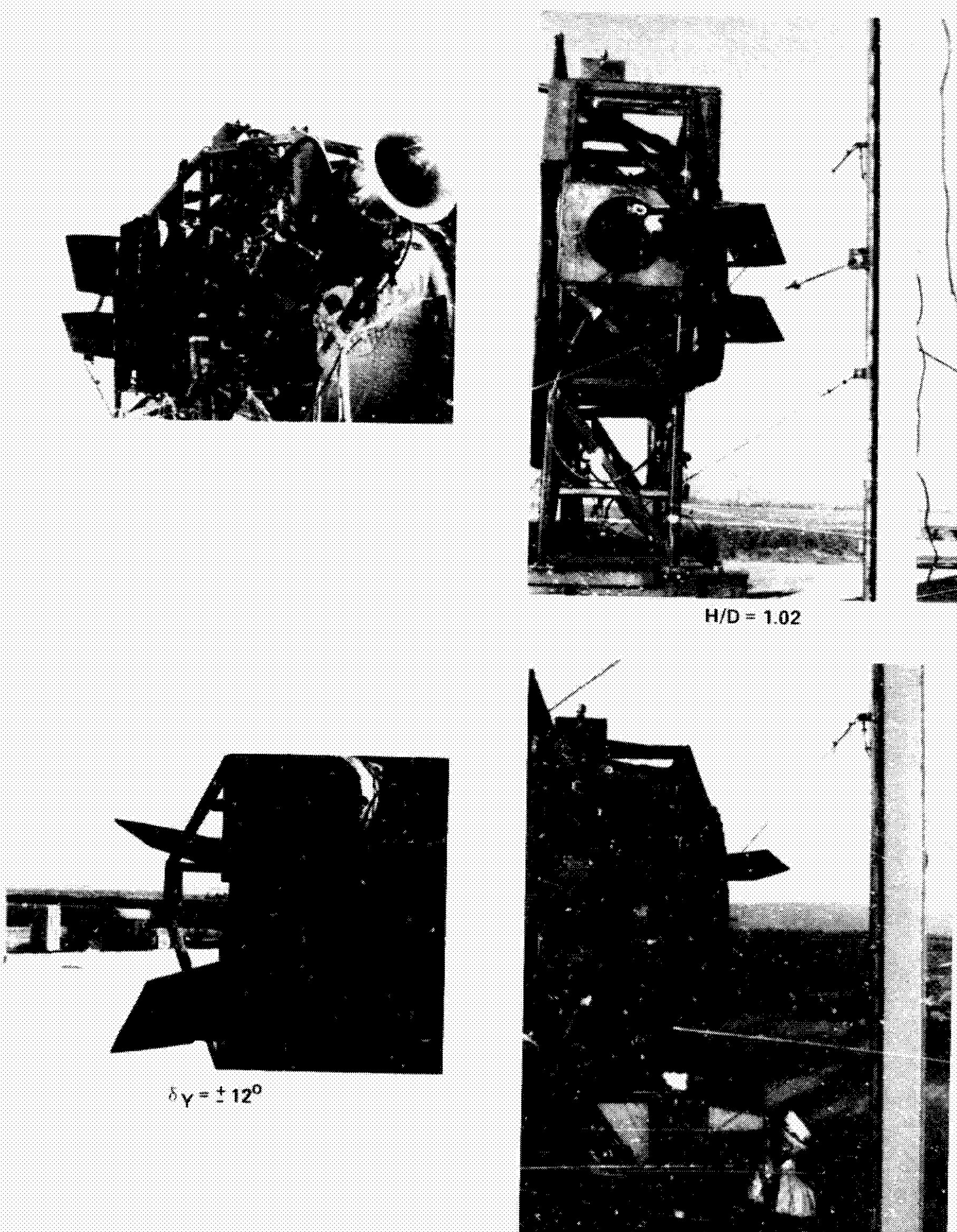

H/D = 1.02

$\delta_Y = \pm 12^o$

$\delta_Y = \pm 12^o$ H/D = 1.02

GP78-1188-142

FIGURE 2-13
X376B/T58 LEFT LIFT/CRUISE UNIT IN GROUND EFFECT
Thrust Stand Assembly

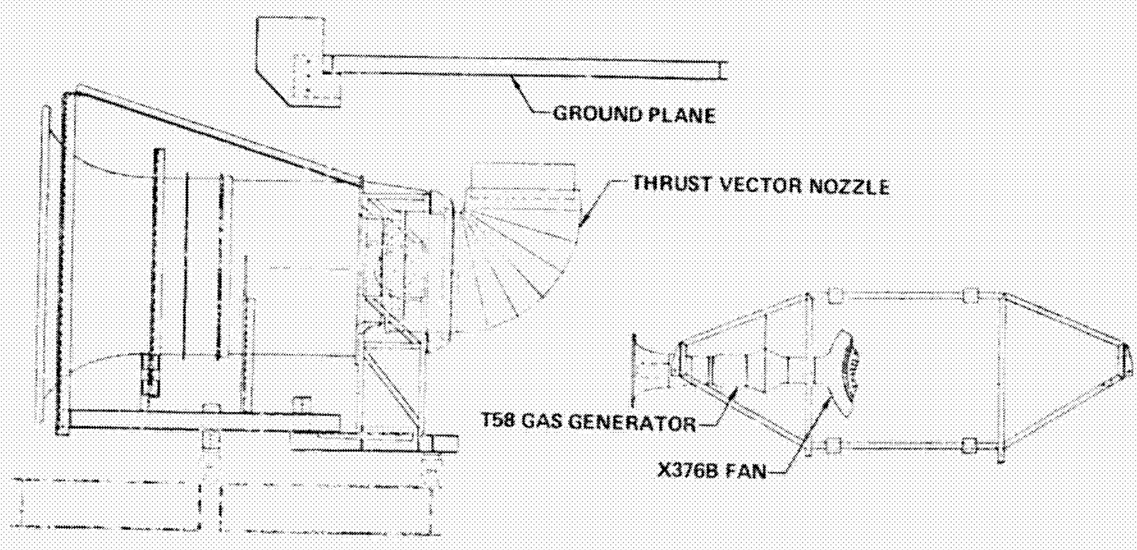

FIGURE 2-14
X376B/T58 LEFT LIFT/CRUISE IN GROUND EFFECT TEST SET-UP

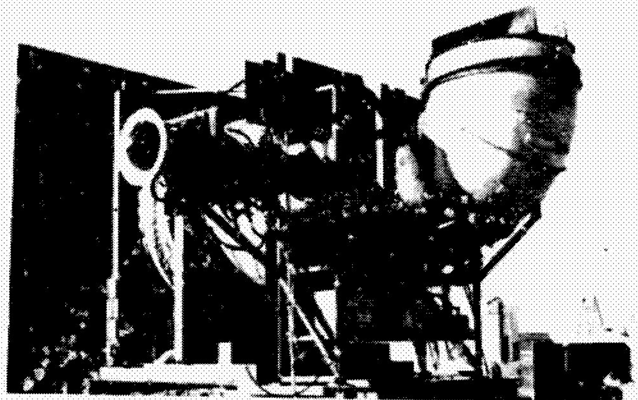

$\delta_{LC} = 95^{o}$

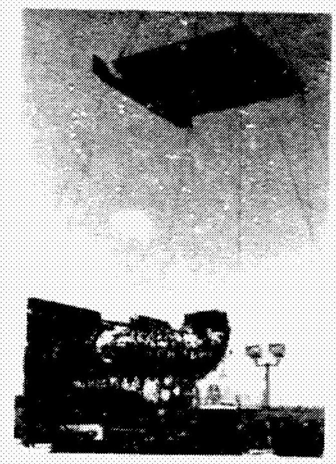

H/D = 6.45

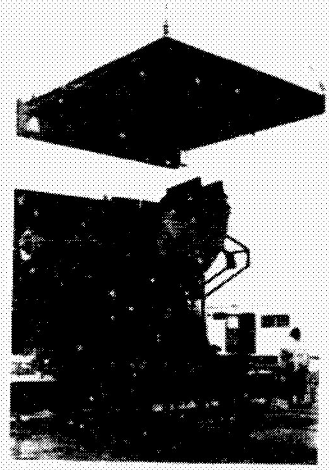

H/D = 1.55

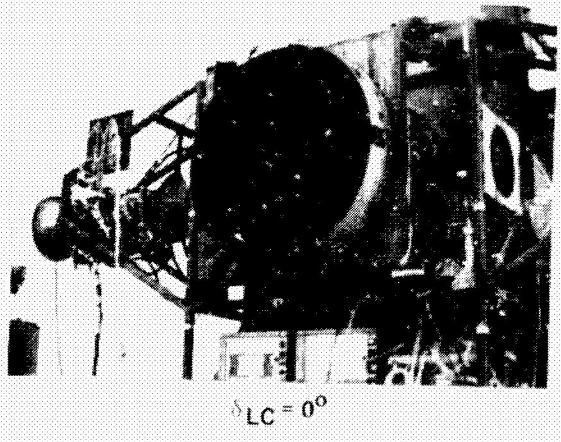

$\delta_{LC} = 0^{o}$

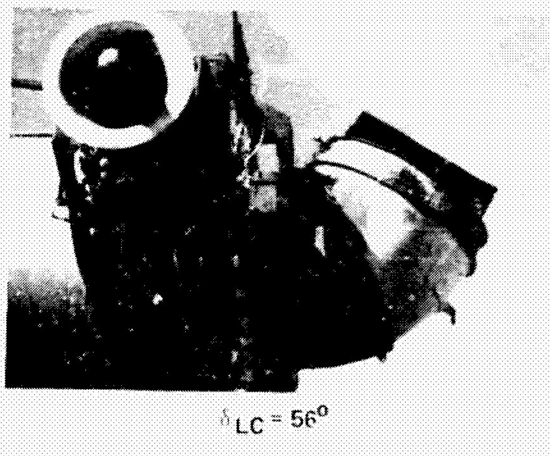

$\delta_{LC} = 56^{o}$

GP78 1188 143

FIGURE 2-15
LF336 NOSE
FAN AND TIP TURBINE EXIT INSTRUMENTATION

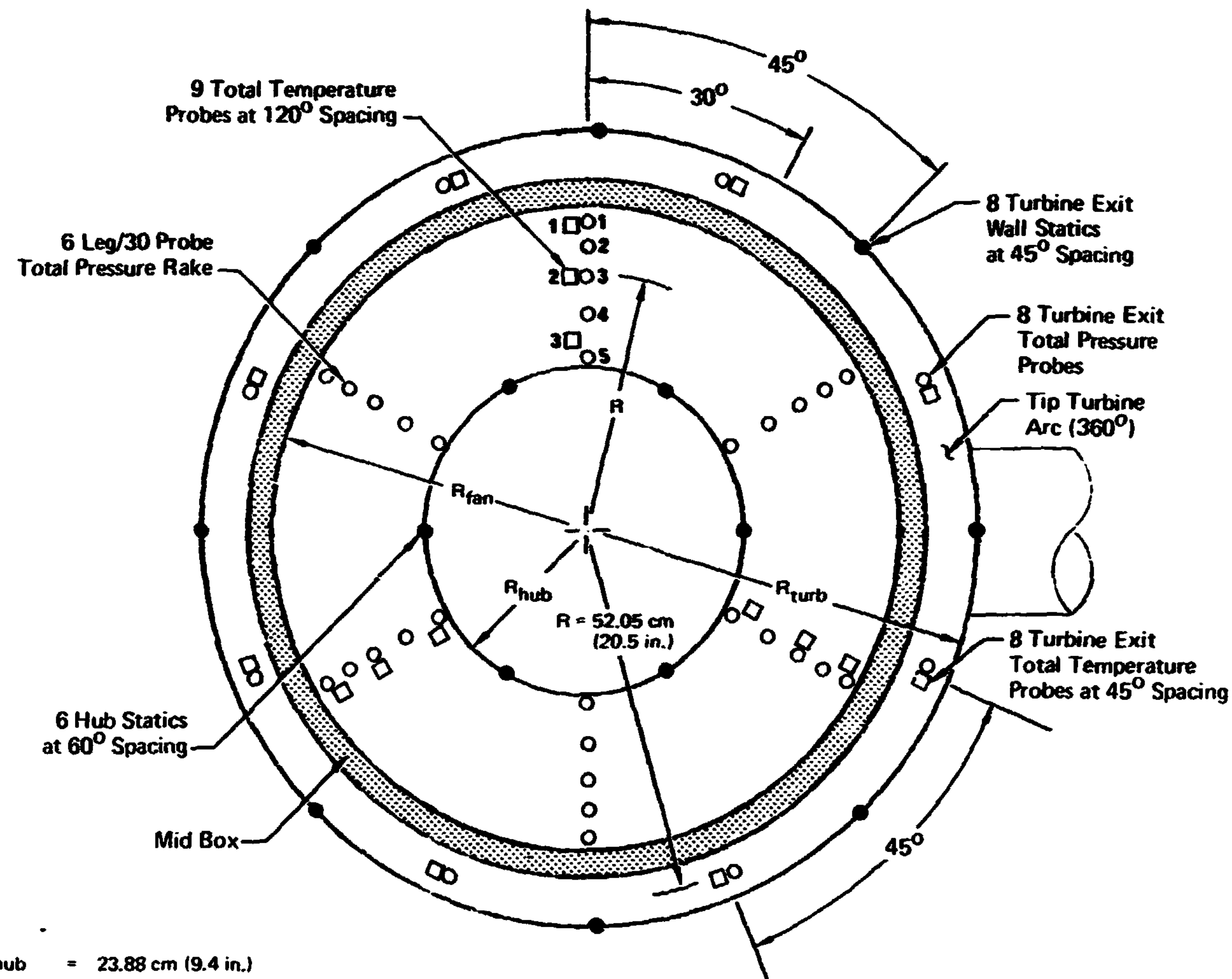

R_{hub} = 23.88 cm (9.4 in.)
R_{fan} = 45.72 cm (18.0 in.)
R_{turb} = 54.61 cm (21.5 in.)

Rear View

Thermocouple Locations

T/C No.	Radius - cm (in.)
1	42.77 (16.84)
2	36.32 (14.30)
3	28.35 (11.16)

Pressure Tube Locations

Tube No.	Radius - cm (in.)
1	43.99 (17.32)
2	40.39 (15.9)
3	36.42 (14.34)
4	31.95 (12.58)
5	26.72 (10.52)

GP78 1188 137

by twelve taps on the calibration nozzle outer wall during fan calibration test runs and by eight taps on the nozzle outer wall during ground effects testing.

2.5.3 X376B/T58 FAN AND TIP TURBINE EXIT - Each of the three X376B fans was instrumented at the stator exit (fan and tip turbine) with the pressure and temperature rakes used in the LSPM. Figure 2-16 depicts the tube and port locations, showing 30 total pressure and 9 total temperature probes at the fan exit and 4 total pressure and 4 total temperature probes at the tip turbine exit. During ground effects testing, fan and tip turbine exit static pressures were obtained from taps as shown on the figure.

2.5.4 NOSE FAN EXIT HUB - The hemispherical hubs used during the ground effects testing of the LF336 and X376B nose fan configurations were instrumented with 21 static pressure taps as shown on Figure 2-17. The flat plate hub also used on the X376B nose fan during ground effects testing was instrumented in a like manner.

2.5.5 LOAD CELLS - Three load cells were used to determine gross thrust and thrust direction. Each load cell was a three component strain gauge balance. Load cell No. 1 (See Figure 2-8) is a unit with 26,690 n (6000 lb) normal force, 17,793 n (4000 lb) axial force and 13,345 n (3000 lb) side force capability. Load cells Nos. 2 and 3 had normal, axial and side force capability of 13,345 n (3000 lb), 8,896 n (2,000 lb) and 4,448 n (1000 lb) respectively.

2.5.6 NOZZLE EXIT - The left lift/cruise unit was instrumented at the nozzle exit. The nozzle exit included 10 total pressure probes attached to the leading edge of the two fixed yaw vane struts and four external nozzle exit base pressure static ports. A schematic of the nozzle exit instrumentaion is presented in Figure 2-18.

2.5.7 ADDITIONAL - Instrumentation to monitor the "health" of the test fan and gas generator and provide diagnostic capability included:

Fans - Speed
- Vibration - Hub Horizontal
  - Hub Axial

Gas Generator - Speed
- Fuel Flow
- Vibration - Compressor Vertical
- Oil Pressure and Temperature
- Exhaust Gas Temperature

Ambient conditions monitored were pressure, temperature, wind velocity, and wind direction.

2.5.8 INSTRUMENTATION SUMMARY - A list of the test instrumentation is presented in Figure 2-19.

2.6 DATA ACQUISITION

The experimental test parameters of pressure, temperature, fan and gas generator speed, and load cell forces were measured, digitized, and recorded on paper punch tape utilizing a VIDAR Corporation digital data system. This system is comprised of analog signal conditioning, an integrating digital voltmeter, and a Teletype Paper-Tape punch. A total of 99 data recording channels are available with

FIGURE 2-16
X376B FAN AND TIP TURBINE EXIT INSTRUMENTATION

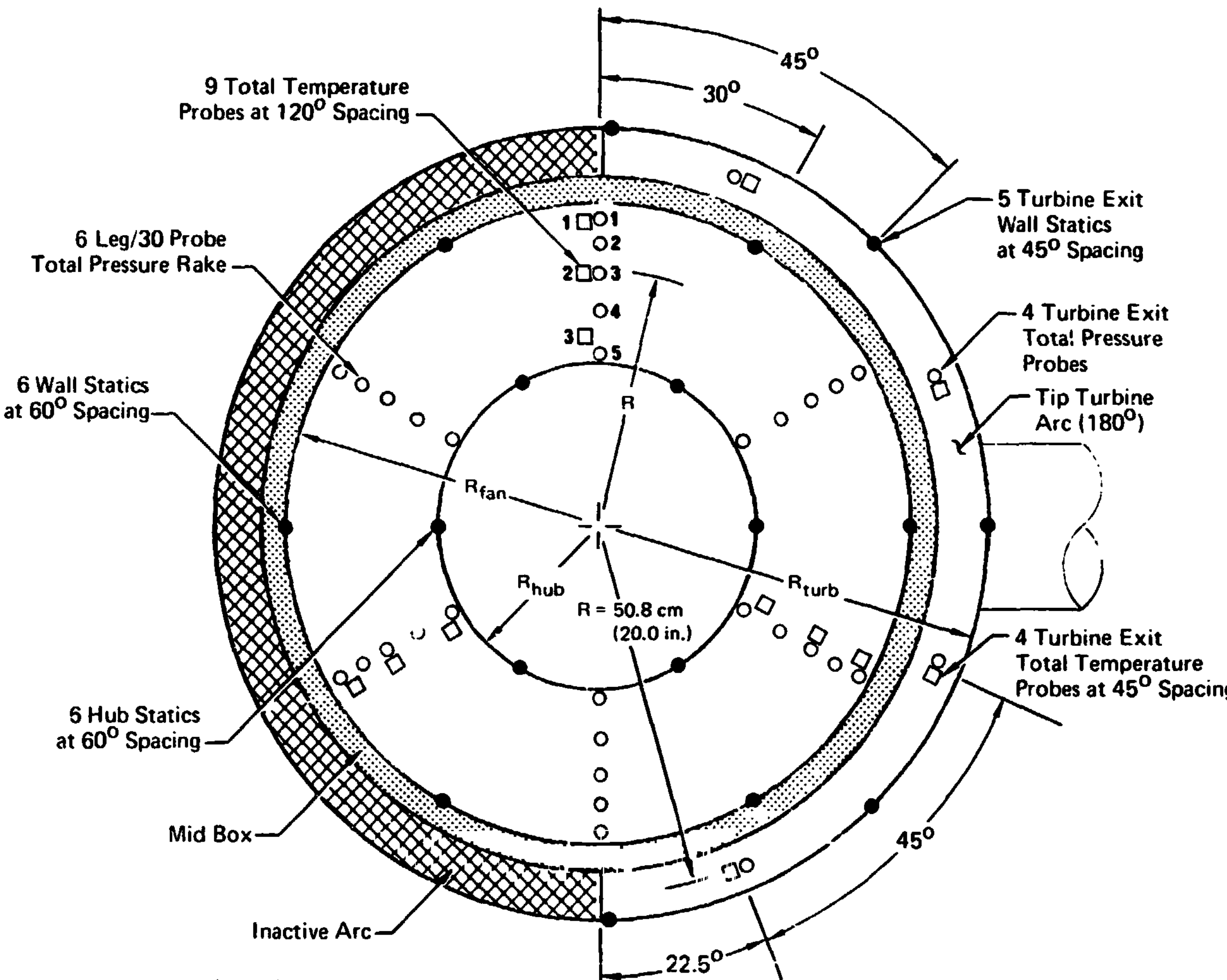

Rear View
Left Side

Thermocouple Locations

T/C No.	Radius - cm (in.)	
	L/C	Fwd
1	40.64 (16.00)	41.73 (16.43)
2	33.07 (13.02)	34.11 (13.43)
3	27.18 (10.70)	28.32 (11.15)

Pressure Tube Locations

Tube No.	Radius - cm (in.)	
	L/C	Fwd
1	43.61 (17.17)	44.81 (17.64)
2	37.54 (14.78)	38.71 (15.24)
3	32.41 (12.76)	33.93 (13.36)
4	28.12 (11.07)	29.49 (11.61)
5	24.28 (9.56)	25.65 (10.10)

GP78-1188-136

FIGURE 2-17

X376B HEMISPHERICAL HUB STATIC PRESSURE TAPS, HP(i), i = 1 THROUGH 21

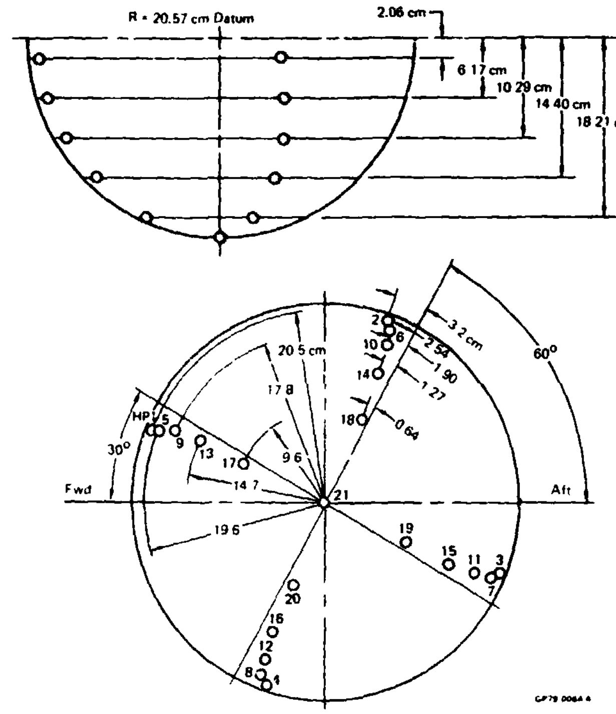

LF336 HEMISPHERICAL HUB STATIC PRESSURES TAPS, HP(i), i = 1 THROUGH 21

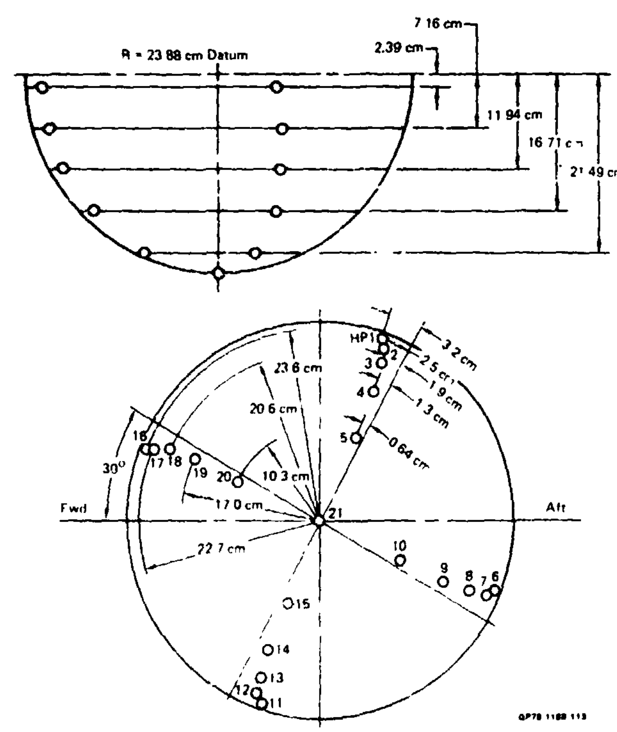

FIGURE 2-18
LIFT/CRUISE NOZZLE EXIT INSTRUMENTATION

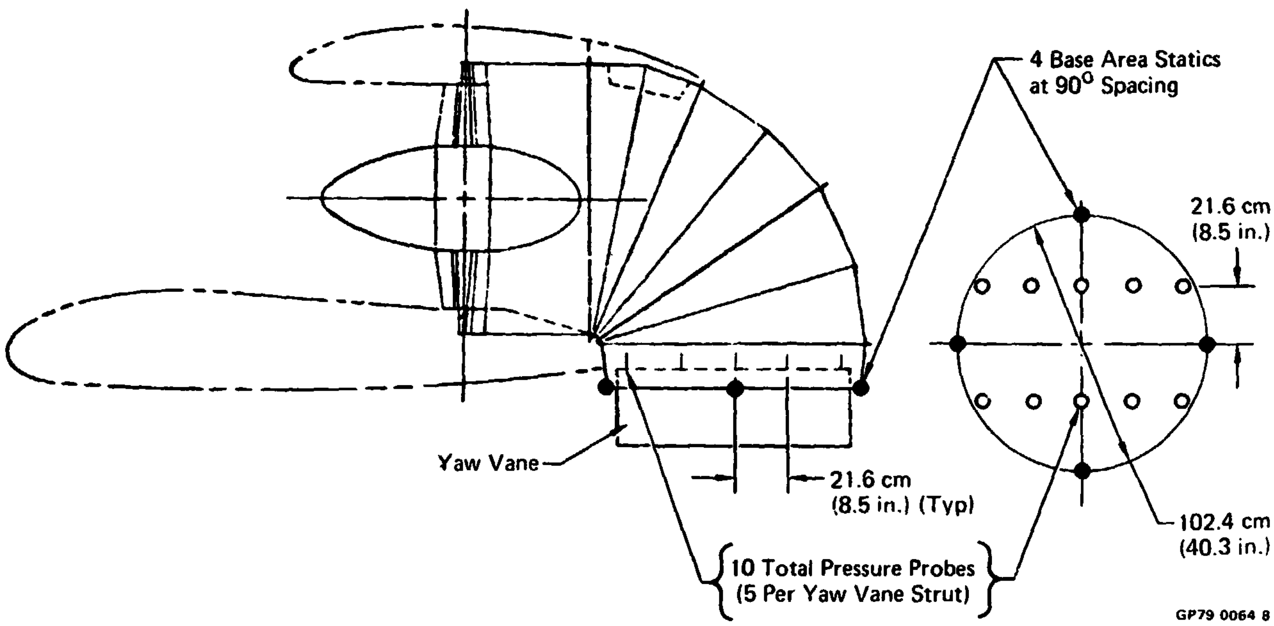

FIGURE 2-19
TEST INSTRUMENTATION SUMMARY

PARAMETER	SYMBOL	NO.	MEASUREMENT DEVICE	RECORDING MODE
AMBIENT CONDITIONS				
TEMPERATURE	TO	1	THERMOCOUPLE	PANEL
PRESSURE	PO	1	PRESSURE GAUGE	PANEL
WIND VELOCITY	VO	1	ANEMOMETER	PANEL
WIND DIRECTION	-	1	-	PANEL/VIDAR
J85 GAS GENERATOR				
RPM	NG	1	TACHOMETER	PANEL/VIDAR
FUEL FLOW	WF	1	FLOWMETER	PANEL/VIDAR
OIL				
PRESSURE	-	1	TRANSDUCER	PANEL
TEMPERATURE	-	1	THERMOCOUPLE	PANEL
EXHAUST GAS				
TEMPERATURE	EGT1-EGT3	3	THERMOCOUPLE	PANEL/VIDAR
PRESSURE	EGP1-EGP3	3	TRANSDUCER	VIDAR
VIBRATION				
COMPRESSOR VERTICAL	-	1	ENGINE STRAIN GAUGE	PANEL
BELLMOUTH				
STATIC PRESSURE	PBG	1	TRANSDUCER	VIDAR
TEMPERATURE	TG1	1	THERMOCOUPLE	VIDAR
LF336 FAN				
RPM	NF	1	TACHOMETER	PANEL/VIDAR
VIBRATION				
HUB HORIZONTAL	-	1	FAN STRAIN GAUGE	PANEL
HUB AXIAL	-	1	FAN STRAIN GAUGE	PANEL
BELLMOUTH				
STATIC PRESSURE	PBF	1	H_2O MANOMETER/TRANSDUCER	PANEL/VIDAR
TEMPERATURE	TB1-TB4	4	THERMOCOUPLE	VIDAR
INLET				
TEMPERATURE	TT1	1	THERMOCOUPLE	VIDAR
EXIT				
FAN				
STATIC PRESSURE	PS1-PS4,6	4-6	S/V	VIDAR
TOTAL PRESSURE	PT1-PT30	30	S/V	VIDAR
TEMPERATURE	TT1-TT9	9	THERMOCOUPLE	VIDAR
TIP TURBINE				
STATIC PRESSURE	PS1-PS8,12	8-12	S/V	VIDAR
TOTAL PRESSURE	PT1-PT8	8	S/V	VIDAR
TEMPERATURE	TT1-TT8	8	THERMOCOUPLE	VIDAR
T58 GAS GENERATOR				
OIL				
PRESSURE	-	1	TRANSDUCER	PANEL
TEMPERATURE	-	1	THERMOCOUPLE	PANEL
EXHAUST GAS				
TEMPERATURE	EGT	1	THERMOCOUPLE	PANEL
BELLMOUTH				
STATIC PRESSURE	PBG	1	H_2O MANOMETER/TRANSDUCER	PANEL/VIDAR
TEMPERATURE	TG1	1	THERMOCOUPLE	VIDAR
X376B FAN				
RPM	NF	-	TACHOMETER	PANEL/VIDAR
VIBRATION				
FAN AXIAL	-	1	-	PANEL
BELLMOUTH				
STATIC PRESSURE	PBF	1	H_2O MANOMETER/TRANSDUCER	PANEL/VIDAR
TEMPERATURE	TB1-TB4	4	THERMOCOUPLE	VIDAR
INLET				
STATIC PRESSURE	PS1,3,5,7	4	S/V	VIDAR
TOTAL PRESSURE	PT1-PT48	48	S/V	VIDAR
TEMPERATURE	TT1-TT8	8	THERMOCOUPLE	VIDAR
EXIT				
FAN				
STATIC PRESSURE	PS1-PS6,12	6-12	S/V	VIDAR
TOTAL PRESSURE	PT1-PT30	30	S/V	VIDAR
TEMPERATURE	TT1-TT9	9	THERMOCOUPLE	VIDAR
TIP TURBINE				
STATIC PRESSURE	PS1-5,6	5-6	S/V	VIDAR
TOTAL PRESSURE	PT1-PT4	4	S/V	VIDAR
TEMPERATURE	TT1-TT4	4	THERMOCOUPLE	VIDAR
FAN EXIT HUB				
HEMISPHERICAL AND FLAT PLATE				
STATIC PRESSURE	HP1-HP21	21	S/V	VIDAR
CALIBRATION NOZZLE AND HUB				
STATIC PRESSURE	PS1-PS35	35	S/V	VIDAR
TEMPERATURE	TS1-12,4	12-14	THERMOCOUPLE	VIDAR
LIFT/CRUISE NOZZLE				
STATIC PRESSURE	PSB1-PSB4	4	S/V	VIDAR
TOTAL TEMPERATURE	PT1-PT10	10	S/V	VIDAR
LOAD CELLS 1,2,3				
AXIAL FORCE	A1-A3	3	STRAIN GAUGE	VIDAR
SIDE FORCE	S1-S3	3	STRAIN GAUGE	VIDAR
NORMAL FORCE	N1-N3	3	STRAIN GAUGE	VIDAR
TEMPERATURE	LCT1-LCT3	3	THERMOCOUPLE	VIDAR

this system. The first 20 channels of the VIDAR system are multiple scan channels, and the remaining channels are single scan. During a recording sequence, the first 20 channels were recorded a total of 48 times, and the remaining channels were recorded once. The total time for one data recording sequence was approximately 90 seconds.

The paper tape data records were processed at NASA-Ames on the 40 x 80 wind tunnel data computer which converted the raw test data to engineering test parameters.

Ambient temperature, wind velocity, wind direction, and barometric pressure were visually monitored and hand recorded.

The gas generator operating conditions were visually monitored and recorded by hand including speed, exhaust gas temperature, oil pressure and temperature, and vibration. The turbotip fan vibration levels, together with fan rpm (as a backup), were also monitored and hand recorded.

3. RESULTS AND DISCUSSION

Four turbotip fan configurations were investigated during this program: the three LSPM X376B/T58 units and an LF336/J85 unit. Fan performance maps were established for each of the fan units except the right lift/cruise unit of the LSPM. Mapping of the right unit was omitted because of program scope limitations. The three X376B/T58 units with their corresponding LSPM exhaust nozzle systems and the LF336/J85 with the LSPM nose louver nozzle were each tested in and out of ground proximity to establish performance trends with ground height.

The primary experimental data gathered during the tests consisted of gross thrust magnitude and direction, fan and gas generator mass flows, and fan and tip turbine stator exit pressures and temperatures. This information was sufficient to determine both fan performance maps and a comparison of the measured thrust and mass flow with values computed using the fan and tip turbine exit pressure and temperature data.

The comparison of thrust information obtained from the load cells, $(F_G)_{MEASURED}$, to that calculated from the fan exit pressure and temperature instrumentation, $(F_G)_{IDEAL}$, and similarly, the comparison of mass flow information from the bellmouths, $(W)_{BELLMOUTH}$, to that obtained from the fan exit instrumentation, $(W)_{RAKE}$, were established in coefficient form using the following expressions:

$$\text{thrust coefficient, CF} = \frac{(F_G)_{MEASURED}}{(F_G)_{IDEAL}}$$

$$\text{fan mass flow coefficient, CAF} = \frac{(W_F)_{BELLMOUTH}}{(W_F)_{RAKE}}$$

$$\text{turbine mass flow coefficient, CAT} = \frac{(W_T)_{BELLMOUTH}}{(W_T)_{RAKE}}$$

The coefficients relate the rake ideal thrust and mass flow to the actual measured values and provide the means to establish installed thrust for the LSPM tests where rake ideal thrust is the measured performance parameter. The present tests established the three coefficients for each fan/nozzle configuration and the effects thereon of ground height variations.

A total of 44 tests runs were carried out with the four fan units according to the schedule in Appendix A. A test run consisted of operation of the fan unit from idle to near 100 percent physical speed followed by a decrease to idle. Test data were recorded during both up and downward speed variations at nominal speeds of 50, 60, 70, 80, 90 and 100 percent.

3.1 X376B/T58 NOSE LIFT UNIT

Tests of the X376B/T58 nose lift unit included mapping runs with the calibration nozzle and ground effect runs with the louvered lift nozzle. The flat plate and hemispherical fan exit hubs were both evaluated during the ground tests to investigate hub geometry variations on performance. In addition, tests with the two yaw vanes each splayed 12° were conducted. The results for each of these test configurations are presented below.

3.1.1 FAN PERFORMANCE MAP - Mapping of the X376B/T58 nose lift unit was accomplished over test runs 19-22. Figure 3-1 presents the fan exit total pressure ratioed to ambient pressure, P_{TFE}/P_0, versus corrected fan speed, $N_F/\sqrt{\theta}$, characteristics for the four calibration nozzle exit areas. The open symbols represent data obtained with increasing fan speed and closed symbols with decreasing speed. The turbine total pressure ratio, P_{TTE}/P_0, versus fan speed data shown in Figure 3-2 indicates no significant differences in total pressure between the fan and turbine streams. Plots of the fan and gas generator bellmouth corrected airflow, $W\sqrt{\theta}/\delta$, variations with fan speed are illustrated in Figure 3-3. The thrust characteristics of the X376B/T58 nose unit with the calibration nozzles are shown in Figure 3-4 as a function of fan speed.

The fan pressure ratio and corrected flow data described above were combined to define the fan map for this unit shown in Figure 3-5. Similarly, thrust performance maps were generated as a function of both fan corrected mass flow and total nozzle flow (fan plus tip turbine flow) and are depicted in Figure 3-6.

Inspection of the fan map indicates that the nose unit falls below the design point pressure ratio of 1.08 at the design airflow of 69.4 kg/sec. The thrust performance map shows, at a constant corrected fan speed, a small variation of thrust with corrected airflow over the range tested with a maximum occurring at a nozzle exit area of 6285 cm^2.

3.1.2 LOUVERED NOZZLE PERFORMANCE IN GROUND PROXIMITY, FLAT PLATE HUB - Tests of the louvered nozzle with the flat plate exit hub installed were carried out for ground heights corresponding to H/D values of ∞ (ground plane removed), 6.45, [illegible], 1.55 and 1.02. The nozzle louver angle, δ_{NL}, and yaw vane angle, δ_Y, were maintained at 95° and 0° respectively for this sequence of runs.

Corrected fan flow and turbine flow versus fan speed are illustrated in Figures 3-7 and 3-8, which also depict the flow data computed by means of the fan exit rake. Corrected measured thrust and ideal thrust values computed via the exit rake are presented in Figure 3-9.

The effect of ground height on fan operating characteristics may be illustrated by superimposing the measured fan operating line at each ground height on the previously determined fan map described under Section 3.1.1. Figure 3-10 provides this illustration where it may be seen that the operating line generated with this nozzle is unchanged for all the heights except the lowest H/D value of 1.02. At this height, a definite shift to the left occurred indicating a reduction in effective nozzle exit area. This reduction in effective nozzle area is typical of nozzle performance in ground effect and is attributed to an increase in pressure above ambient at the nozzle exit plane.

Comparison, at a constant corrected fan speed, of the measured thrust data for the several ground heights reveals no significant change except at the lowest height. At the lowest ground position a definite increase in thrust magnitude was recorded. The improvement in thrust is associated with a change in pressure level on the fan exit hub which occurs at the lowest height. Figure 3-11 shows the fan exit hub pressure data recorded on the centerline tap as a function of fan speed for the two lowest heights. An increase in magnitude and a change in slope with fan speed is evident at the lowest height.

Evaluation of the thrust and mass flow coefficients for the fan exit rake was determined from the data of Figures 3-7, 3-8 and 3-9, by forming the ratio of measured to rake computed data at a given fan speed. Figure 3-12 shows the variation

of the three rake coefficients as a function of H/D. (The light curves represent the coefficients at particular corrected fan speeds, while the dark curve represents the average value over the test speed range. Since, in most instances, the data for individual corrected fan speeds resulted in closely bunched curves, it was not practical to label these curves with respect to RPM. The reader is directed to Appendix C for the coefficient data at a specific corrected fan speed.) The average values for the mass flow coefficients, CAF and CAT, remain relatively constant over the range of ground heights tested. The thrust coefficient is relatively constant except for the lowest height where an increase of approximately 10 percent is indicated. The thrust coefficient improvement is a result of the measured thrust increase previously discussed.

The thrust vector angle and line of thrust action generated by this arrangement of the louvered exhaust nozzle is shown in Figure 3-13. A nominal thrust vector angle, τ, of 23 degrees was measured with an average moment arm from the fan centerline of 3.3 cm.

3.1.3 LOUVERED NOZZLE PERFORMANCE IN GROUND PROXIMITY, HEMISPHERICAL HUB - The louvered nozzle with the hemispherical fan exit hub installed was tested in a similar fashion as the above described flat plate hub configuration.

The fan and turbine airflow information recorded at the five ground heights is given in Figures 3-14 and 3-15, and the corrected thrust data versus fan speed is presented in Figure 3-16.

The location of the fan operating lines on the fan map for the five ground heights is depicted in Figure 3-17. A reduction in effective nozzle exit area is indicated as was the case with the flat plate hub, however the change is not quite as large.

Figure 3-16 indicates that thrust performance was unchanged, at a constant corrected fan speed, except at the lowest height where an increase in thrust of approximately 3 percent was measured. Hub pressure information is displayed in Figure 3-18 for the hemispherical hub test runs and is similar to the flat plate data of Figure 3-11, however the change in pressure between H/D of 1.55 and 1.02 is slightly lower for the hemispherical hub geometry.

Fan exit rake coefficients for this configuration are shown in Figure 3-19 and are similar to the flat plate hub rake coefficients. The increase in thrust coefficient at H/D = 1.02 is 5 percent for the hemispherical hub, whereas 10 percent was the increment obtained with the flat plate hub.

The thrust vector angle and moment arm data recorded for the hemispherical hub geometry is shown in Figure 3-20 and again is similar to the flat plate hub information.

The effect of the fan exit hub shape on the thrust performance of the X376B/T58 nose lift unit appears to be small over the range of ground heights tested. No thrust change at and above an H/D of 1.55 was greater than 2 percent. Pressurization of the fan exit hub region was observed with both hub shapes and served to cause an increase in thrust at a ground height of H/D = 1.02. Pressure-area integration of pressure distribution on the fan hub (21 pressure taps), obtained from the Reference 6 test, yielded hub forces as shown in Figure 3-21 and represents confirmation of the hub pressurization effect at the lowest ground height.

3.1.4 LOUVERED NOZZLE PERFORMANCE IN GROUND PROXIMITY, FLAT PLATE HUB WITH YAW VANES SPLAYED - Splaying of the nose unit exhaust flow by deflecting the two yaw vanes to each side was a technique investigated on the LSPM to reduce gas generator ingestion levels. As a consequence, this nozzle configuration was included in the fan calibration test matrix.

The airflow, thrust, fan operating line, rake coefficient, thrust vector angle and moment arm test data for this configuration is shown in Figures 3-22 through 3-27. Review of the test results shows no significant variations from the results obtained with either the flat plate or hemispherical hub tests with the yaw vanes undeflected. It was expected that a 12° splay of the nozzle exit vanes would cause a decrease in gross thrust performance of the nose unit, however, if this is indeed true, the effect is within the uncertainty band of the present thrust measurement technique.

3.2 X376B/T58 LEFT LIFT/CRUISE UNIT

The tests of the left lift/cruise unit encompassed mapping of the fan with the calibration nozzles and evaluation of the vectoring nozzle performance for hood deflection angles, δ_{LC}, of 0°, 56° and 95°.

3.2.1 FAN PERFORMANCE MAP - Calibration of the left lift/cruise unit was accomplished over test runs 15 through 18. Figures 3-28 and 3-29 present the fan pressure ratio and turbine discharge pressure ratio characteristics as a function of fan speed for the four calibration nozzle exit areas. Fan airflow data versus fan speed is shown in Figure 3-30, whereas the gross thrust produced with the calibration nozzle is illustrated in Figure 3-31.

Construction of the fan map was performed and is shown in Figure 3-32. The thrust performance maps are provided in Figure 3-33. Comparison of these maps with the nose unit maps shows, as expected, good agreement in both pressure rise and thrust performance.

3.2.2 LIFT/CRUISE NOZZLE PERFORMANCE IN GROUND PROXIMITY - The effect of ground proximity on the left lift/cruise nozzle in its 95° deflected position was evaluated at the same five heights covered with the nose lift unit. The performance data set isting of airflow and thrust as a function of corrected fan speed is plotted in es 3-34 through 3-36.

Superposition of the fan operating line for each height on the fan map for this unit is shown in Figure 3-37. No relative movement of the fan operating line with ground height is indicated and is in contrast to the nose unit which exhibited back pressure effects at H/D = 1.02. It is hypothesized that this difference is a result of differences in nozzle configuration and exit flow distribution between the lift/cruise and nose units.

The fan exit rake coefficient variation with ground height is shown in Figure 3-38. The data used to make-up this figure may be found in Appendix C.

3.2.3 LIFT/CRUISE NOZZLE VECTOR PERFORMANCE - The change in fan and nozzle performance with lift/cruise nozzle deflection angle was evaluated out of ground effect. Figures 3-39 through 3-41 depict the fan and gas generator mass flow and thrust characteristics as a function of fan speed for hood deflection angles of 0° and 56°.

Fan exit rake coefficient, thrust vector angle, and moment arm information is shown in Figures 3-42 and 3-43. The general effect of increasing hood deflection angle on gross thrust is slight. A nominal thrust level of 5600 newtons was measured at 3600 RPM for each of the three vector positions.

3.3 X376B/T58 RIGHT LIFT/CRUISE UNIT

Testing of the right lift/cruise unit was confined to evaluation of the unit in ground effect. Mapping was not carried out due to program scope limitations. An additional ground height at H/D = 2.0 was included in the test runs on this unit.

The results of the ground effects testing of the right lift/cruise unit are shown in Figures 3-44 through 3-46.

The fan exit rake coefficients for the right lift/cruise unit are provided in Figure 3-47. The average values remain relatively constant with respect to H/D, although the thrust coefficient shows a drop in value of approximately 4 percent from H/D = 2.0 to 1.02.

The thrust vector angle and moment arm characteristics for the right unit are given in Figure 3-48.

3.4 LF336/J85 NOSE LIFT UNIT

Testing of the LF336/J85 turbotip fan unit was included in the test program primarily to establish the effects of higher fan pressure ratio on the ground height characteristics of the LSPM louvered nozzle. It was expected that the hub pressurization effect would be a function of fan total pressure. The LF336/J85 fan system has a design pressure ratio of 1.3 compared to 1.08 for the X376B/T58 units and possesses an exit geometry compatible with the LSPM louvered nozzle.

The test of the LF336/J85 system included both fan mapping and ground effects runs with the louvered lift nozzle at H/D values of ∞, 6.45, 2.55 and 1.55. Data at H/D equal to 1.02 was not obtained so that testing could be focused on the units of primary importance: the three X376B/T58 LSPM units.

3.4.1 FAN PERFORMANCE MAP - Calibration of the LF336/J85 unit was accomplished over test runs 1-3 using three of the four calibration nozzle areas. Fan pressure ratio and turbine discharge pressure ratio as a function of fan speed is presented in Figures 3-49 and 3-50. Unlike the X376B/T58 fan units a sizeable difference in fan and turbine pressure ratio exists on this unit. Fan and gas generator airflow information is given in Figure 3-51 and the measured thrust data is provided in Figure 3-52. Operation of this fan unit was restricted to speeds of 90 percent and below due to minor tip turbine bucket damage, and as a consequence, the full design point performance of this fan could not be utilized.

The fan map for the LF336 fan is shown in Figure 3-53, whereas the thrust maps as a function of fan and total corrected flow are given in Figure 3-54. These performance maps compare closely with test results obtained during a previous nozzle test program described in Reference 7.

3.4.2 LOUVERED NOZZLE PERFORMANCE IN GROUND PROXIMTIY - Tests of the louvered nozzle with the LF336/J85 were conducted with a hemispherical exit hub installed, with the louvers set at 95°, and with yaw vanes undeflected.

Figures 3-55 through 3-58 show the airflow and thrust data recorded at the four ground heights. Figure 3-59 illustrates the location of operating lines on the fan map for each ground height. As was observed with the X376B/T58 louvered nozzle test, no change in the operating line is indicated for H/D = 1.55 and above.

The fan exit rake coefficients were also calculated for this fan and are illustrated in Figure 3-60 as a function of ground height. No significant change in either thrust or flow coefficients is indicated. This same result was obtained with the X376B/T58 unit (down to an H/D = 1.55), consequently, it is concluded that the effect of fan pressure ratio changes on the performance of the nose nozzle in ground proximity is negligible for the range of pressure ratio and ground heights covered here. It is noted that turbine mass flow coefficient, CAT, for this unit is greater than 1.0. This result implies that all of the gas generator flow did not pass through the annular tip turbine exhaust duct. Flow leakage from the tip turbine section into the fan duct at the gas seal location (see Figure 2-2) is possible on this unit and is the probable reason for the turbine flow coefficient to have a value above 1.0.

FIGURE 3-1

X376B/T58 NOSE LIFT UNIT PRESSURE RATIO CHARACTERISTICS
FAN PRESSURE RATIO vs FAN SPEED
Calibration Nozzle

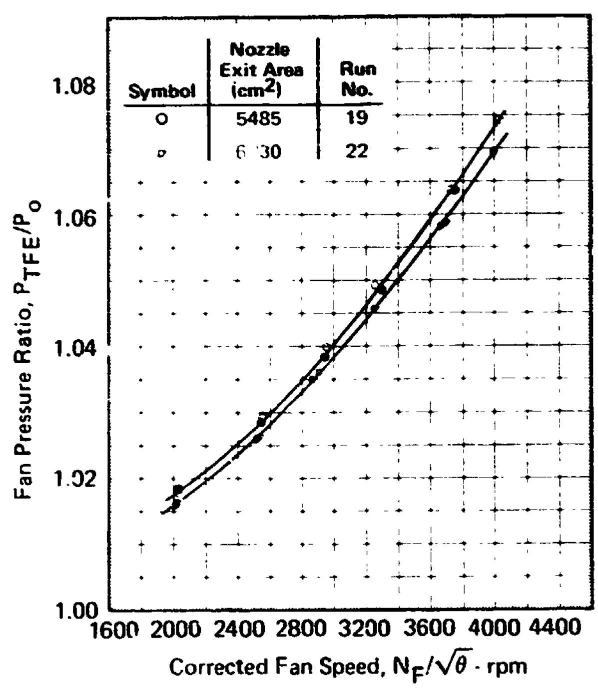

GP78-1188-15

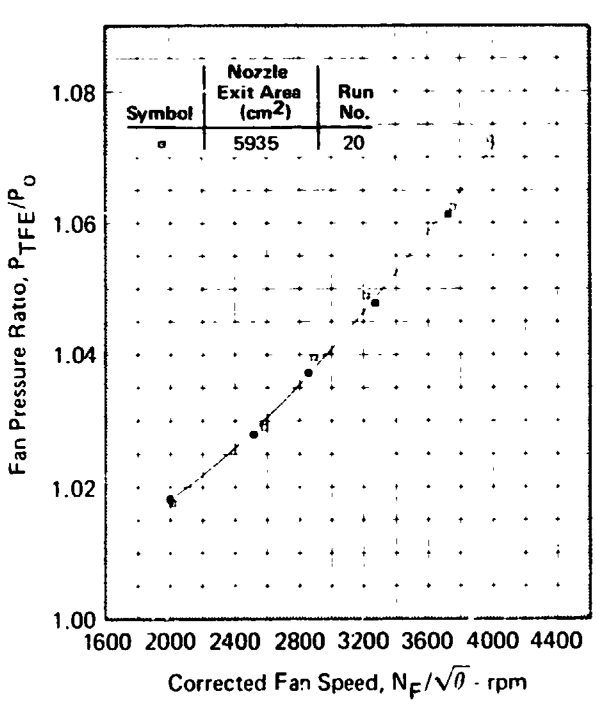

GP78 1188 16

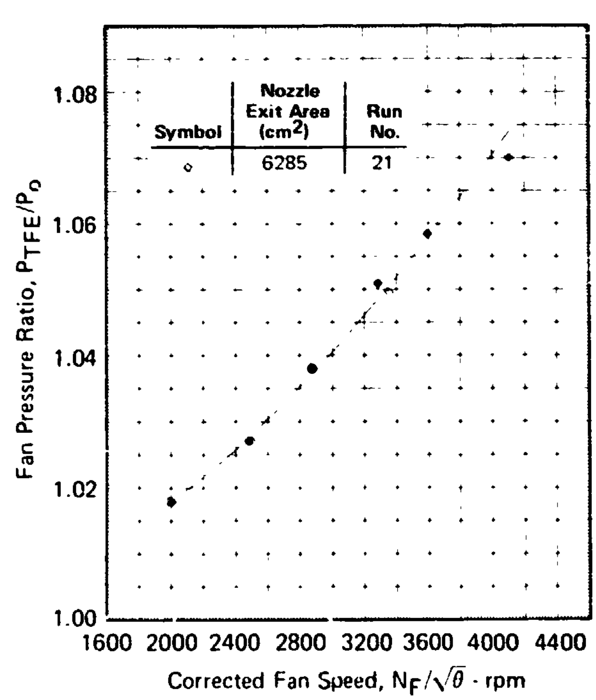

GP78 1188 12

FIGURE 3-2
X376B/T58 NOSE LIFT UNIT PRESSURE RATIO CHARACTERISTICS
TURBINE PRESSURE RATIO vs FAN SPEED
Calibration Nozzle

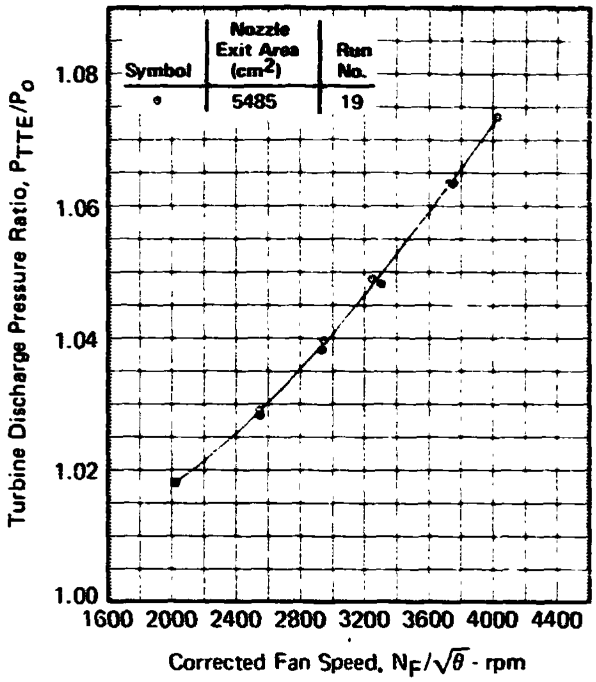

GP78-1188-13

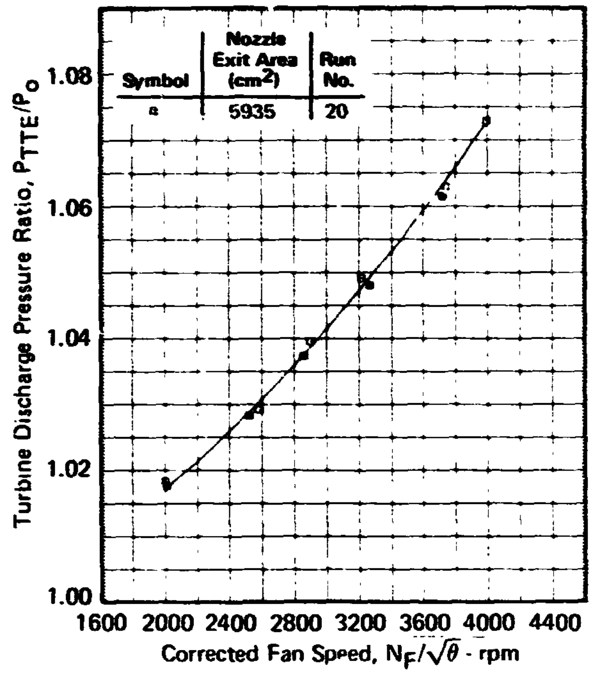

GP78-1188-11

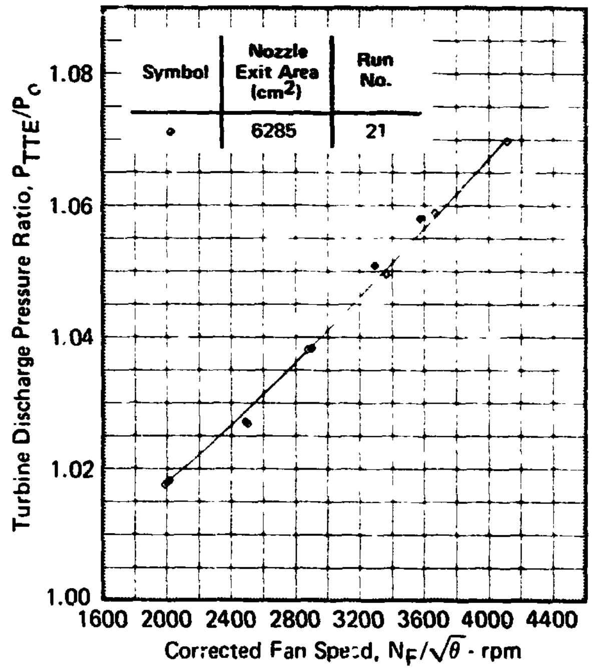

GP7P 1188 10

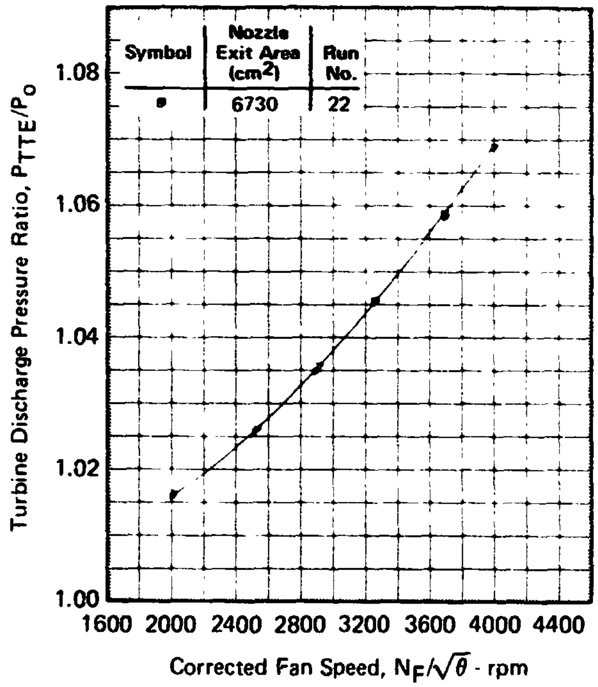

GP78-1188 9

FIGURE 3-3
X376B/T58 NOSE LIFT UNIT AIRFLOW CHARACTERISTICS
AIRFLOW vs FAN SPEED
Calibration Nozzles

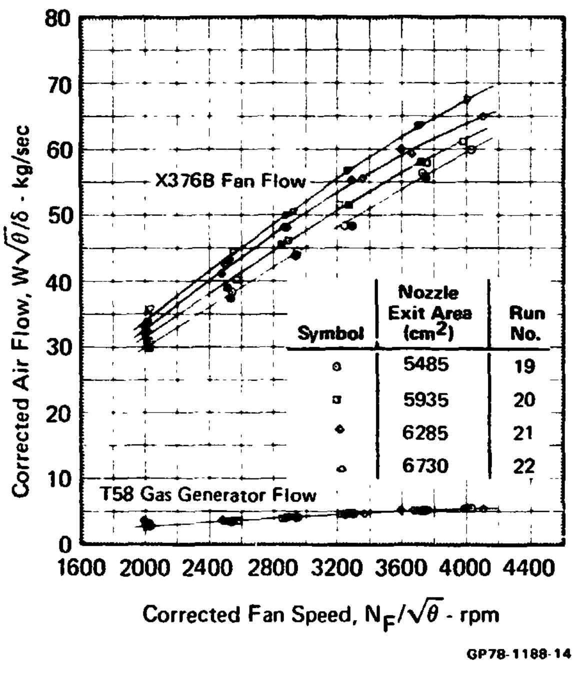

FIGURE 3-4
X376B/T58 NOSE LIFT UNIT CALIBRATION NOZZLE PERFORMANCE
THRUST vs FAN SPEED

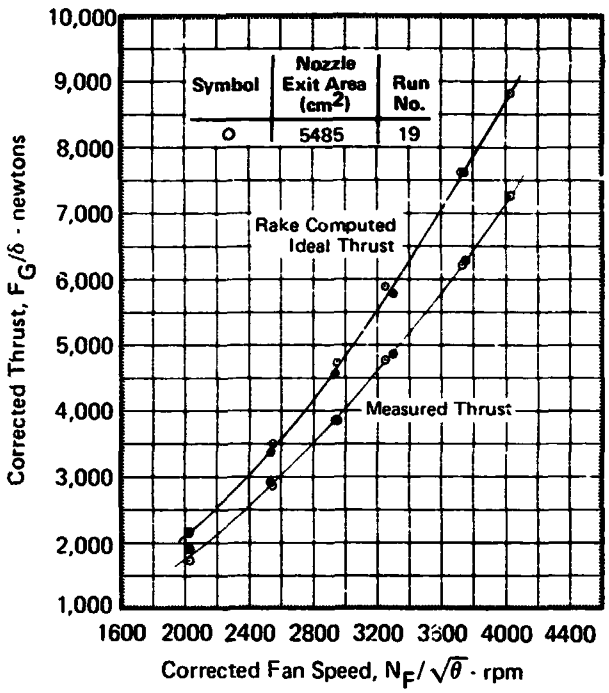

GP78-1188-119

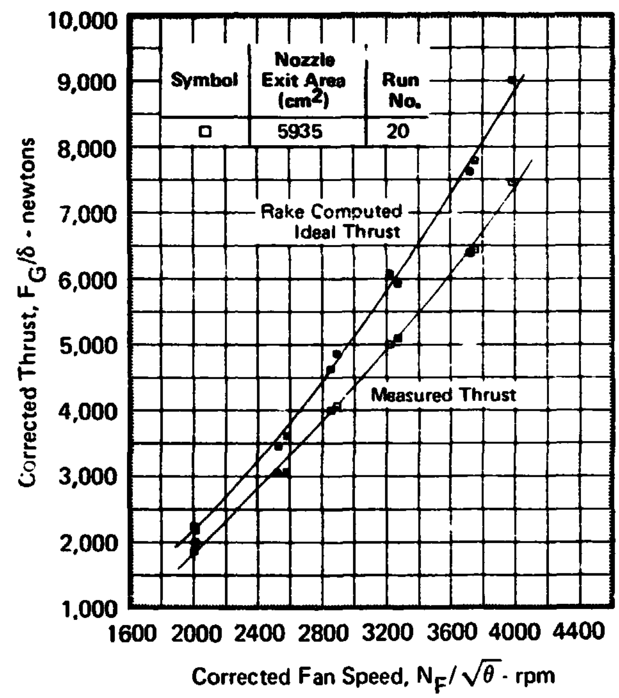

GP78-1188-121

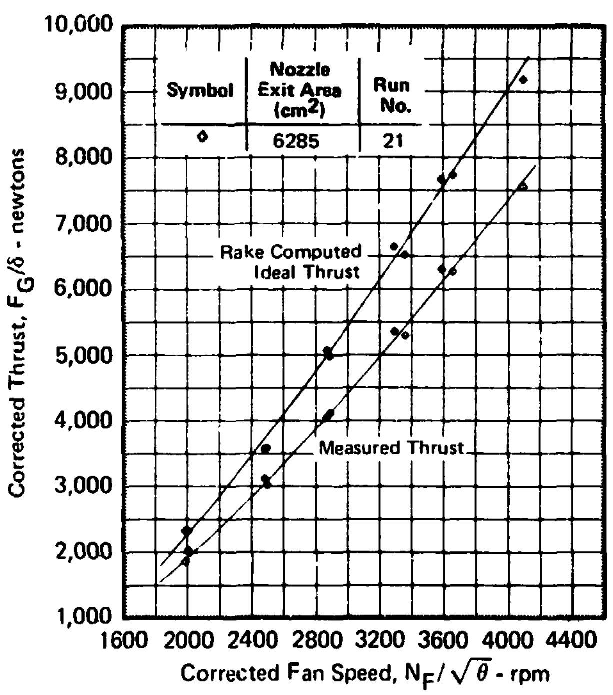

GP78-1188-120

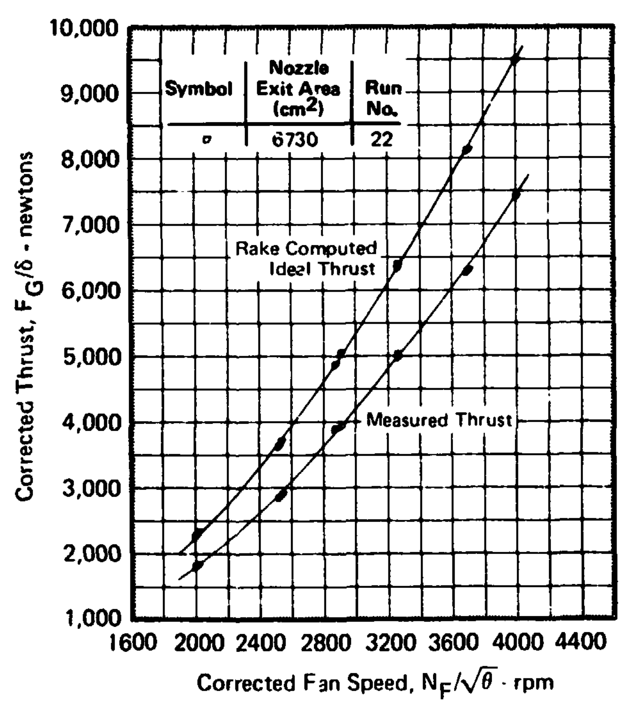

GP78 1188-114

FIGURE 3-5
X376B/T58 NOSE LIFT UNIT FAN MAP CHARACTERISTICS
Calibration Nozzles

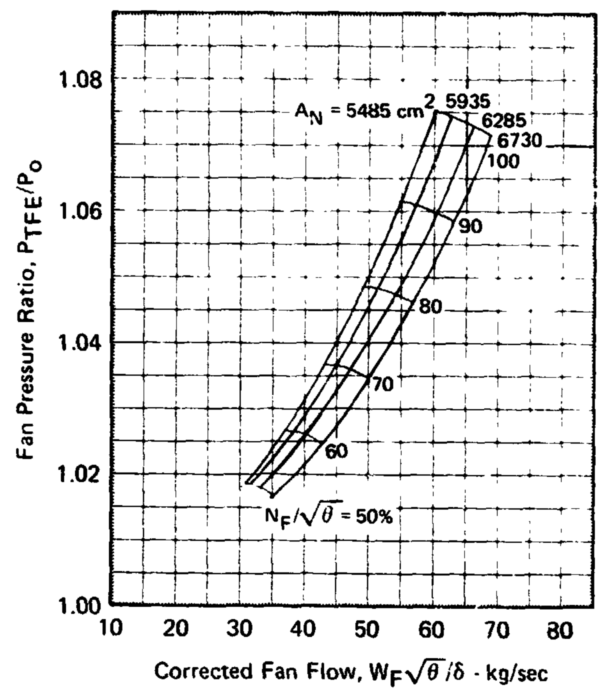

GP78-1188-8

FIGURE 3-6
X376B/T58 NOSE LIFT UNIT PERFORMANCE MAP
THRUST vs FAN FLOW, TOTAL FLOW
Calibration Nozzles

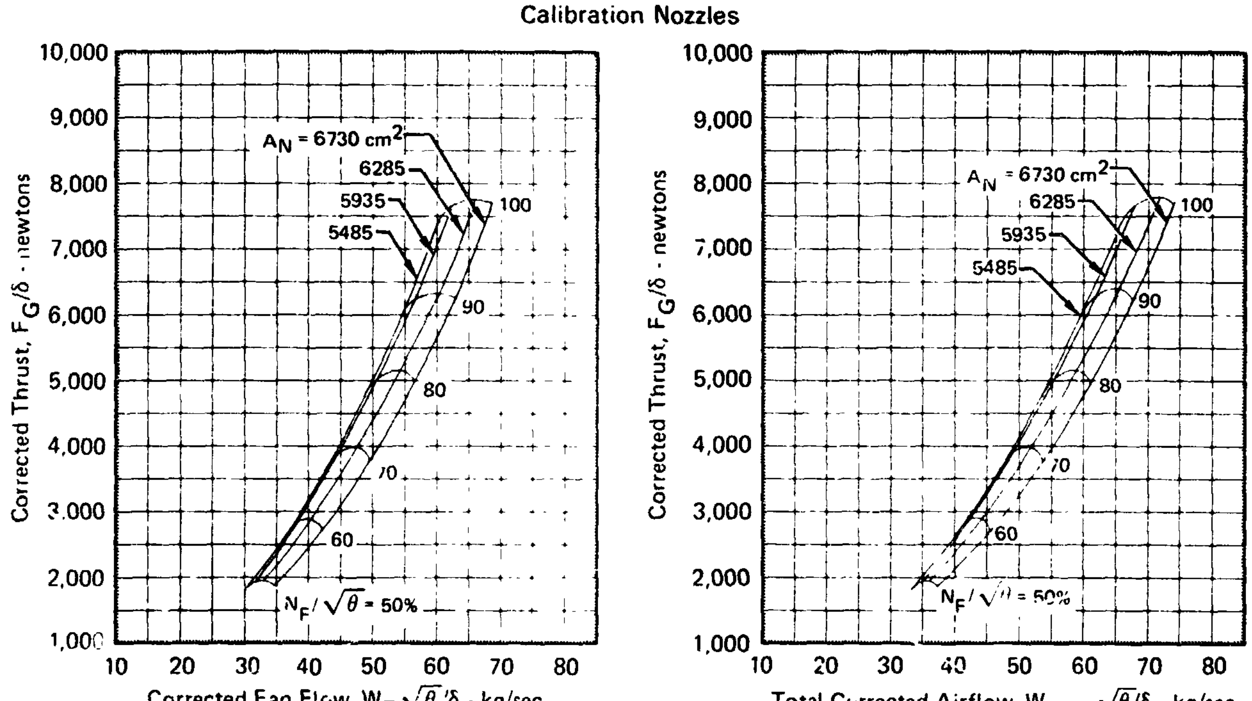

GP78-1188-122

GP78-1188-123

FIGURE 3-7
X376B/T58 NOSE LIFT UNIT PERFORMANCE IN GROUND EFFECT
FAN FLOW vs FAN SPEED

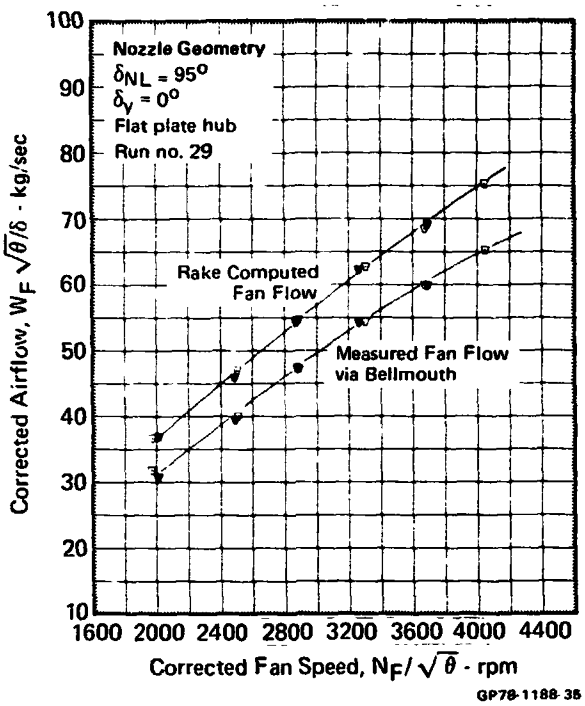

H/D = ∞

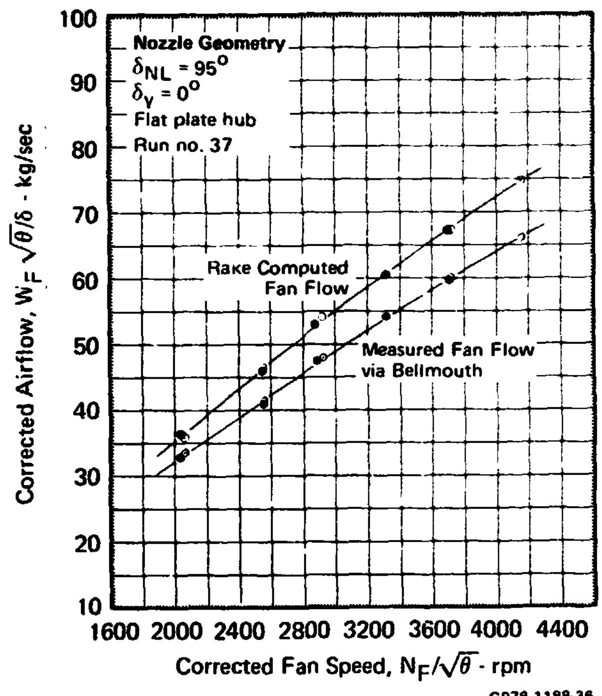

H/D = 6.45

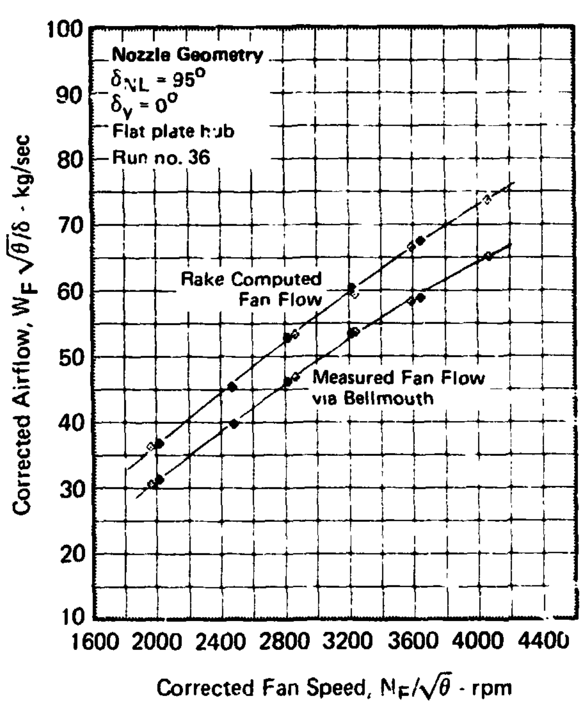

H/D = 2.55

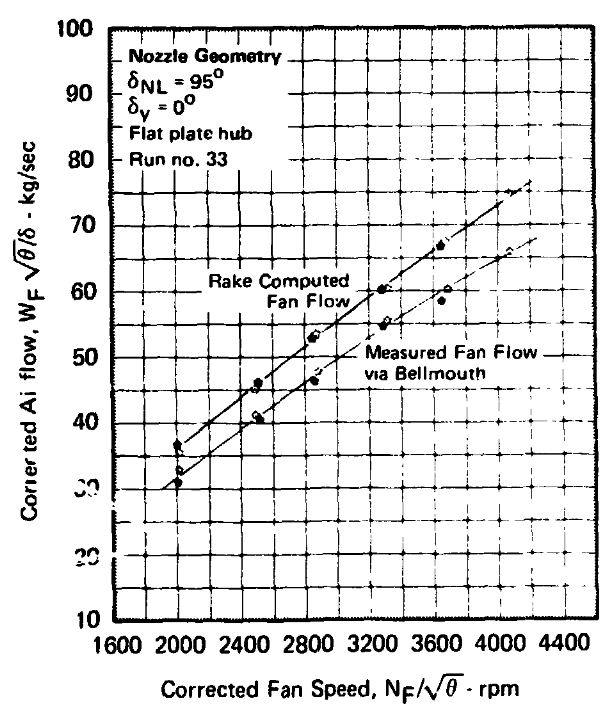

H/D = 1.55

FIGURE 3-7 (Continued)
X376B/T58 NOSE LIFT UNIT PERFORMANCE IN GROUND EFFECT
FAN FLOW vs FAN SPEED
H/D = 1.02

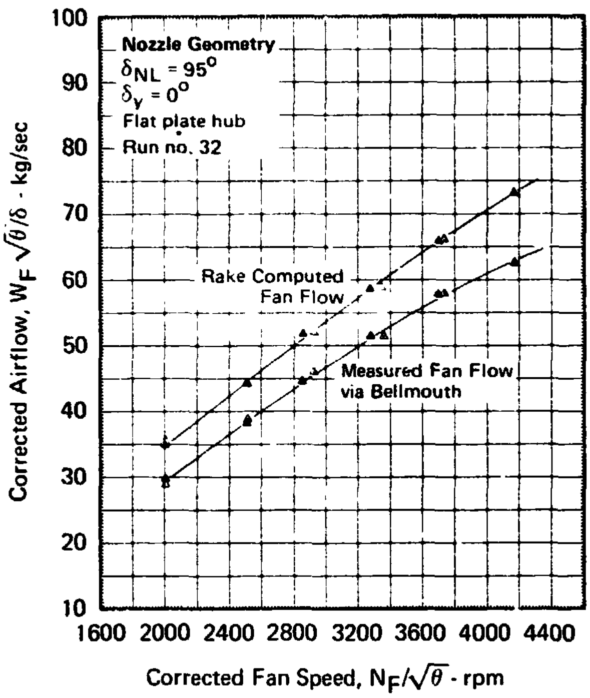

FIGURE 3-8
X376B/T58 NOSE LIFT UNIT PERFORMANCE IN GROUND EFFECT
TURBINE FLOW vs FAN SPEED
δ_{NL} = 95° δ_y = 0° Flat Plate Hub
H/D = ∞, 6.45, 2.55, 1.55, 1.02

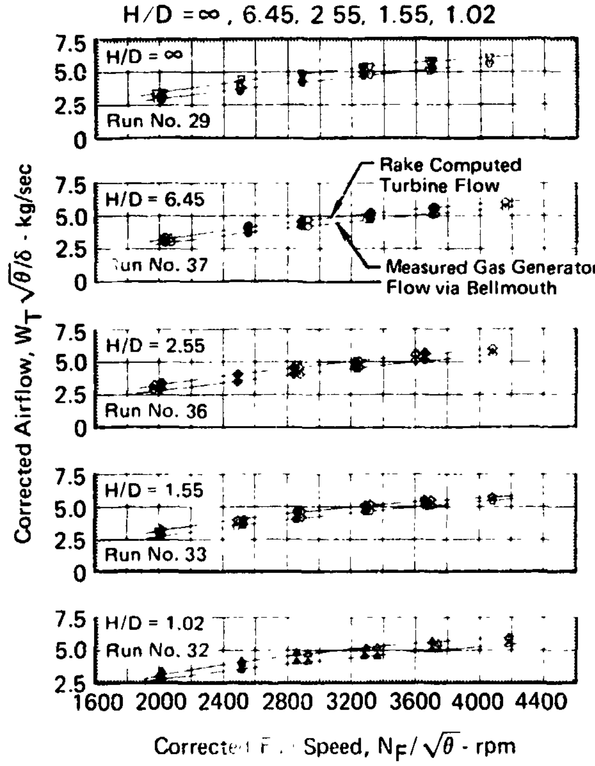

FIGURE 3-9
X376B/T58 NOSE LIFT UNIT PERFORMANCE IN GROUND EFFECT
THRUST vs FAN SPEED

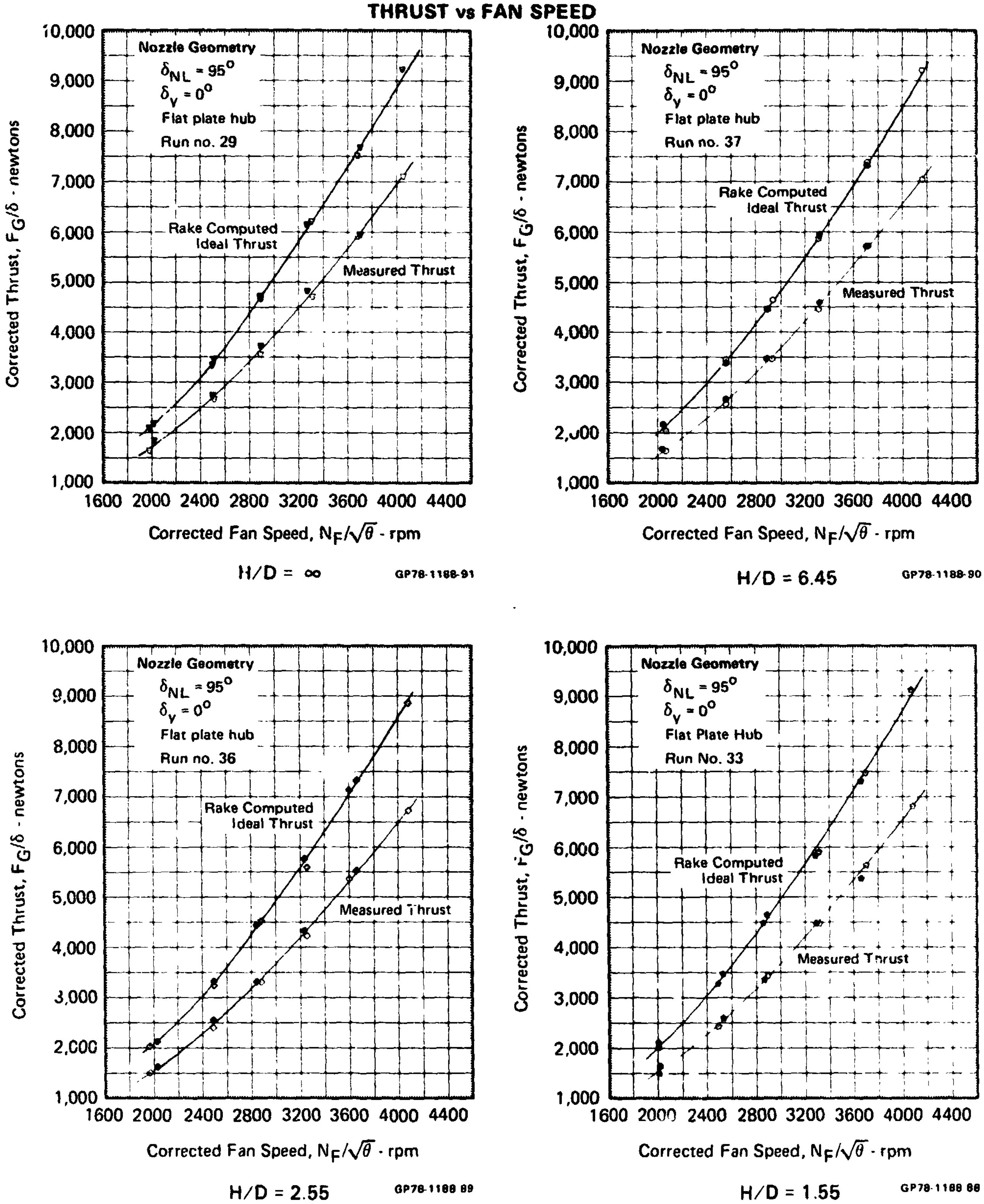

FIGURE 3-9 (Continued)
X376B/T58 NOSE LIFT UNIT PERFORMANCE IN GROUND EFFECT THRUST vs FAN SPEED
H/D = 1.02

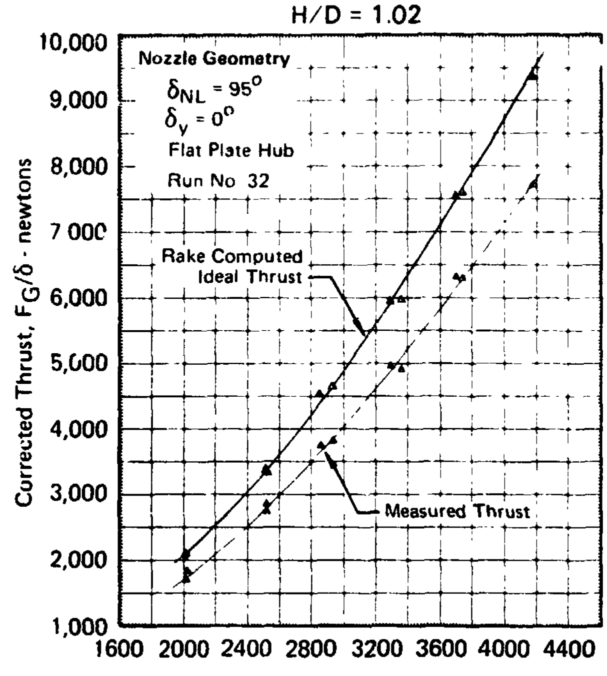

GP78 1188 87

FIGURE 3-10
X376B/T58 NOSE LIFT UNIT FAN PERFORMANCE IN GROUND EFFECT
Louvered Lift Nozzle

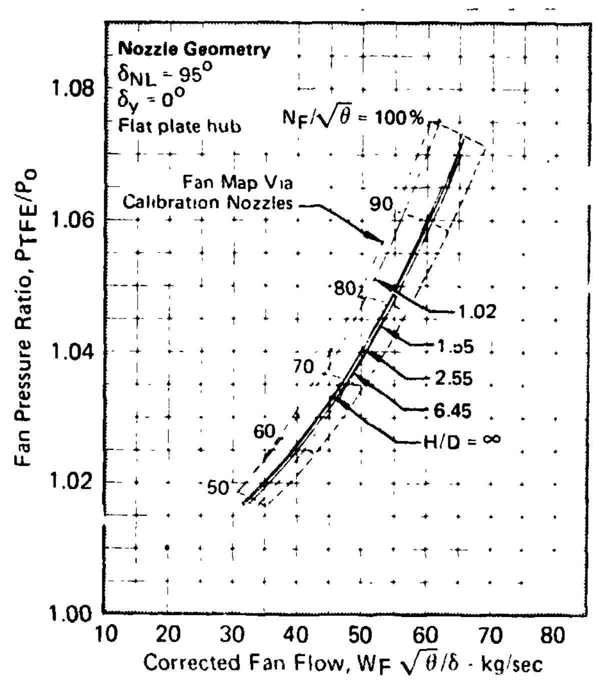

GP78 1188 6

FIGURE 3-11
X376B/T58 NOSE LIFT UNIT
EXIT HUB PRESSURE DATA
FLAT PLATE HUB
δ_{NL} = 95° δ_Y = 0°

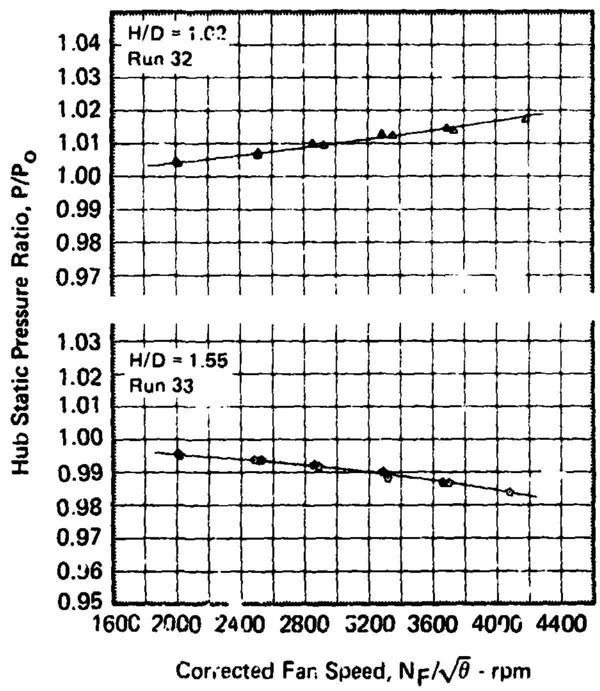

FIGURE 3-12
X376B/T58 NOSE LIFT UNIT EXIT RAKE COEFFICIENTS
δ_{NL} = 95° δ_Y = 0°   Flat Plate Hub

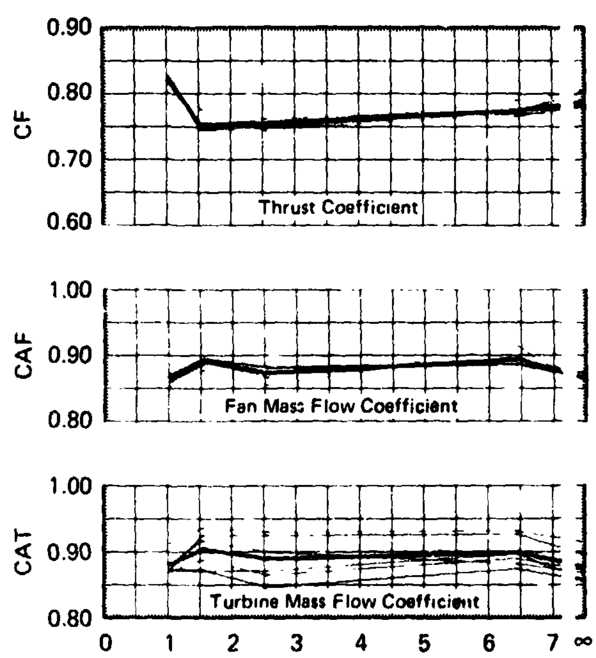

FIGURE 3-13
X376B/T58 NOSE LIFT UNIT THRUST VECTOR ANGLE AND MOMENT ARM CHARACTERISTICS
H/D = ∞

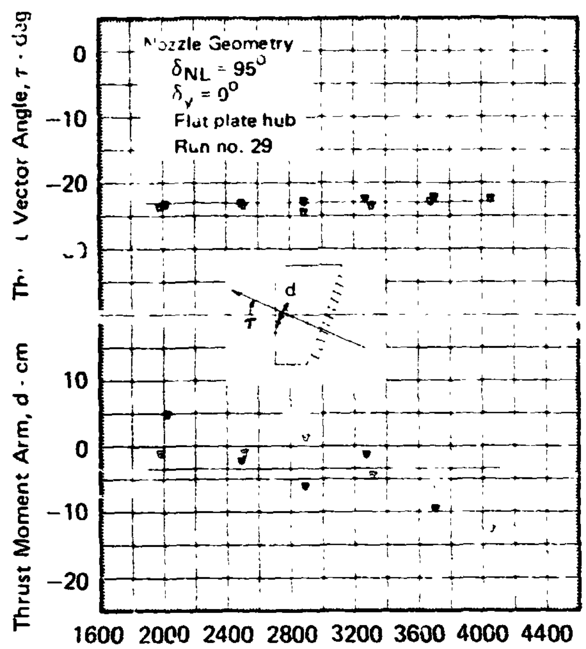

GP78-1188 126

FIGURE 3-14
X376B/T58 NOSE LIFT UNIT PERFORMANCE IN GROUND EFFECT FAN FLOW vs FAN SPEED
H/D = ∞

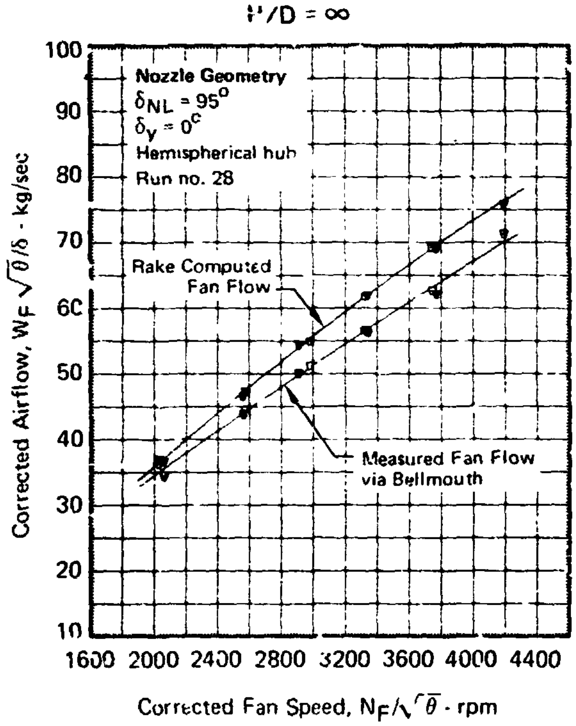

GP78 1183-66

FIGURE 3-14 (Continued)
X376B/T58 NOSE LIFT UNIT PERFORMANCE IN GROUND EFFECT
FAN FLOW vs FAN SPEED

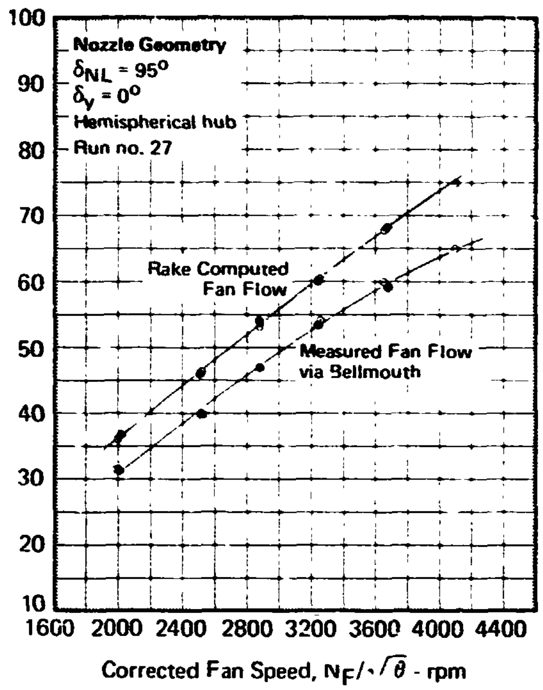

GP78 1188-45

H/D = 6.45

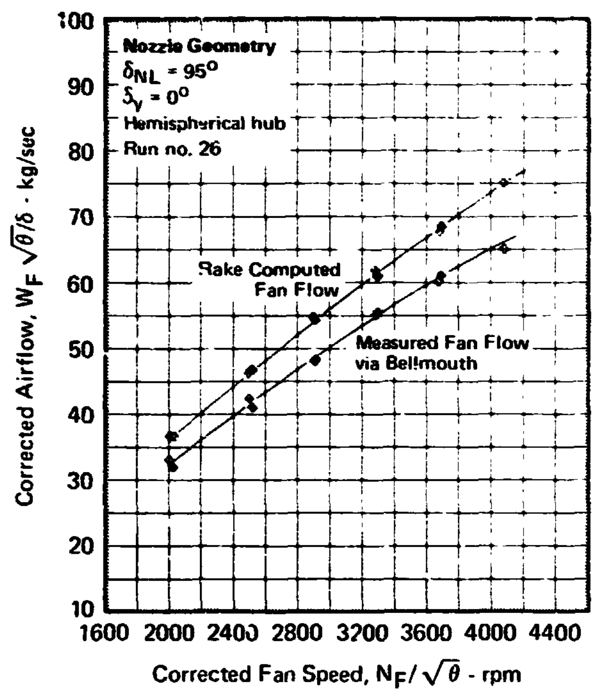

GP78-1188-46

H/D = 2.55

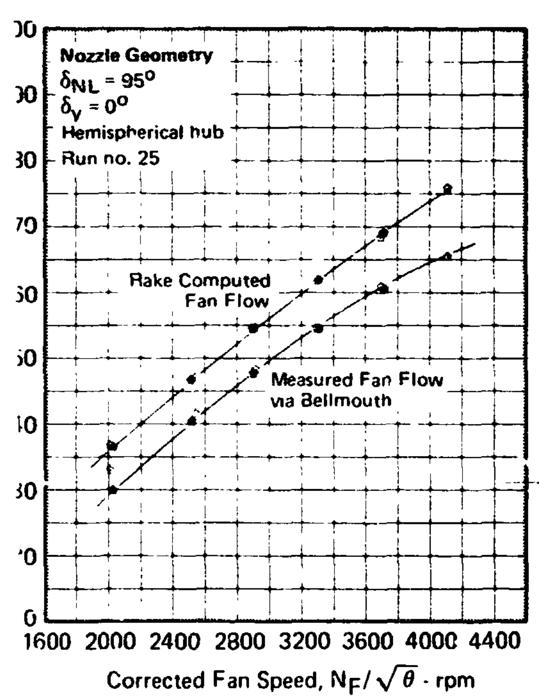

GP78 1188 47

H/D = 1.55

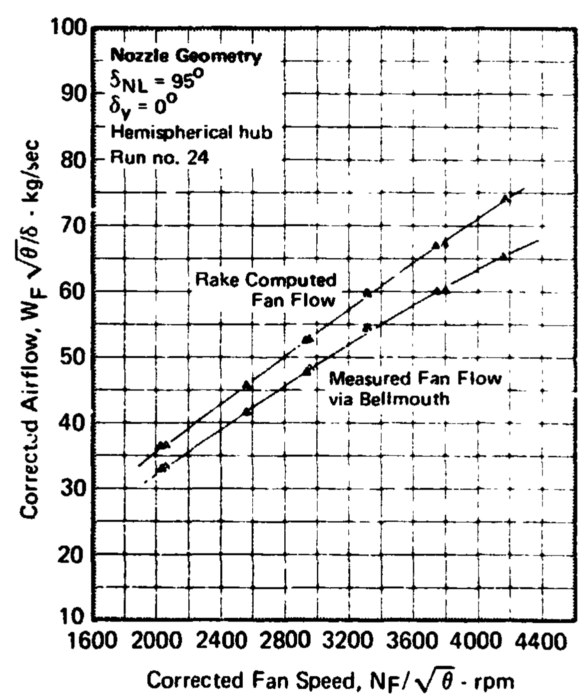

GP78-1188-48

H/D = 1.02

FIGURE 3-15
X376B/T58 NOSE LIFT UNIT PERFORMANCE IN GROUND EFFECT
TURBINE FLOW vs FAN SPEED

δ_{NL} = 95 δ_{v} = 0° Hemispherical Hub
H/D = ∞, 6.45, 2.55, 1.55, 1.02

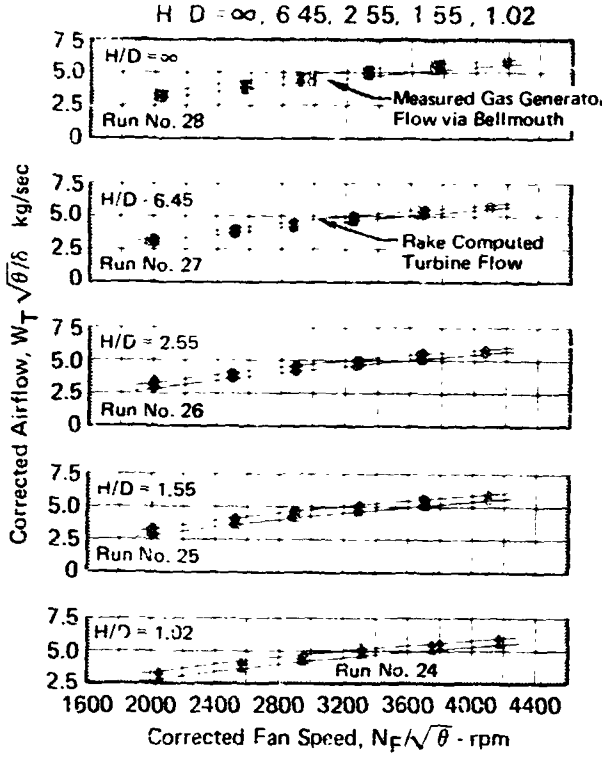

GP78-1188-60

FIGURE 3-16
X376B/T58 NOSE LIFT UNIT PERFORMANCE IN GROUND EFFECT
THRUST vs FAN SPEED
H/D = ∞

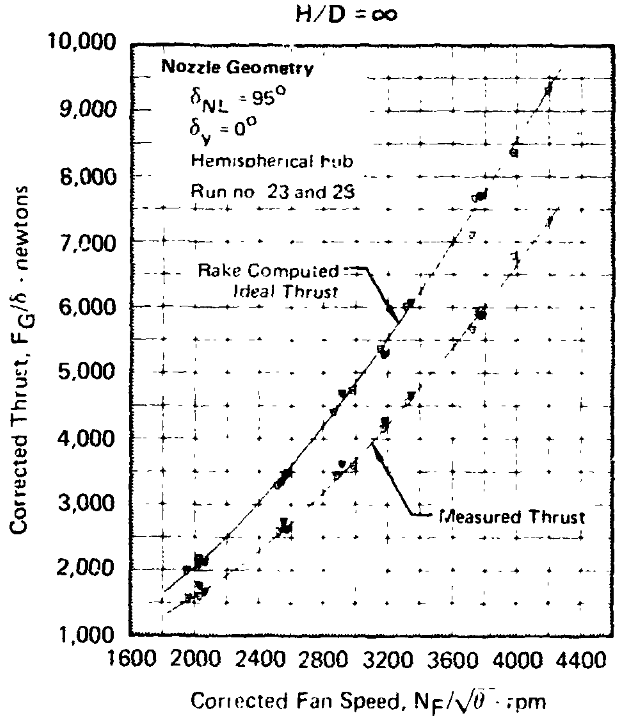

GP78 1183 92

FIGURE 3-16 (Continued)
X376B/T58 NOSE LIFT UNIT PERFORMANCE IN GROUND EFFECT
THRUST vs FAN SPEED

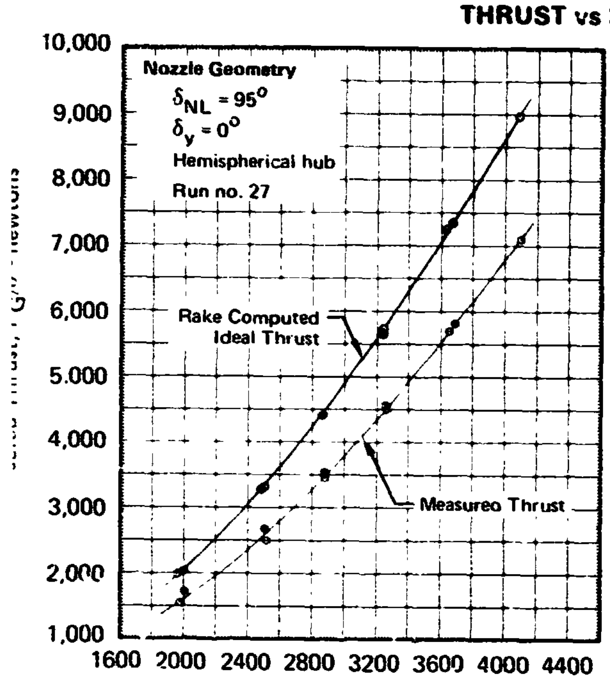

H/D = 6.45

GP78-1188-93

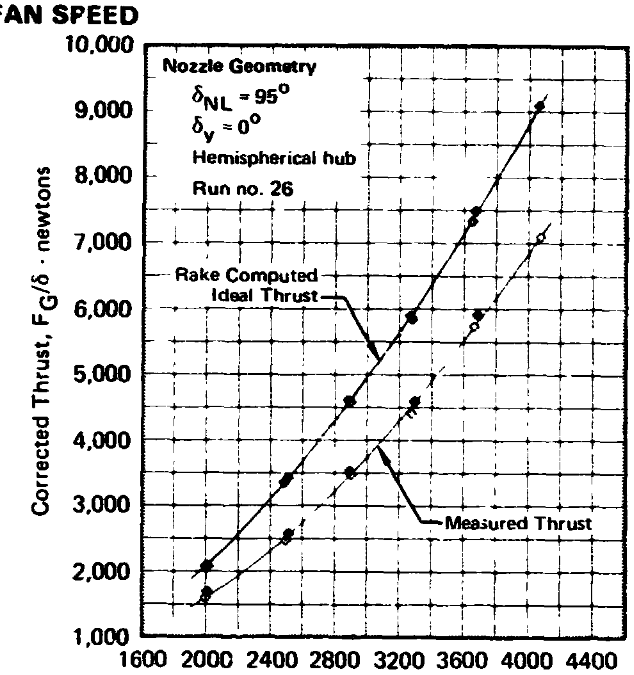

GP78-1188-94

H/D = 2.55

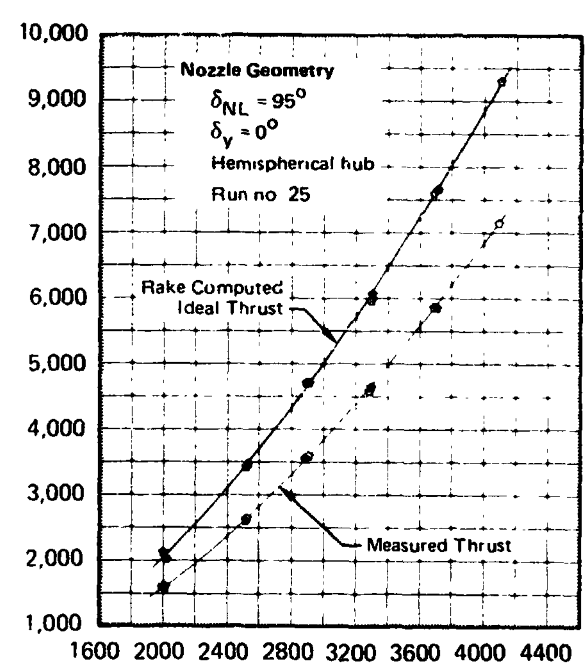

GP78-1188-95

H/D = 1.55

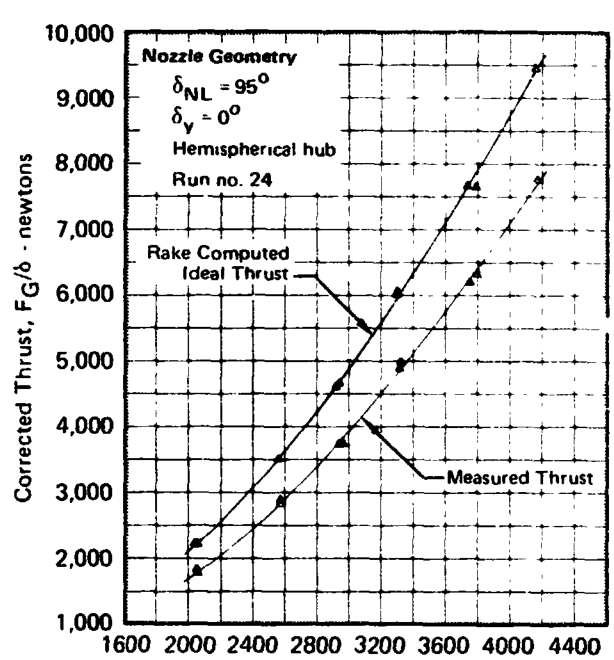

GP78 1188 96

H/D = 1.02

ORIGINAL PAGE IS OF POOR QUALITY

FIGURE 3-17
X376B/T58 NOSE LIFT UNIT FAN PERFORMANCE
IN GROUND EFFECT
Louvered Lift Nozzle

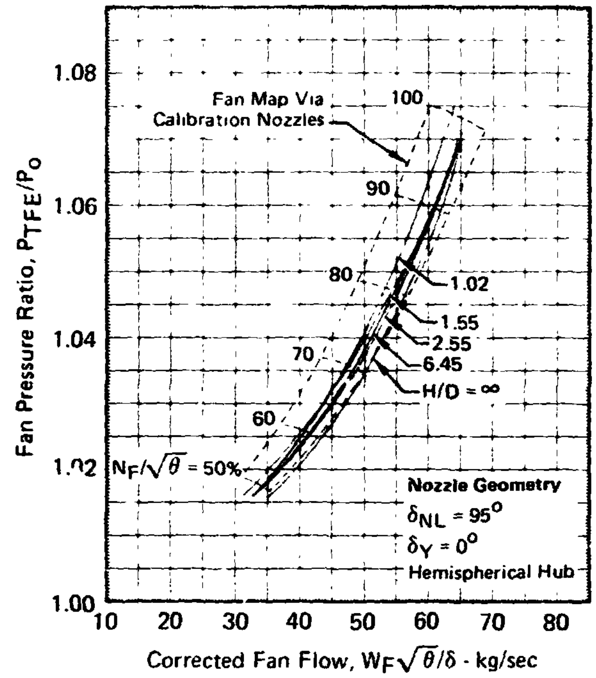

GP78-1188-7

FIGURE 3-18
X376B/T58 NOSE LIFT UNIT
EXIT HUB PRESSURE DATA
HEMISPHERICAL HUB
δ_{NL} = 95° δ_Y = 0°

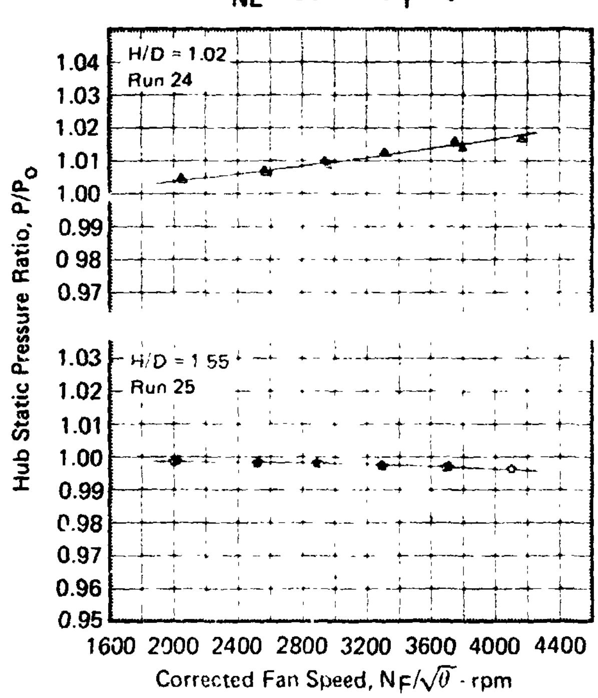

GP78-1188-147

FIGURE 3-19
X376B/T58 NOSE LIFT UNIT EXIT RAKE COEFFICIENTS
$\delta_{NL} = 95°$ $\delta_y = 0°$ Hemispherical Hub

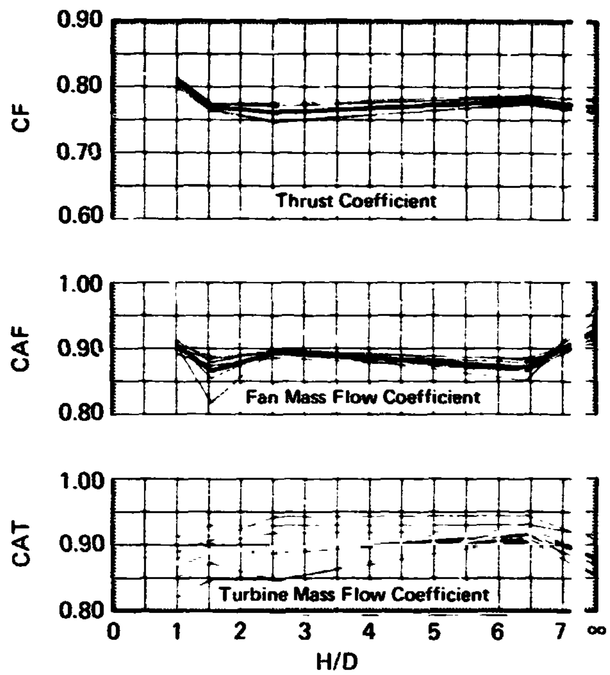

GP78-1188-82

FIGURE 3-20
X376B/T58 NOSE LIFT UNIT THRUST VECTOR ANGLE AND MOMENT ARM CHARACTERISTICS
$H/D = \infty$

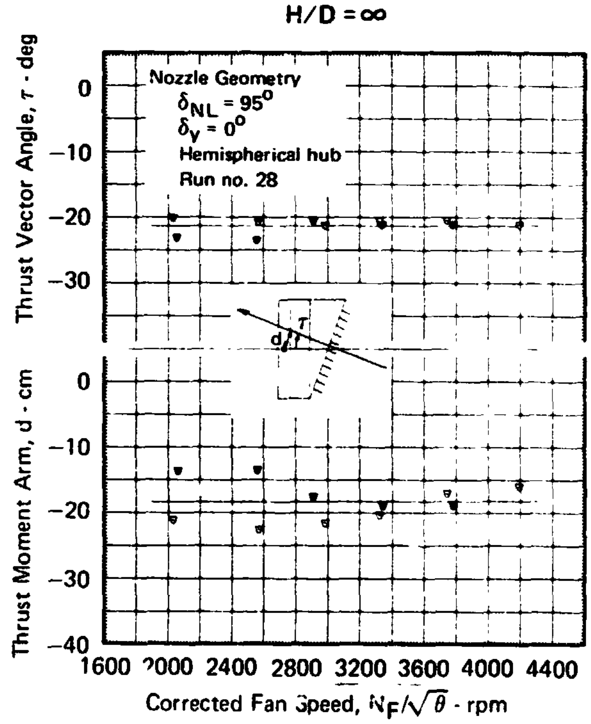

GP78-1188-129

FIGURE 3-21
X376B/T58 NOSE LIFT UNIT
FAN EXIT HUB FORCES

$N_F/\sqrt{\theta}$ = 3600 rpm

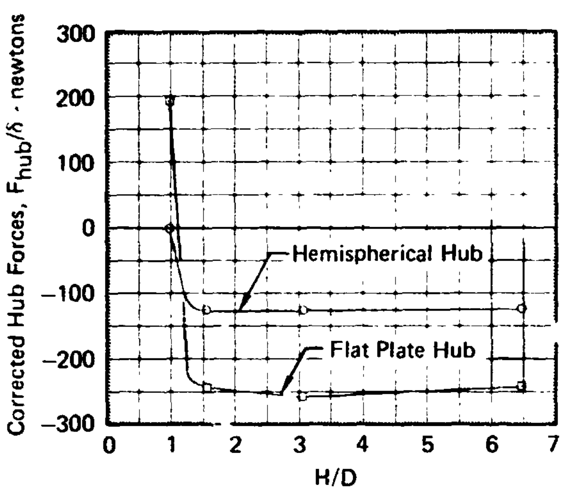

GP78-1188-146

FIGURE 3-22
X376B/T58 NOSE LIFT UNIT PERFORMANCE IN GROUND EFFECT
FAN FLOW vs FAN SPEED

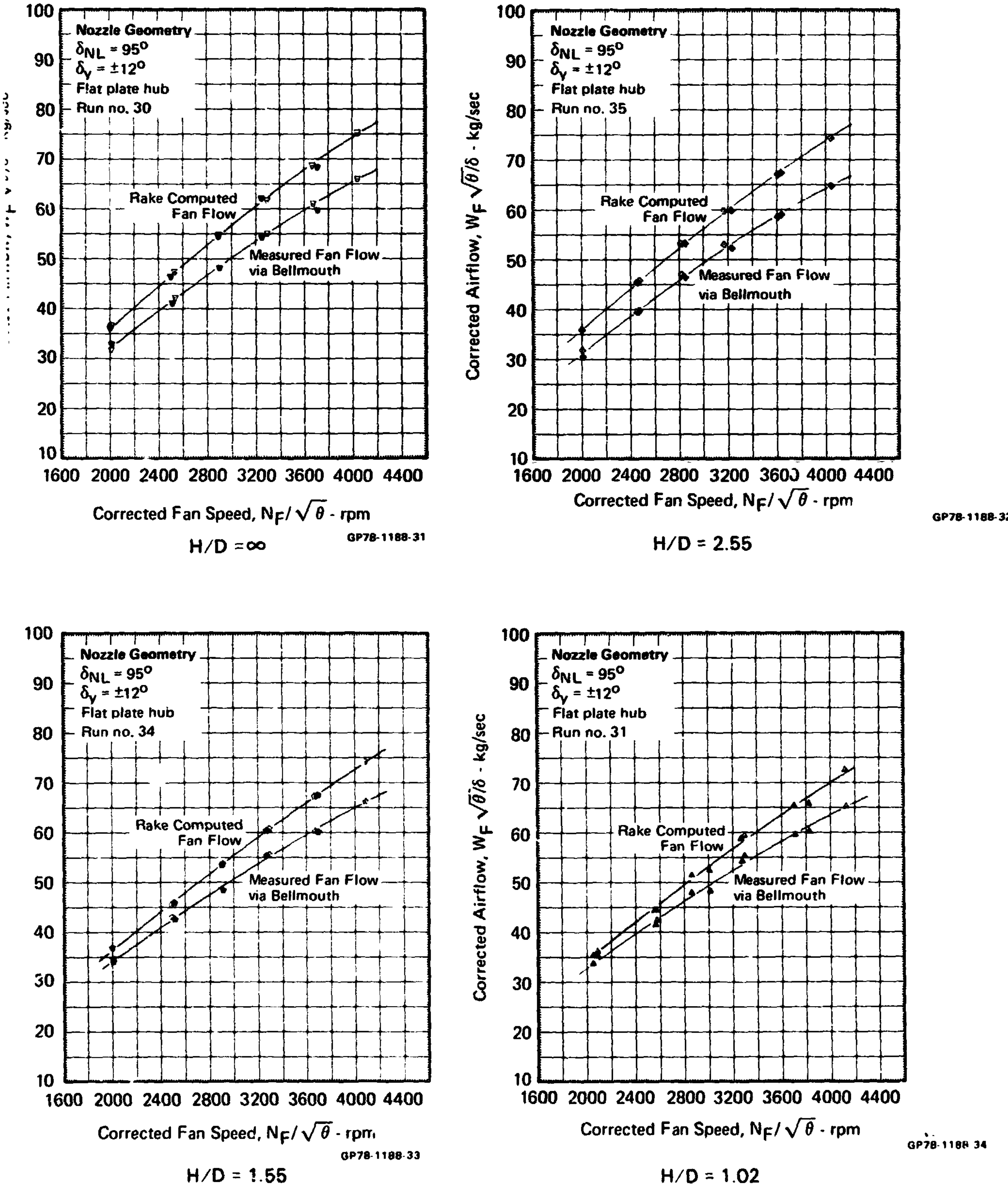

FIGURE 3-23
X376B/T58 NOSE LIFT UNIT PERFORMANCE IN GROUND EFFECT
TURBINE FLOW vs FAN SPEED
$\delta_{NL} = 95°$ $\delta_y = \pm 12°$ Flat Plate Hub
H/D = ∞, 2.55, 1.55, 1.02

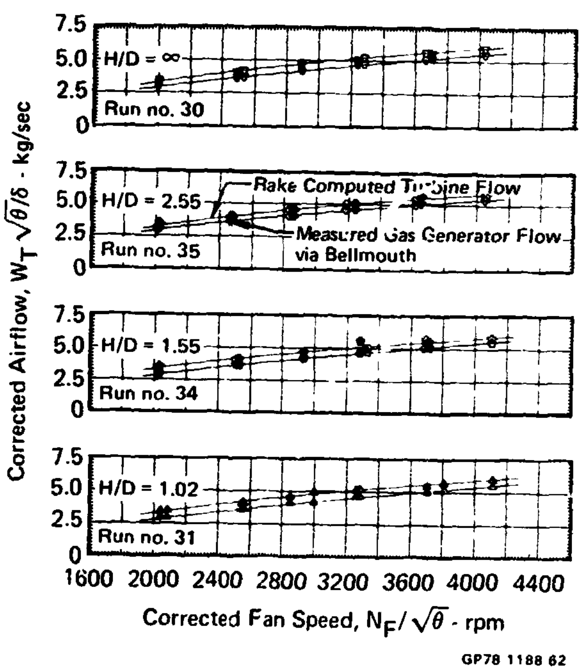

FIGURE 3-24
X376B/T58 NOSE LIFT UNIT PERFORMANCE IN GROUND EFFECT
THRUST vs FAN SPEED

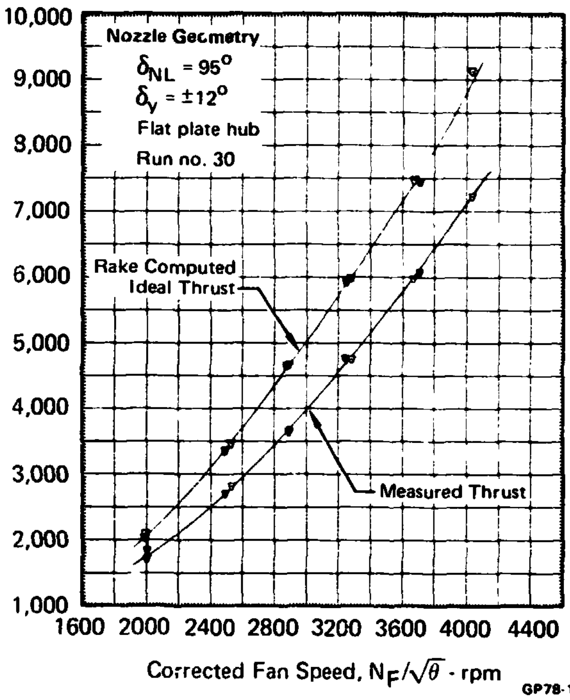

GP78-1188-100

H/D = ∞

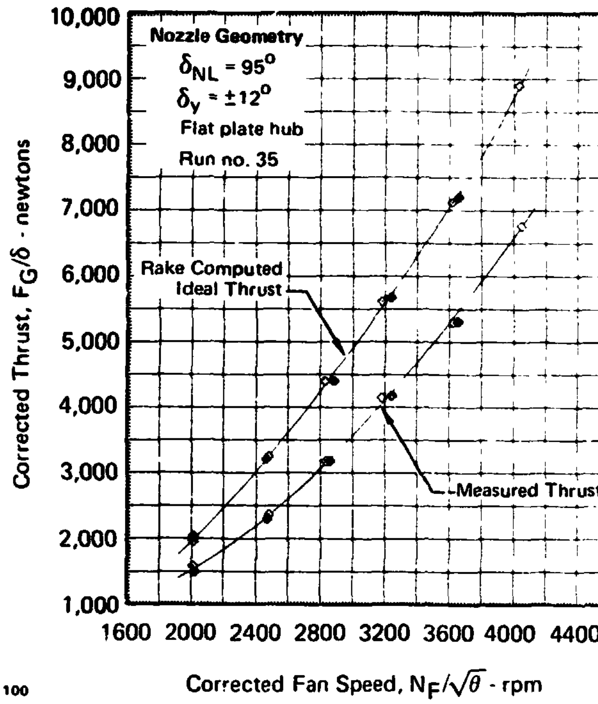

GP78-1188-99

H/D = 2.55

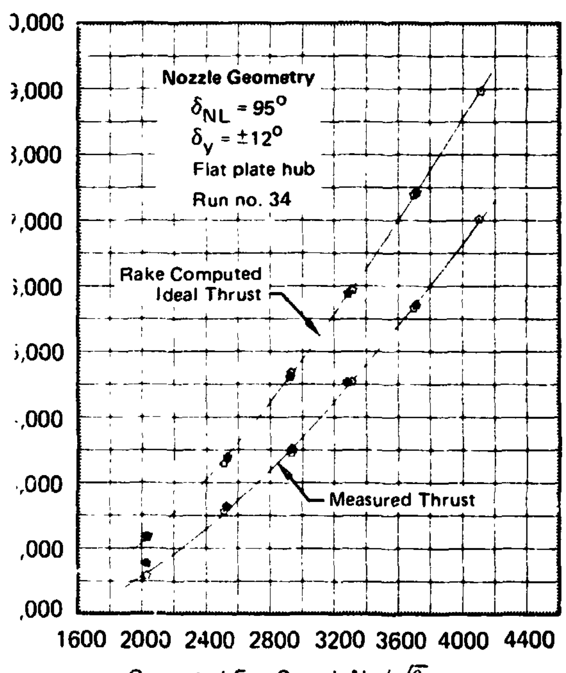

GP78-1188-98

H/D = 1.55

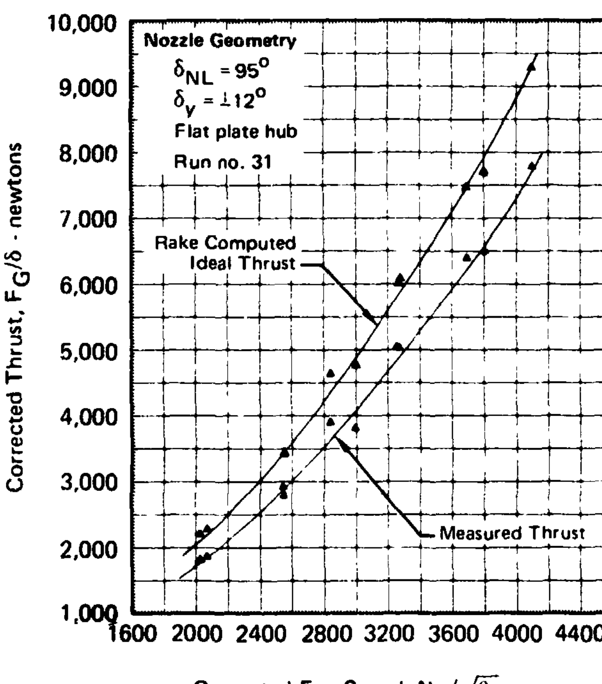

GP78-1188-97

H/D = 1.02

FIGURE 3-25
X376B/T58 NOSE LIFT UNIT FAN PERFORMANCE IN GROUND EFFECT
Louvered Lift Nozzle

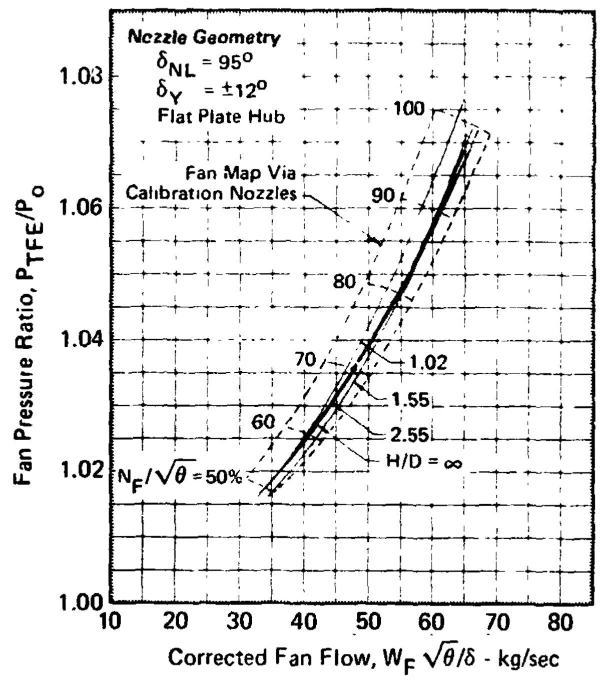

GP78-1188-18

FIGURE 3-26
X376B/T58 NOSE LIFT UNIT EXIT RAKE COEFFICIENTS
δ_{NL} = 95° δ_y = ±12° Flat Plate Hub

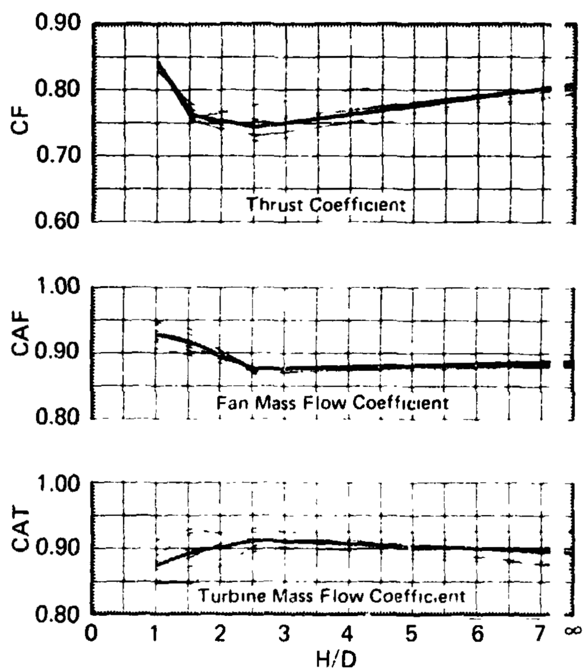

GP78 1188 86

FIGURE 3-27
X376B/T58 NOSE LIFT UNIT THRUST VECTOR ANGLE AND MOMENT ARM CHARACTERISTICS
H/D = ∞

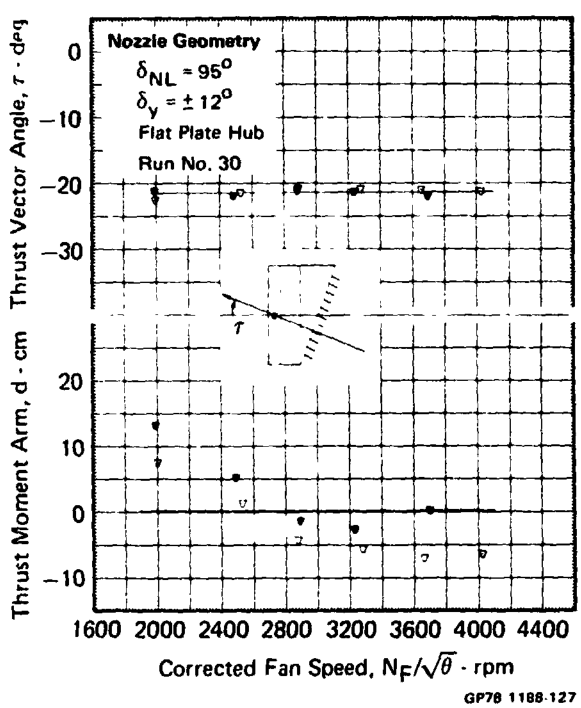

FIGURE 3-28
X376B/T58 LEFT LIFT/CRUISE UNIT PRESSURE RATIO CHARACTERISTICS
FAN PRESSURE RATIO vs FAN SPEED
Calibration Nozzles

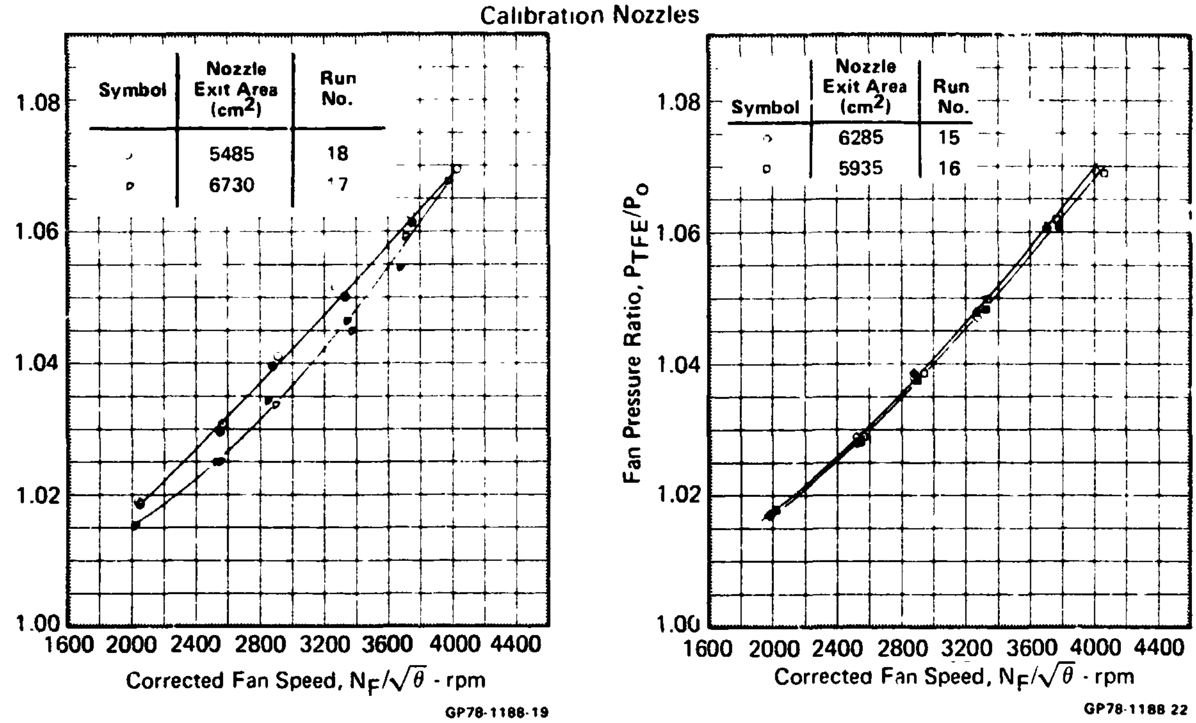

FIGURE 3-29
X376B/T58 LEFT LIFT/CRUISE UNIT PRESSURE RATIO CHARACTERISTICS
TURBINE PRESSURE RATIO vs FAN SPEED
Calibration Nozzles

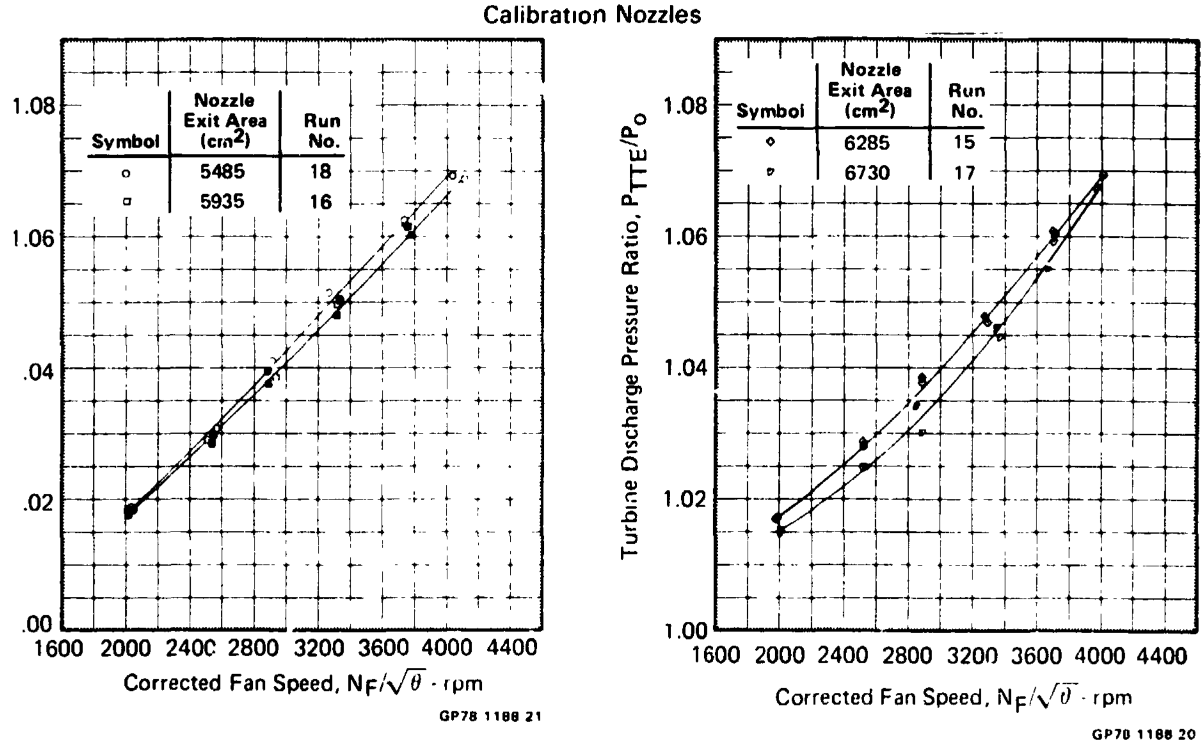

FIGURE 3-30
X376B/T58 LEFT LIFT/CRUISE AIRFLOW CHARACTERISTICS
FAN AIRFLOW vs FAN SPEED

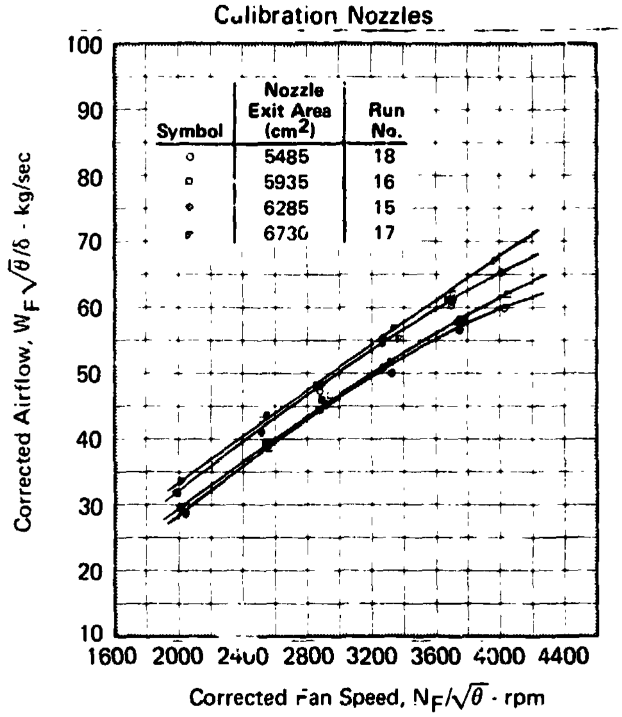

GP78-1188-29

FIGURE 3-31
X376B/T58 LEFT LIFT/CRUISE UNIT CALIBRATION NOZZLE PERFORMANCE
THRUST vs FAN SPEED

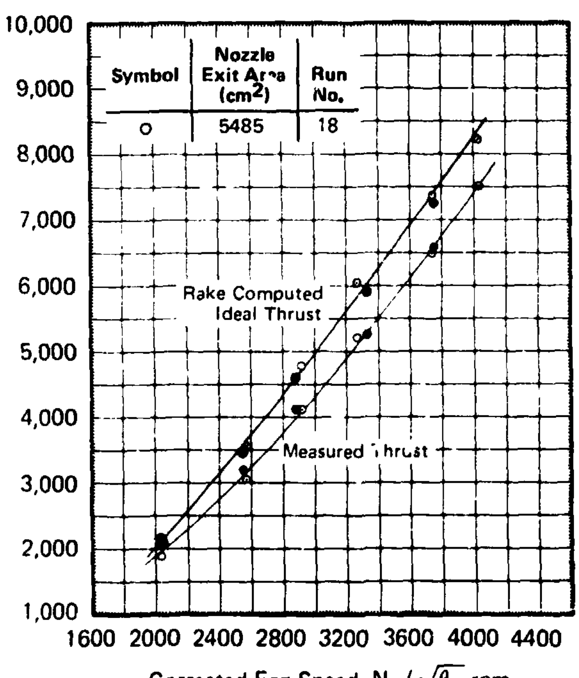

GP78 1188 118

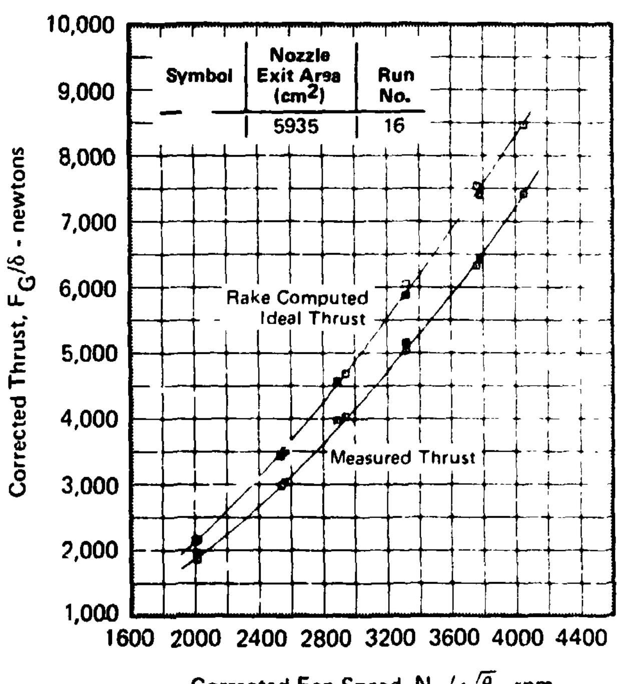

GP78 1188 117

FIGURE 3-31 (Continued)

X376B/T58 LEFT LIFT/CRUISE CALIBRATION NOZZLE PERFORMANCE THRUST vs FAN SPEED

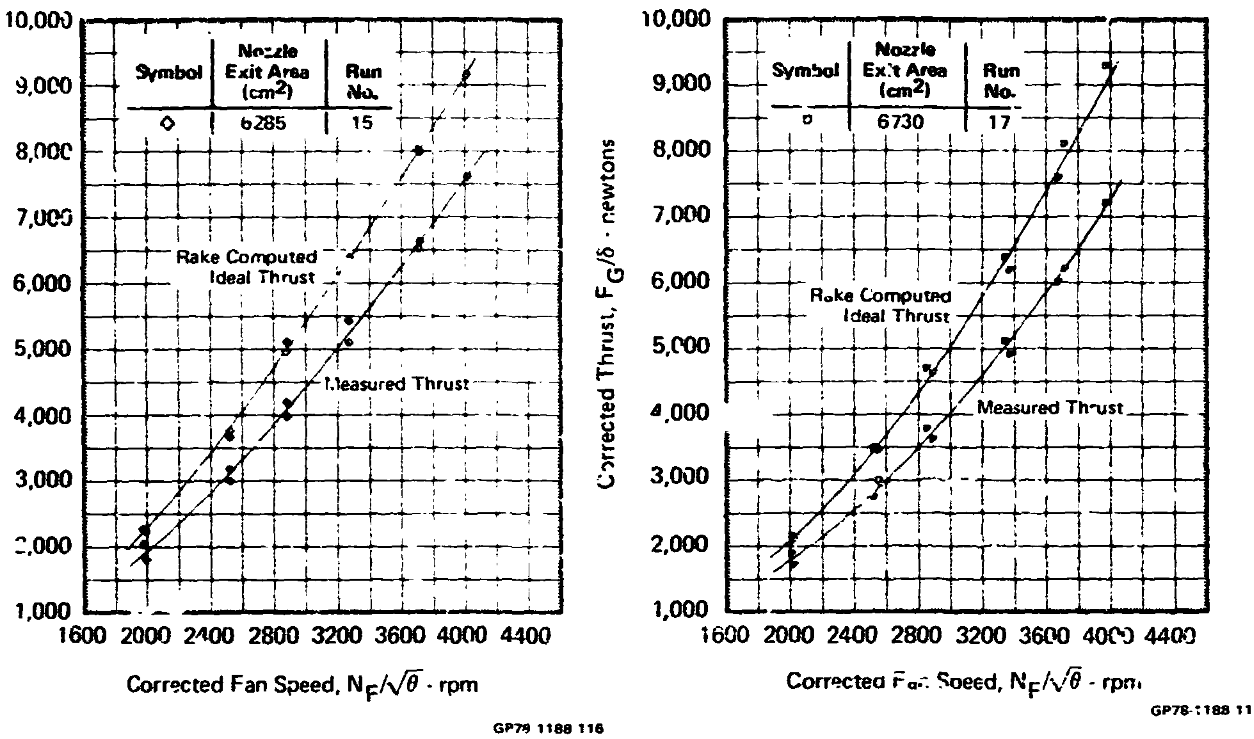

FIGURE 3-32

X376B/T58 LEFT LIFT/CRUISE UNIT FAN MAP CHARACTERISTICS

Calibration Nozzles

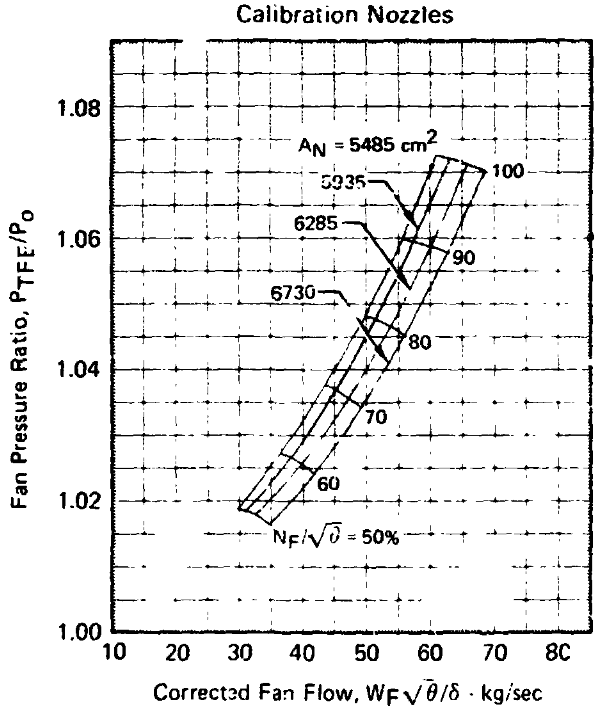

FIGURE 3-33
X376B/T58 LEFT LIFT/CRUISE UNIT PERFORMANCE MAP
THRUST vs FAN FLOW, TOTAL FLOW
Calibration Nozzles

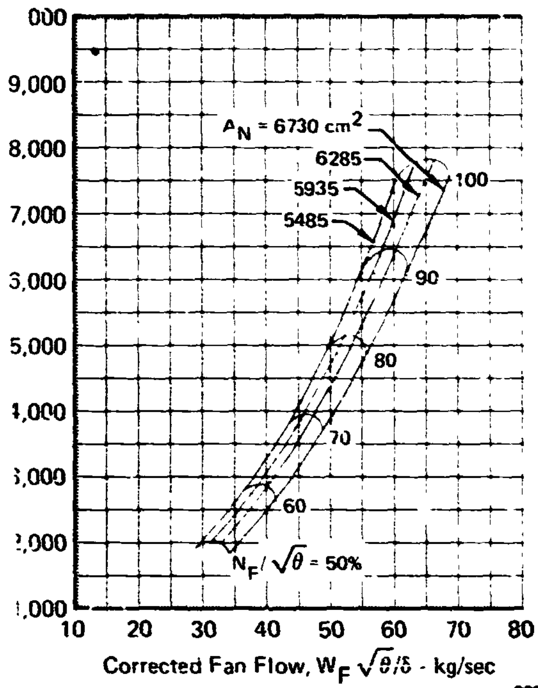

GP78-1188-124

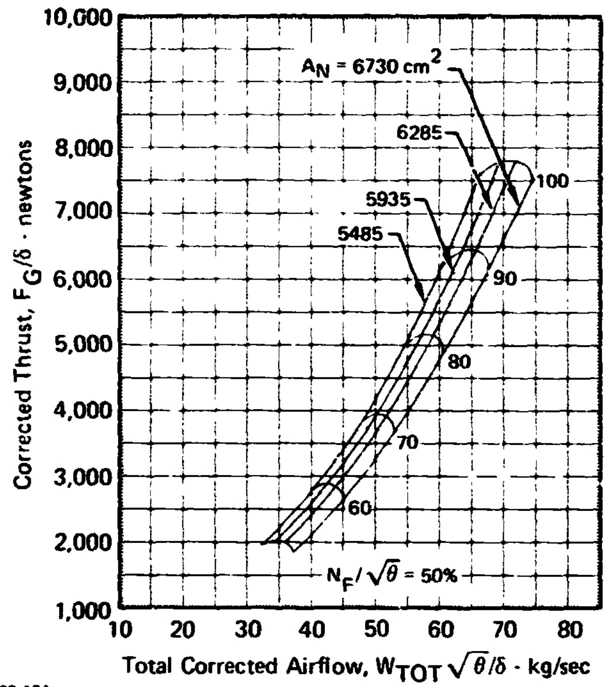

GP78-1188-125

FIGURE 3-34
X376B/T58 LEFT LIFT/CRUISE UNIT PERFORMANCE IN GROUND EFFECT
FAN FLOW vs FAN SPEED
$H/D = \infty$

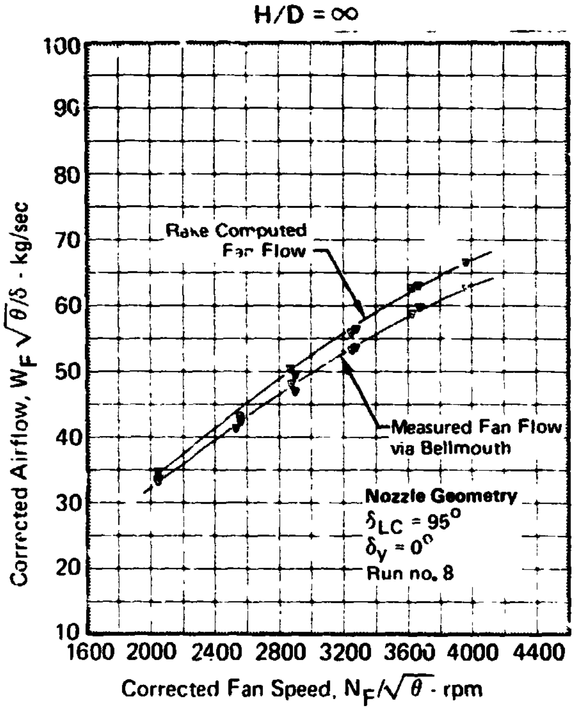

GP78-1188 69

ORIGINAL PAGE IS OF POOR QUALITY

FIGURE 3-34 (Continued)
X376B/T58 LEFT LIFT/CRUISE UNIT PERFORMANCE IN GROUND EFFECT
FAN FLOW vs FAN SPEED

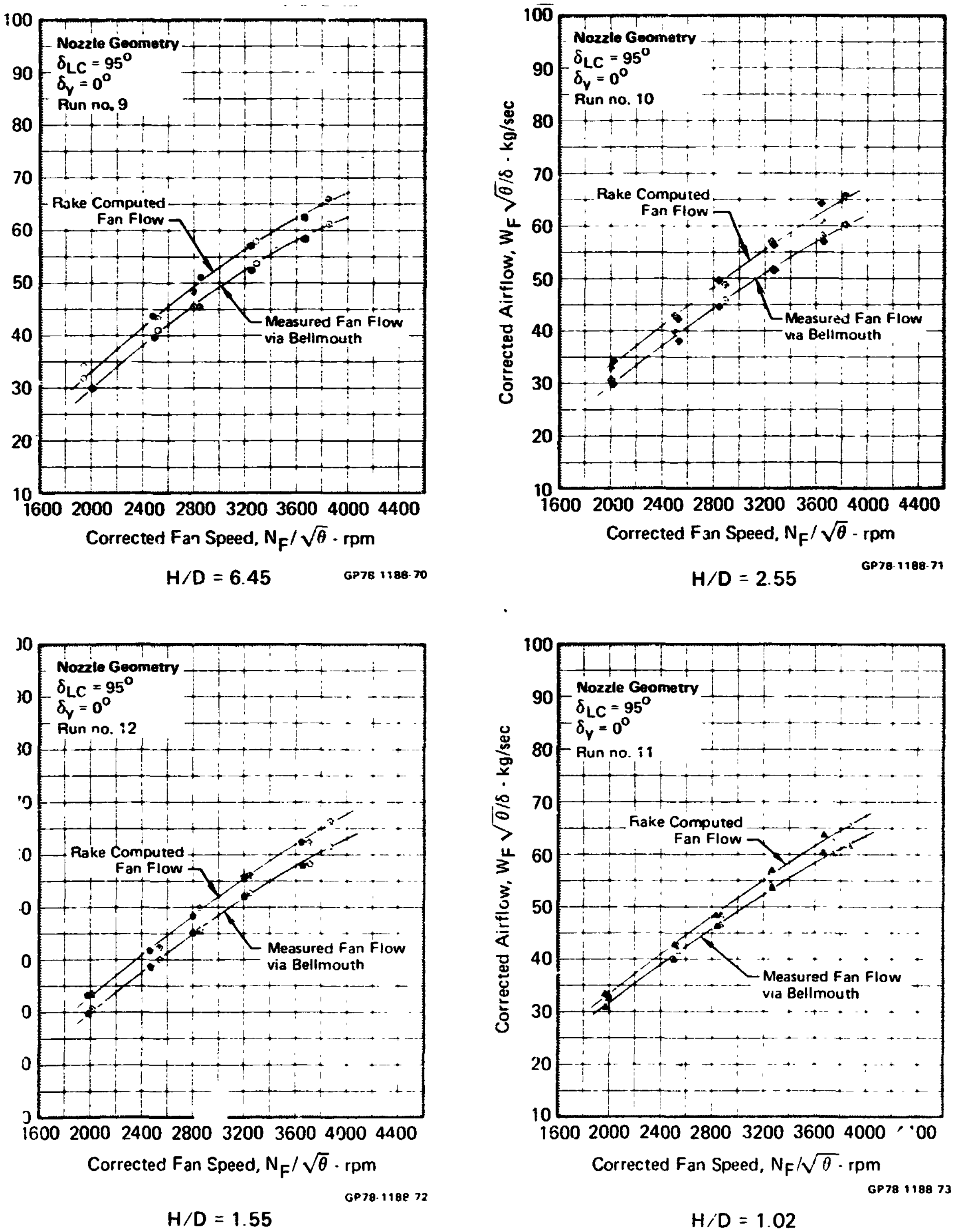

ORIGINAL PAGE IS OF POOR QUALITY

FIGURE 3-35
X376B/T58 LEFT LIFT/CRUISE UNIT PERFORMANCE IN GROUND EFFECT
TURBINE FLOW vs FAN SPEED
δ_{LC} = 95° δ_V = 0°
H/D = 6.45, 2.55, 1.55, 1.02

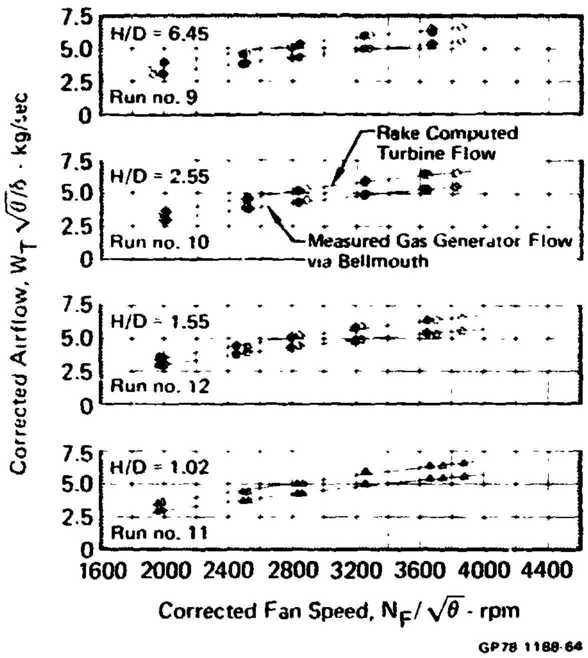

FIGURE 3-36
X376B/T58 LEFT LIFT/CRUISE UNIT PERFORMANCE IN GROUND EFFECT
THRUST vs FAN SPEED
H/D = ∞

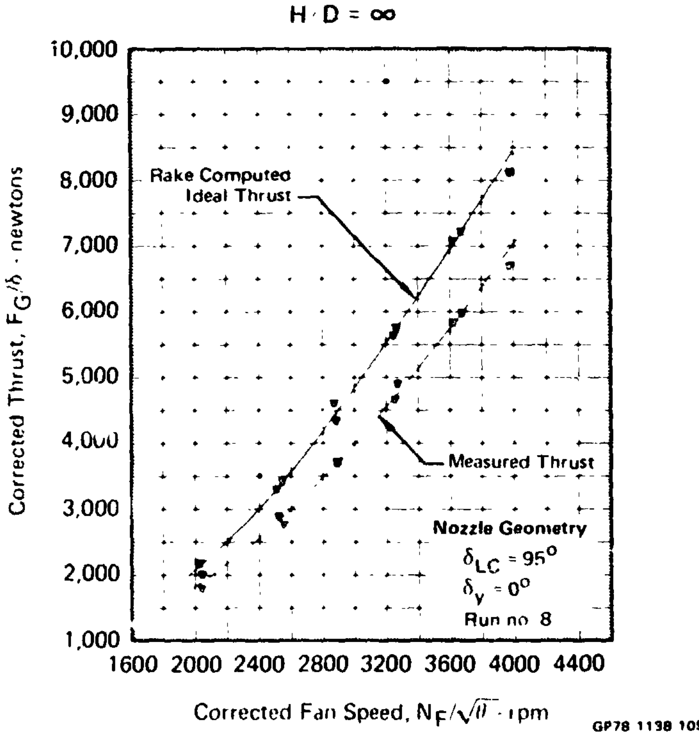

FIGURE 3-36 (Continued)
X376B/T58 LEFT LIFT/CRUISE UNIT PERFORMANCE IN GROUND EFFECT
THRUST vs FAN SPEED

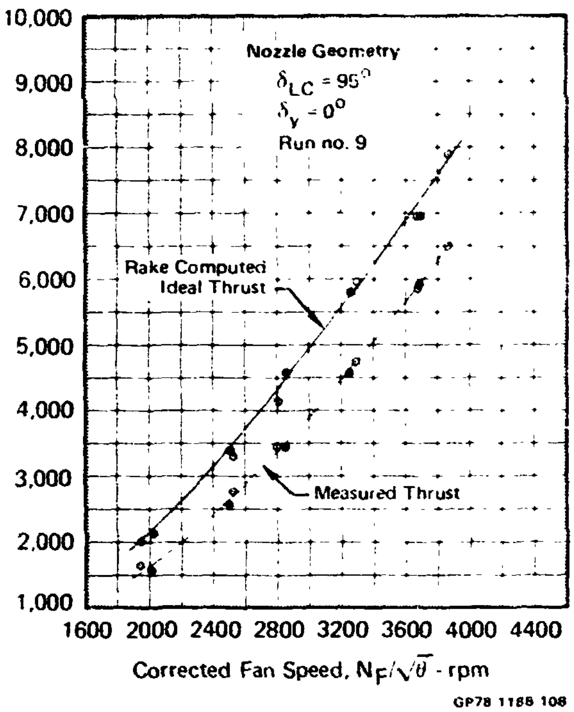

H/D = 6.45

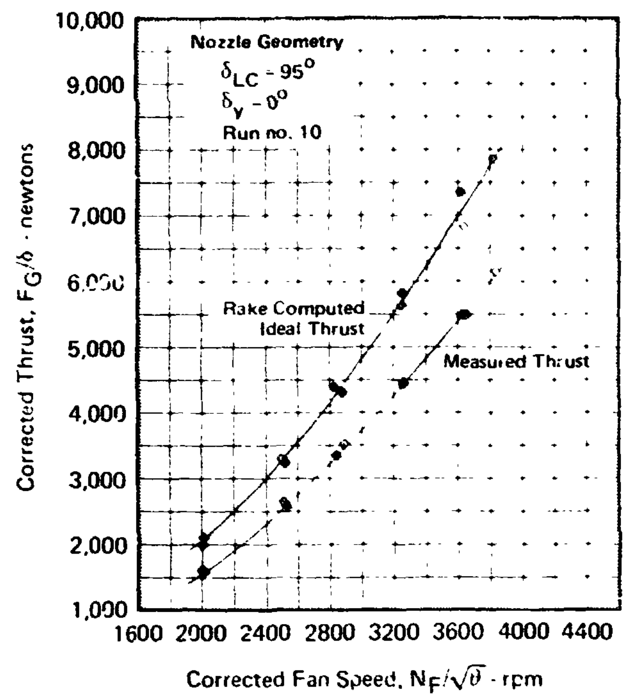

H/D = 2.55 GP78 1188 107

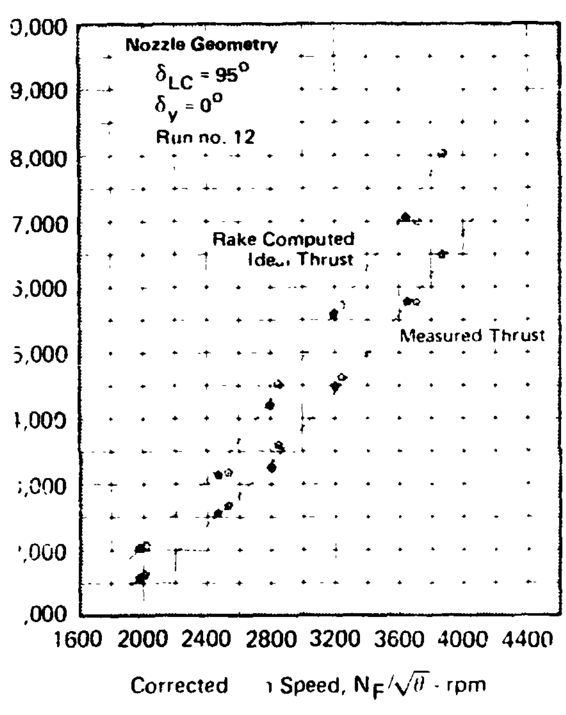

H/D = 1.55

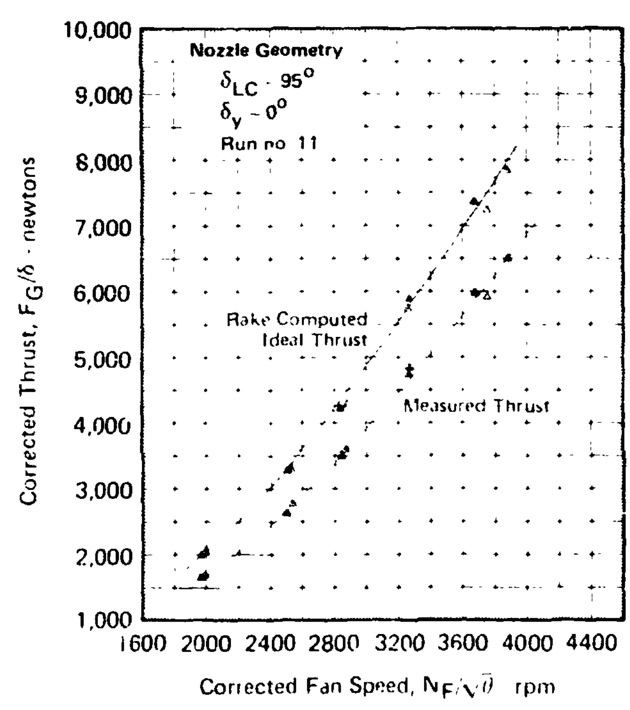

H/D = 1.02

ORIGINAL PAGE IS OF POOR QUALITY

FIGURE 3-37
X376B/T58 LEFT LIFT/CRUISE UNIT FAN PERFORMANCE IN GROUND EFFECT
Lift/Cruise Vectoring Nozzle

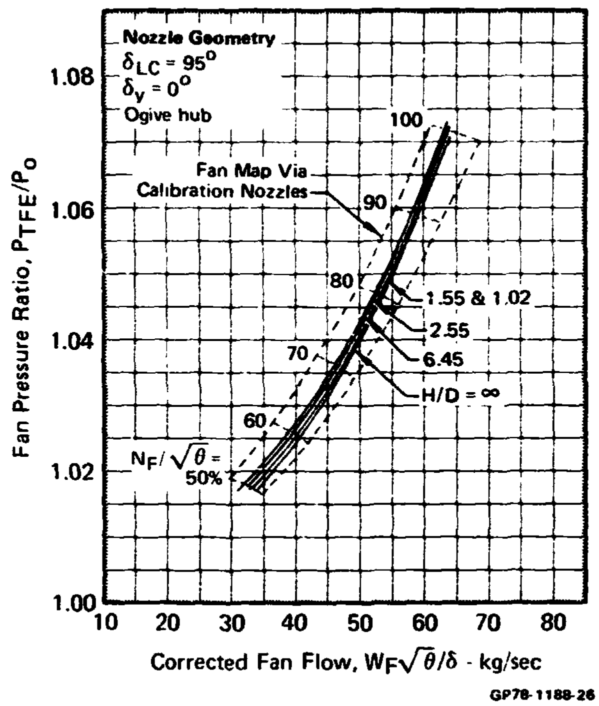

FIGURE 3-38
X376B/T58 LEFT LIFT/CRUISE UNIT EXIT RAKE COEFFICIENTS
δ_{LC} = 95° δ_y = 0°

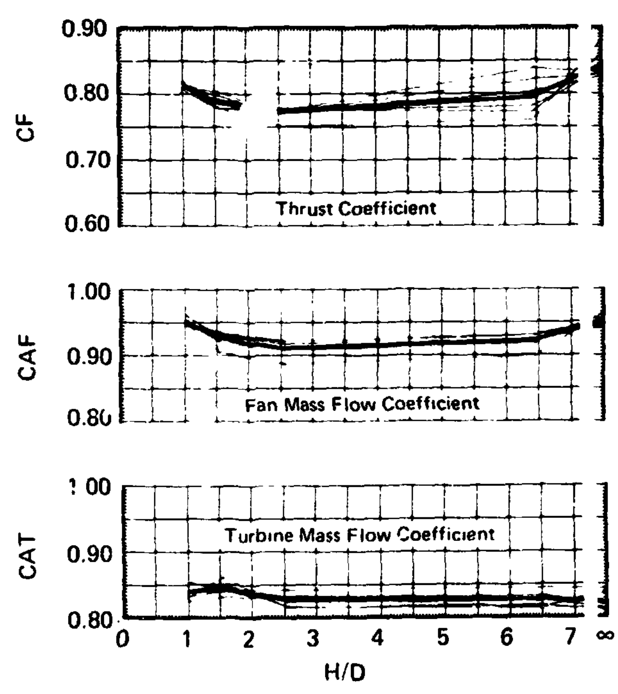

FIGURE 3-39
X376B T58 LEFT LIFT CRUISE UNIT PERFORMANCE
FAN FLOW vs FAN SPEED
H/D = ∞

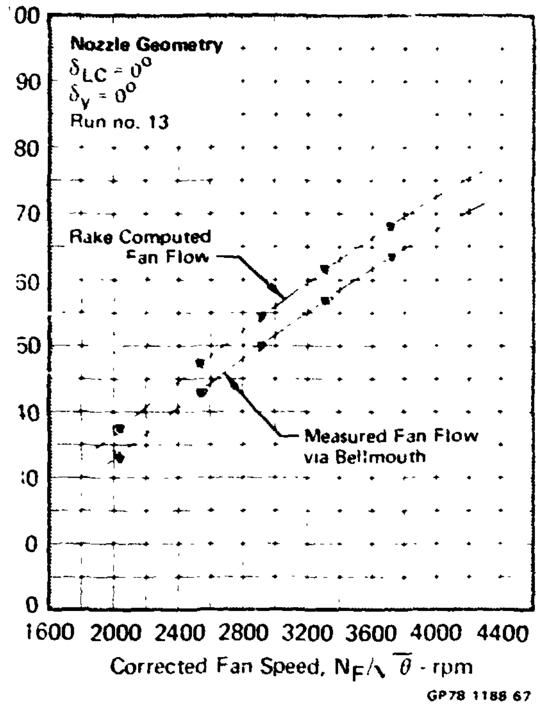

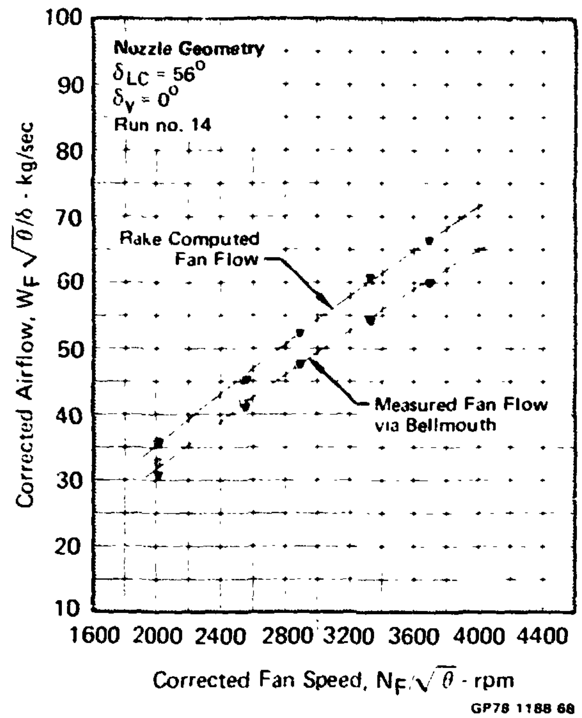

FIGURE 3-40
X376B/T58 LEFT LIFT CRUISE UNIT PERFORMANCE
TURBINE FLOW vs FAN SPEED
H/D = ∞ $\delta_y = 0°$

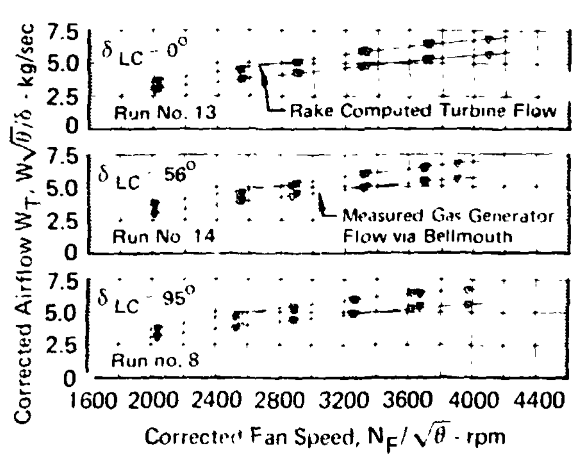

FIGURE 3-41
X376B/T58 LEFT LIFT/CRUISE UNIT PERFORMANCE
THRUST vs FAN SPEED
H/D = ∞

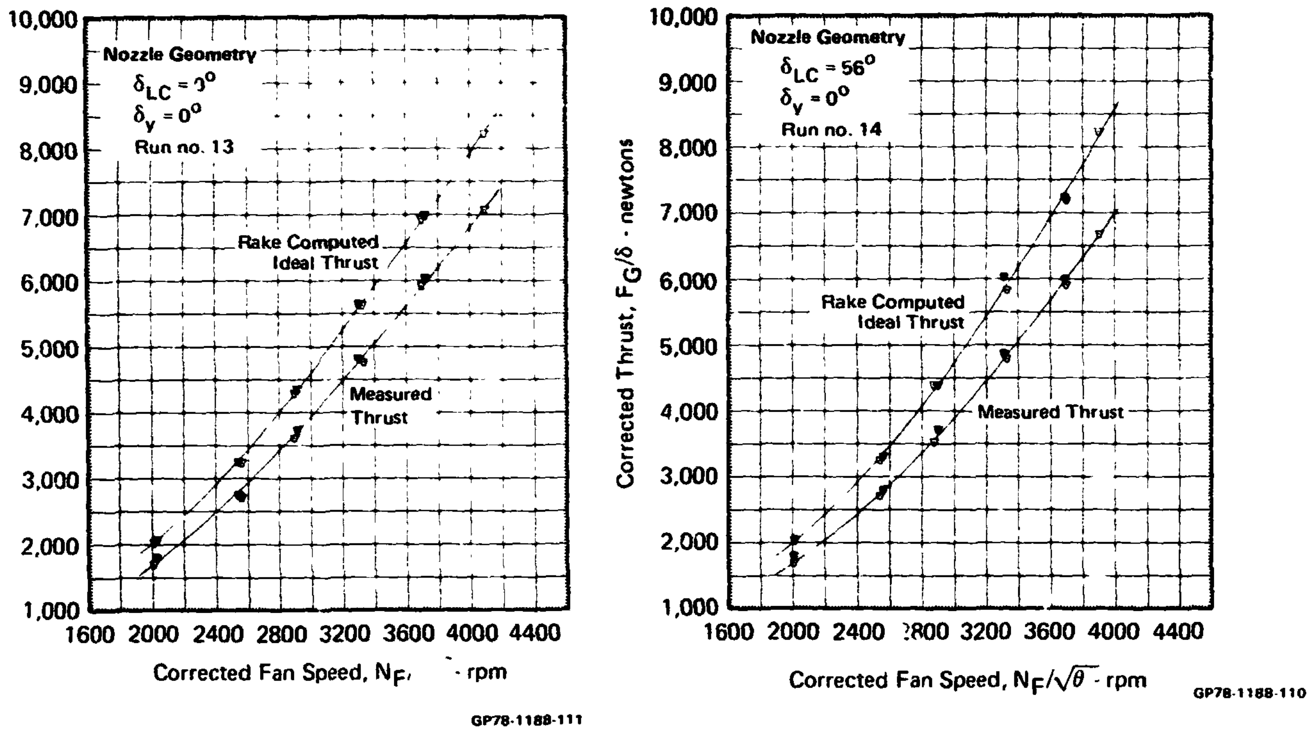

FIGURE 3-42
X376B/T58 LEFT LIFT/CRUISE UNIT EXIT RAKE COEFFICIENTS
H/D = ∞ δ_y = 0°

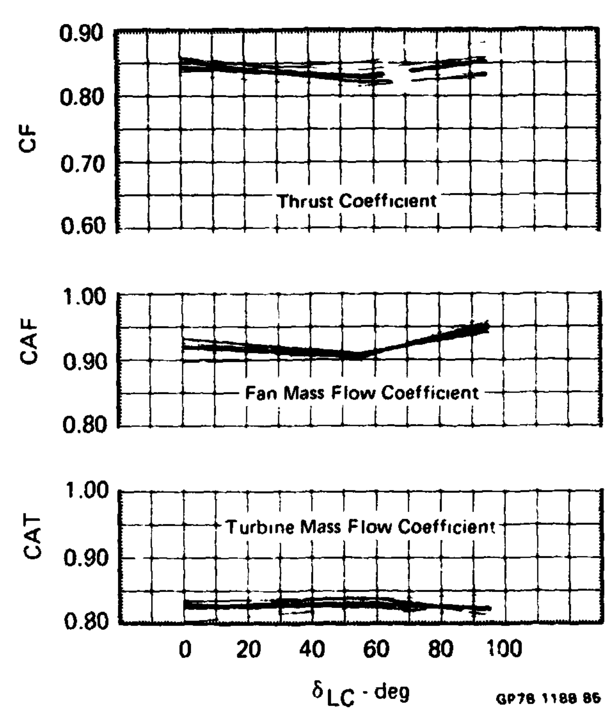

FIGURE 3-43
X376B/T58 LEFT LIFT/CRUISE UNIT THRUST VECTOR ANGLE AND MOMENT ARM CHARACTERISTICS
H/D = ∞

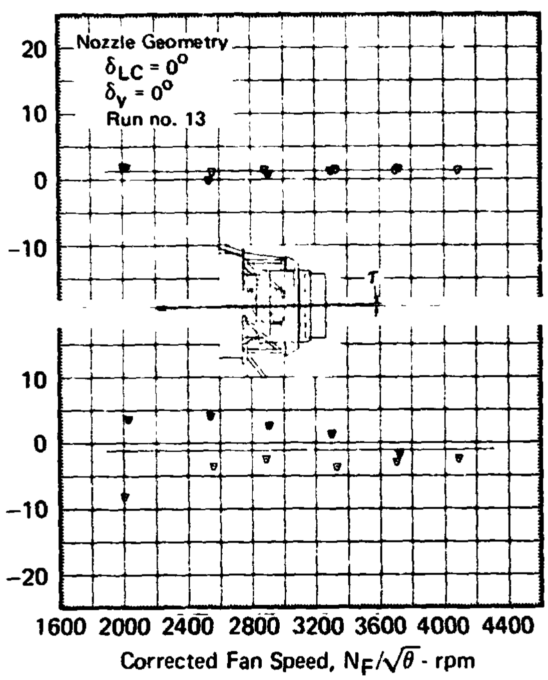

GP78-1188-130

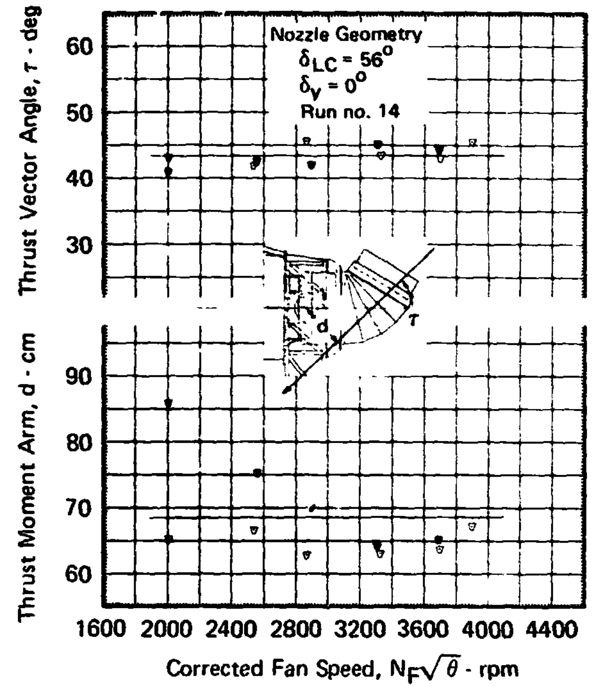

GP78-1188-131

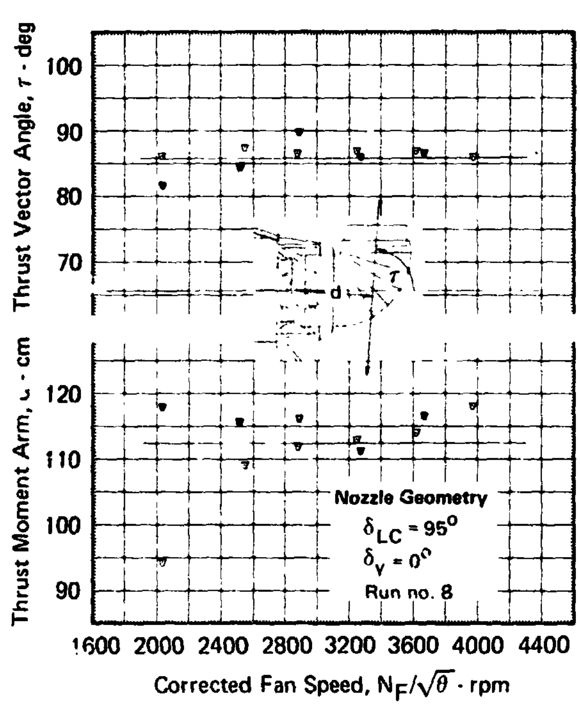

GP78 1188-132

FIGURE 3-44

X376B/T58 RIGHT LIFT/CRUISE UNIT PERFORMANCE IN GROUND EFFECT

FAN FLOW vs FAN SPEED

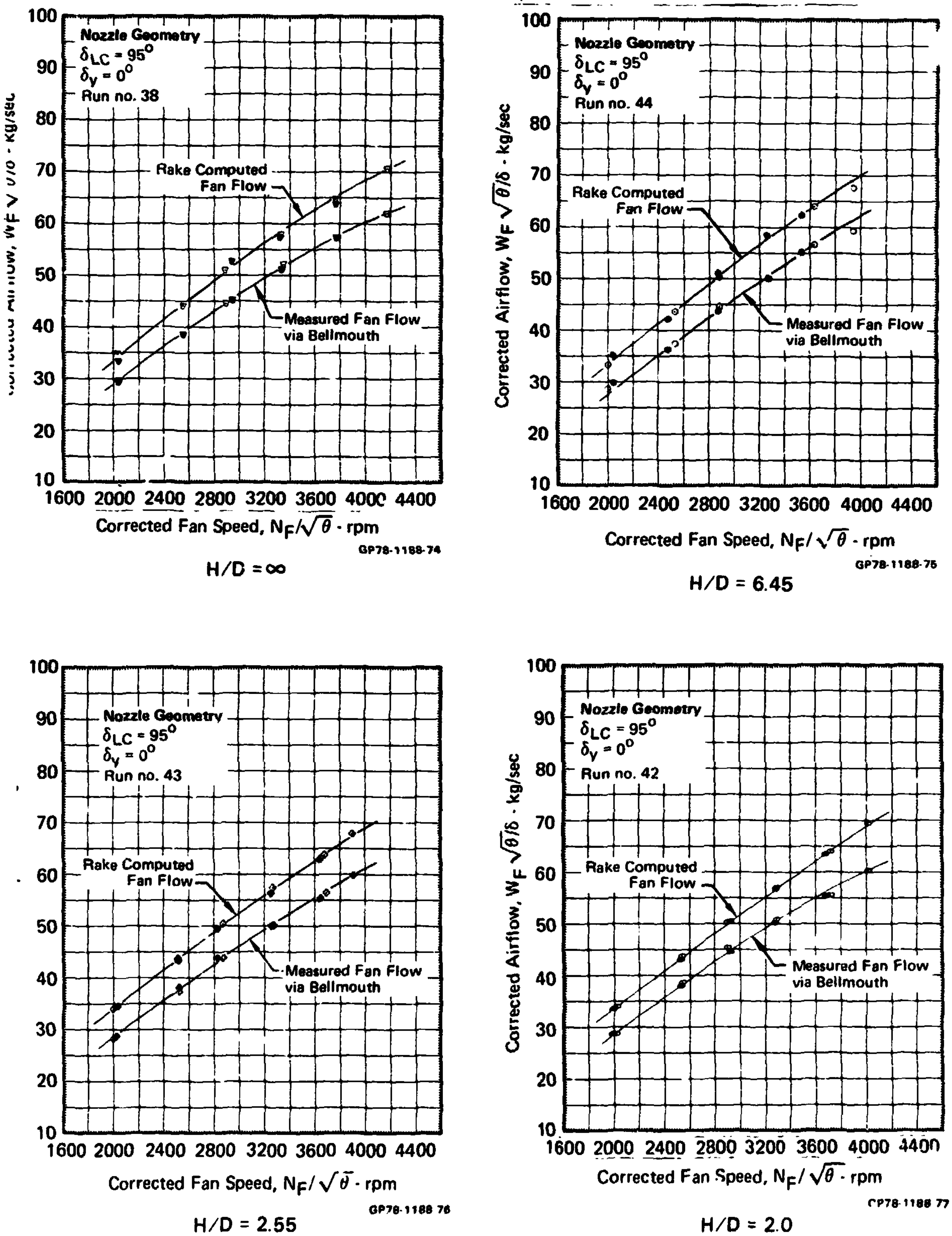

FIGURE 3-44 (Continued)
X376B/T58 RIGHT LIFT/CRUISE UNIT PERFORMANCE IN GROUND EFFECT
FAN FLOW vs FAN SPEED

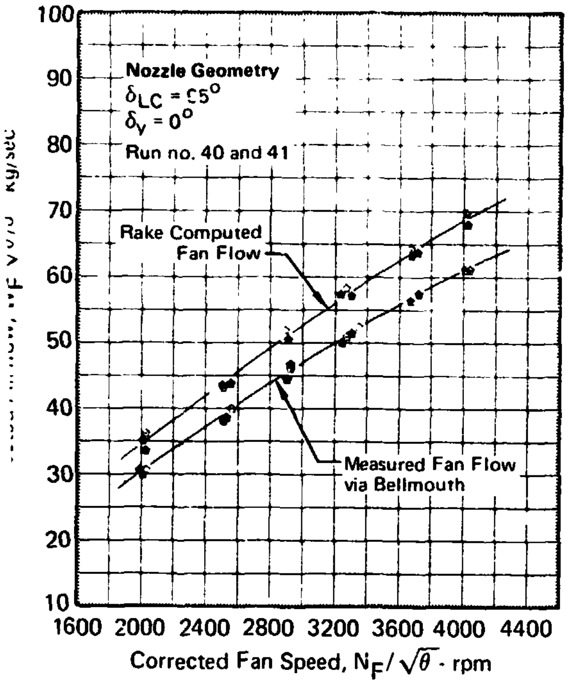

H/D = 1.55

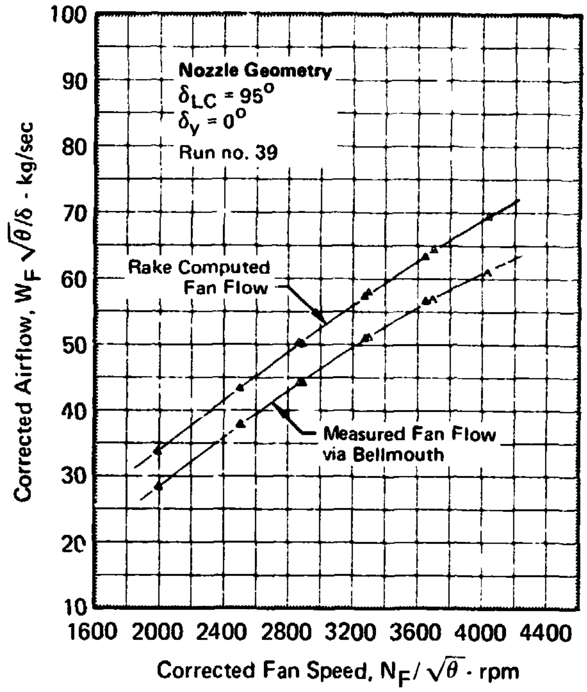

H/D = 1.02

FIGURE 3-45
X376B/T58 RIGHT LIFT/CRUISE UNIT PERFORMANCE IN GROUND EFFECT
TURBINE FLOW vs FAN SPEED
δ_{LC} = 95° δ_y = 0°
H/D = ∞, 6.45, 2.55, 2.00, 1.55, 1.02

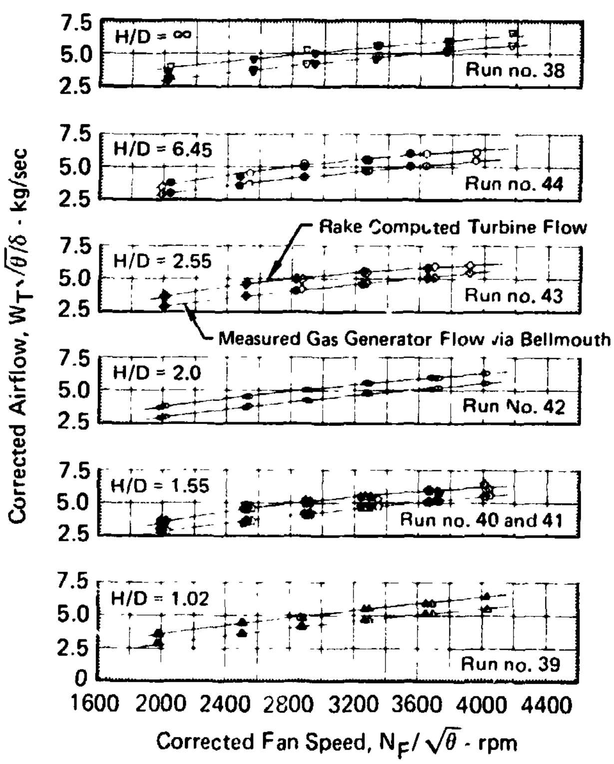

FIGURE 3-46
X376B/T58 RIGHT LIFT/CRUISE UNIT PERFORMANCE IN GROUND EFFECT
THRUST vs FAN SPEED

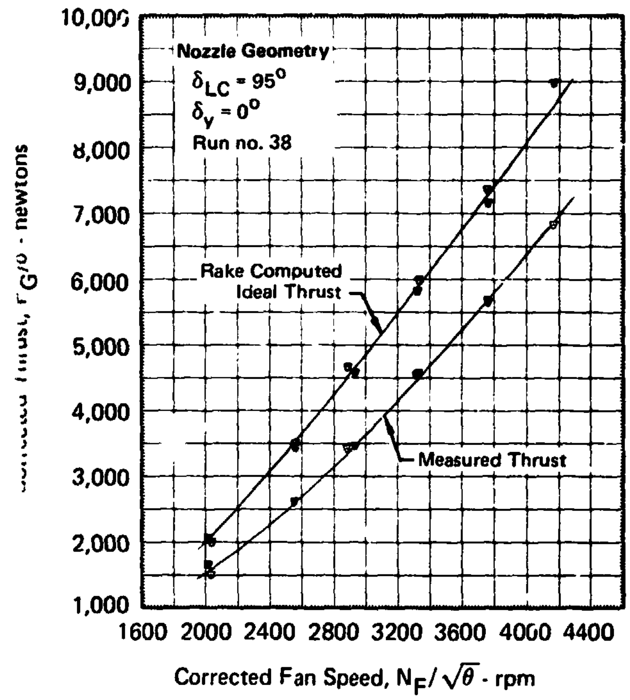

GP78-1188-53

H/D = ∞

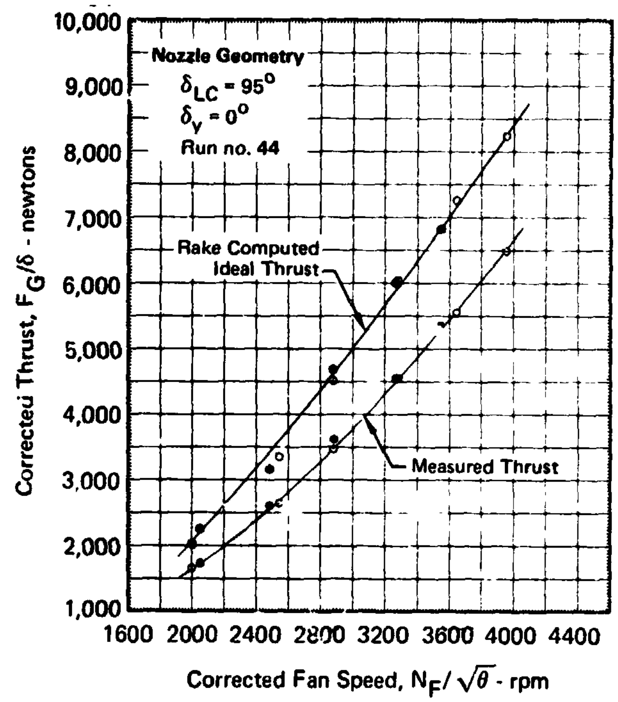

GP78-1188-54

H/D = 6.45

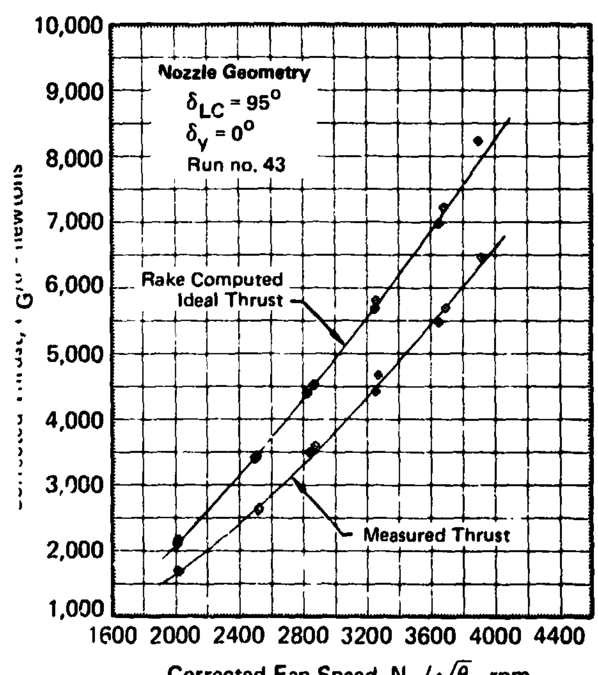

GP78 1188-55

H/D = 2.55

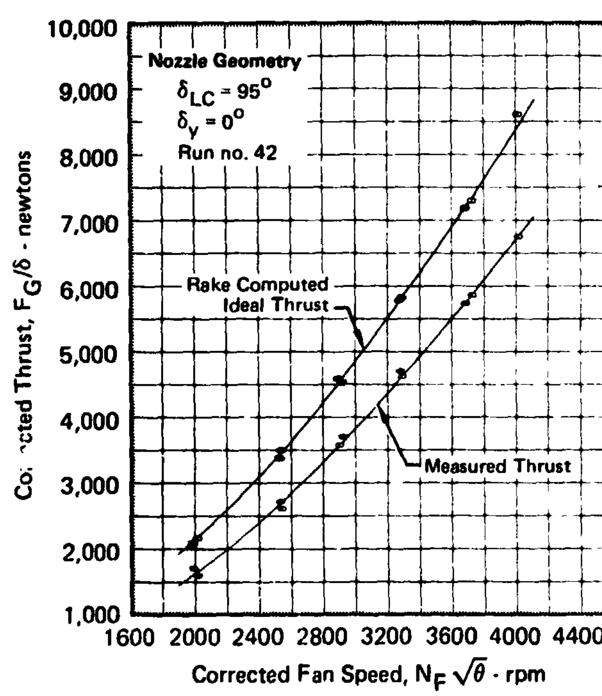

GP78 1188 56

H/D = 2.0

FIGURE 3-46 (Continued)
X376B/T58 RIGHT LIFT/CRUISE UNIT PERFORMANCE IN GROUND EFFECT
THRUST vs FAN SPEED

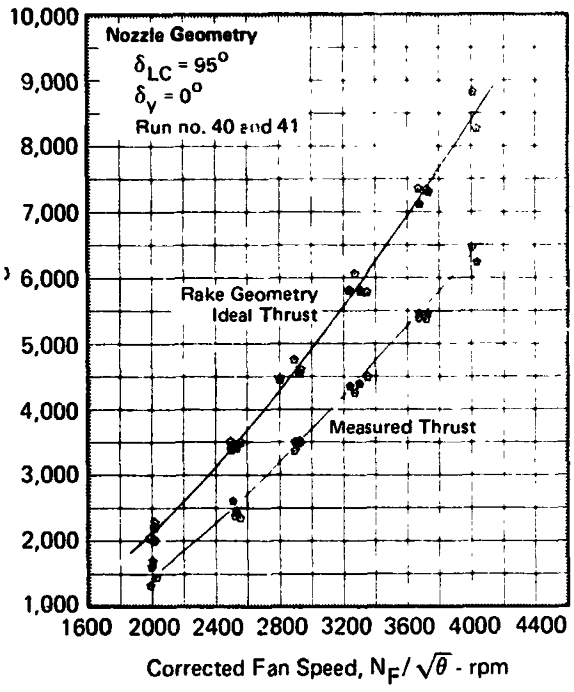

H/D = 1.55

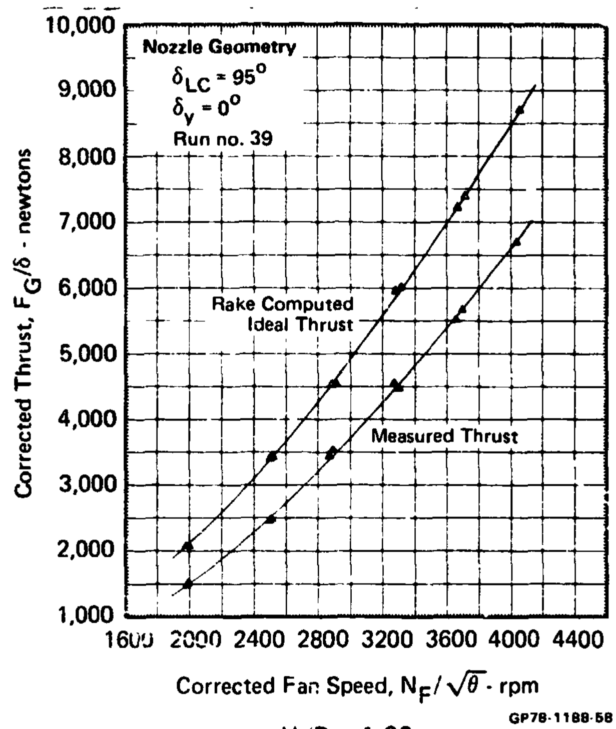

H/D = 1.02

FIGURE 3-47
X376B/T58 RIGHT LIFT/CRUISE UNIT EXIT RAKE COEFFICIENTS
δ_{LC} = 95° δ_y = 0°

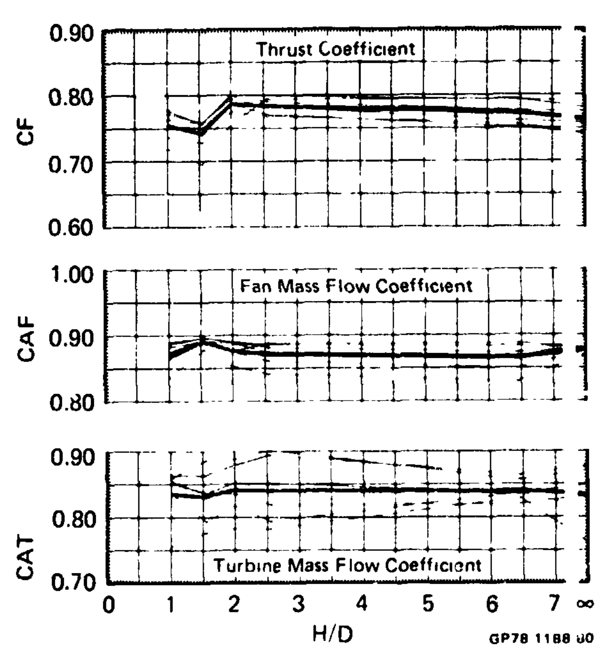

FIGURE 3-48
X376B/T58 RIGHT LIFT/CRUISE UNIT
THRUST VECTOR ANGLE AND MOMENT ARM CHARACTERISTICS
H/D =∞

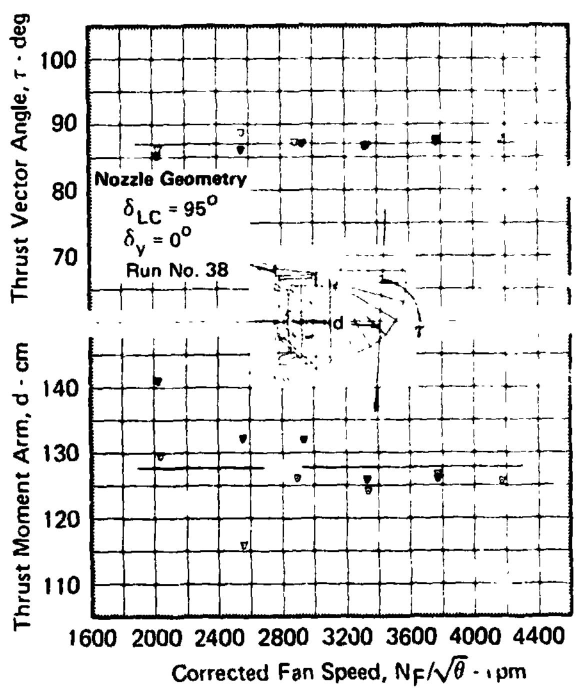

GP78 1188 133

FIGURE 3-49
LF336/J85 PRESSURE RATIO CHARACTERISTICS
FAN PRESSURE RATIO vs FAN SPEED
Calibration Nozzles

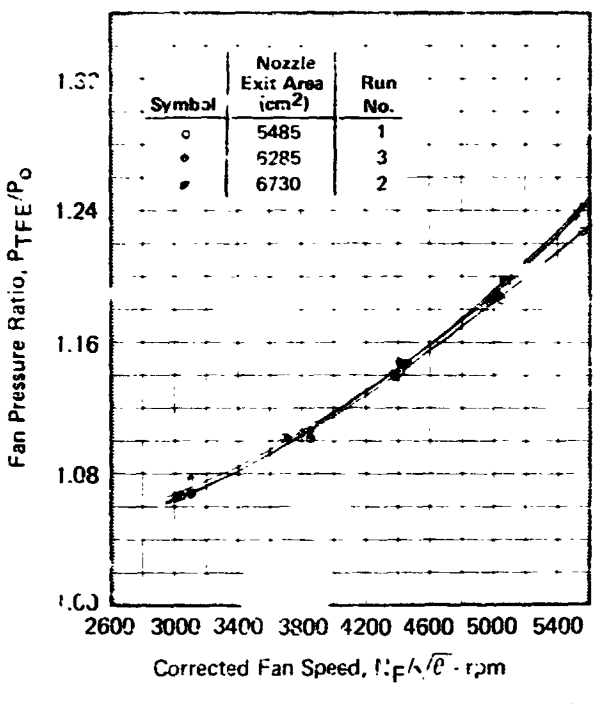

FIGURE 3-50
LF336/J85 PRESSURE RATIO CHARACTERISTICS
TURBINE PRESSURE RATIO vs FAN SPEED
Calibration Nozzles

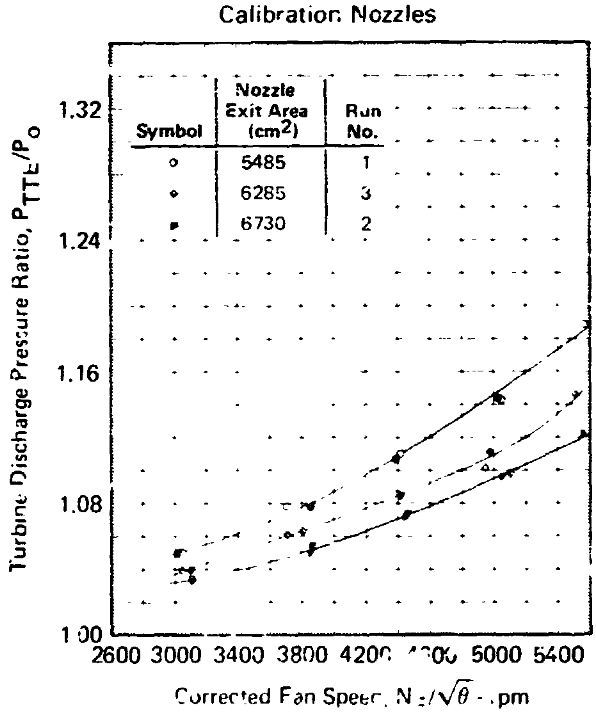

FIGURE 3-51
LF336/J85 AIRFLOW CHARACTERISTICS
AIRFLOW vs FAN SPEED
Calibration Nozzles

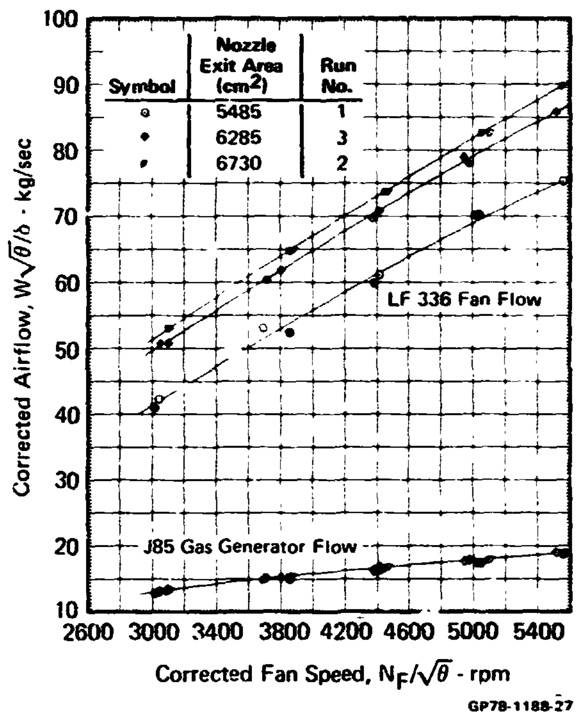

FIGURE 3-52
LF336/J85 CALIBRATION NOZZLE PERFORMANCE
THRUST vs FAN SPEED

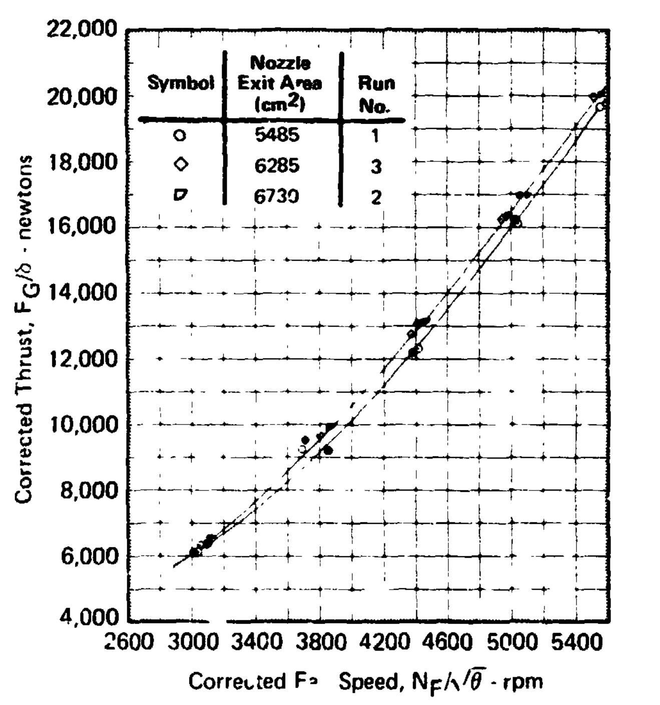

FIGURE 3-53
LF336/J85 FAN MAP CHARACTERISTICS
Calibration Nozzles

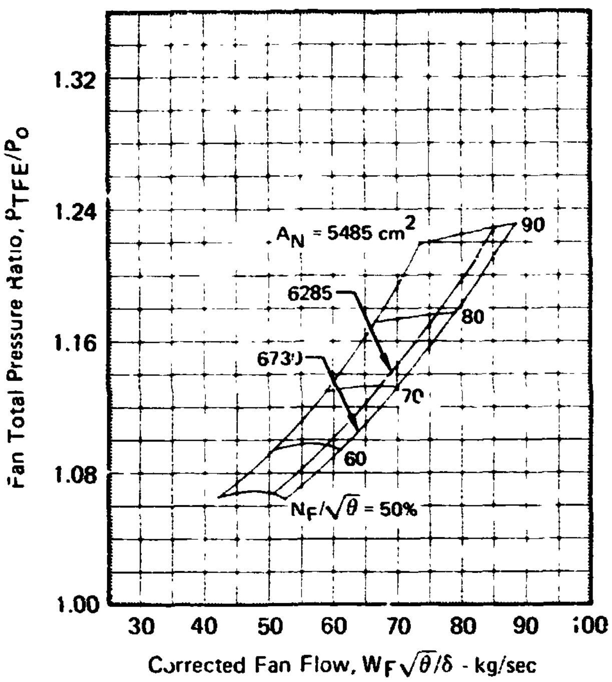

FIGURE 3-54
LF336/J85 PERFORMANCE MAP
THRUST vs FAN FLOW, TOTAL FLOW
Calibration Nozzles

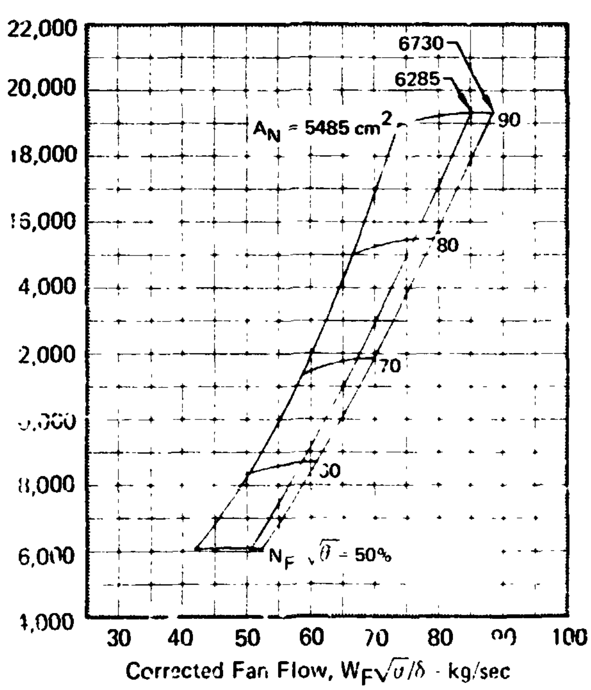

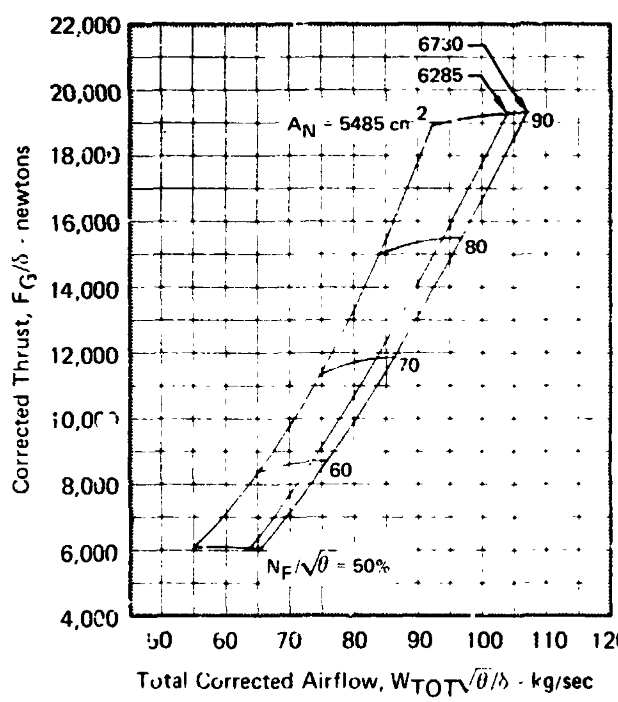

FIGURE 3-66
LF336/J85 NOSE LIFT UNIT PERFORMANCE IN GROUND EFFECT
FAN FLOW vs FAN SPEED

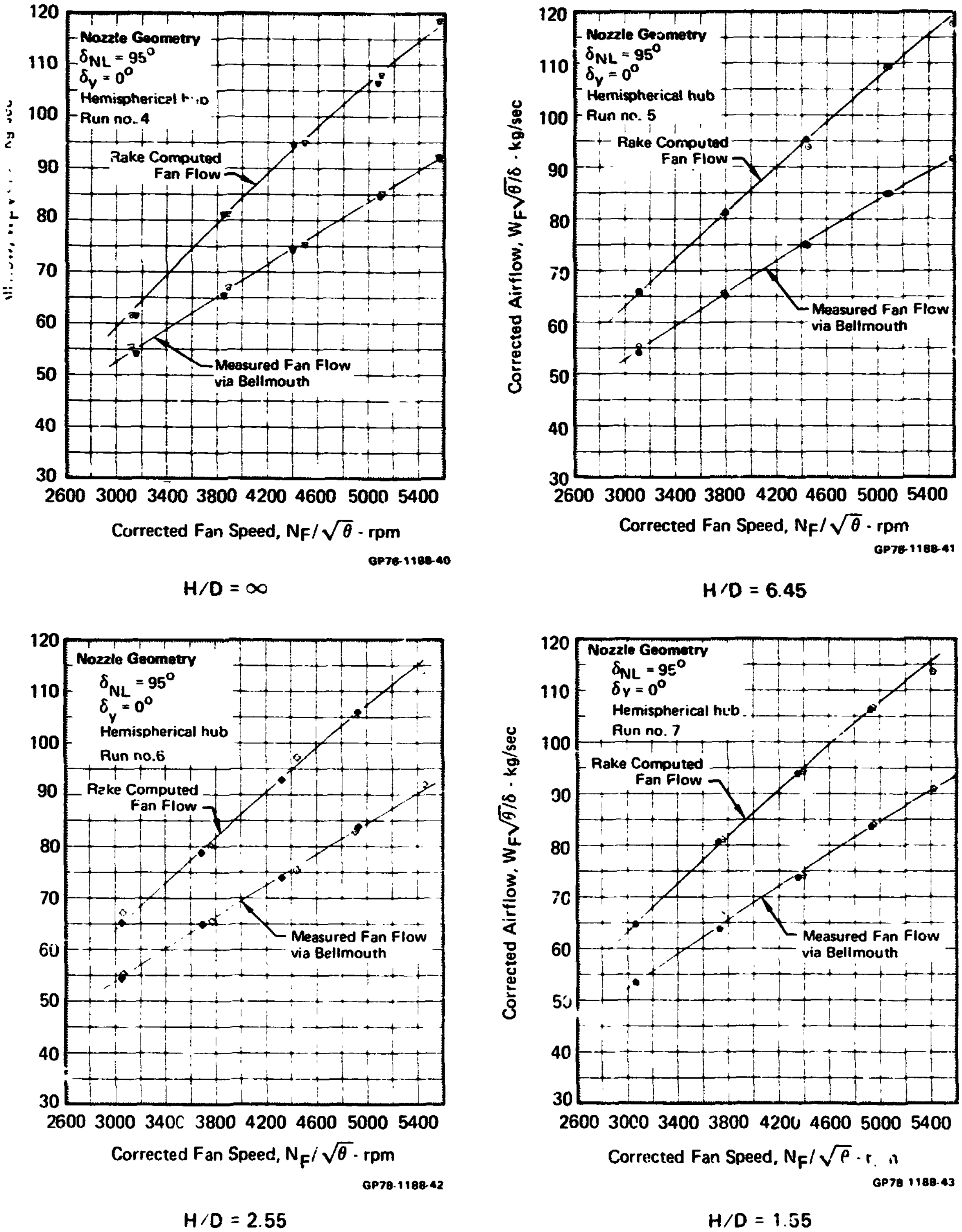

FIGURE 3-56
LF336/J85 NOSE LIFT UNIT PERFORMANCE IN GROUND EFFECT
TURBINE FLOW vs FAN SPEED

δ_{NL} = 95° δ_y = 0° Hemispherical Hub

H/D = ∞, 6.45, 2.55, 1.55

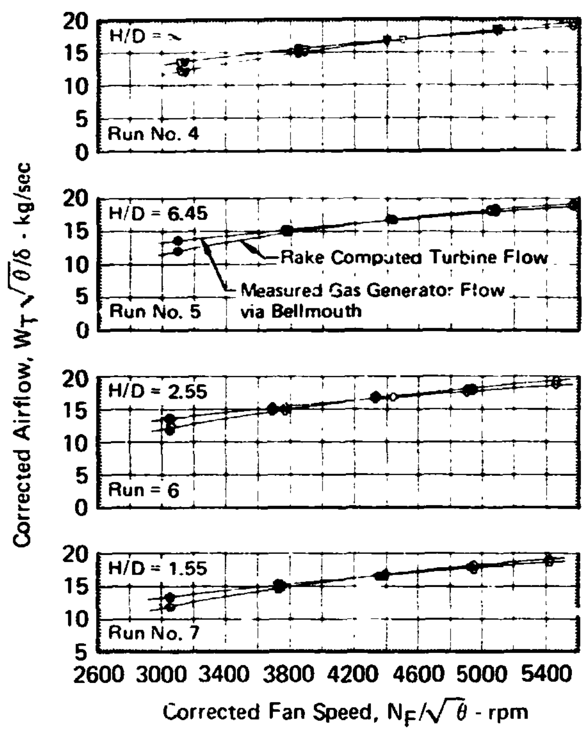

FIGURE 3-57
LF336/J85 NOSE LIFT UNIT PERFORMANCE IN GROUND EFFECT
THRUST vs FAN SPEED

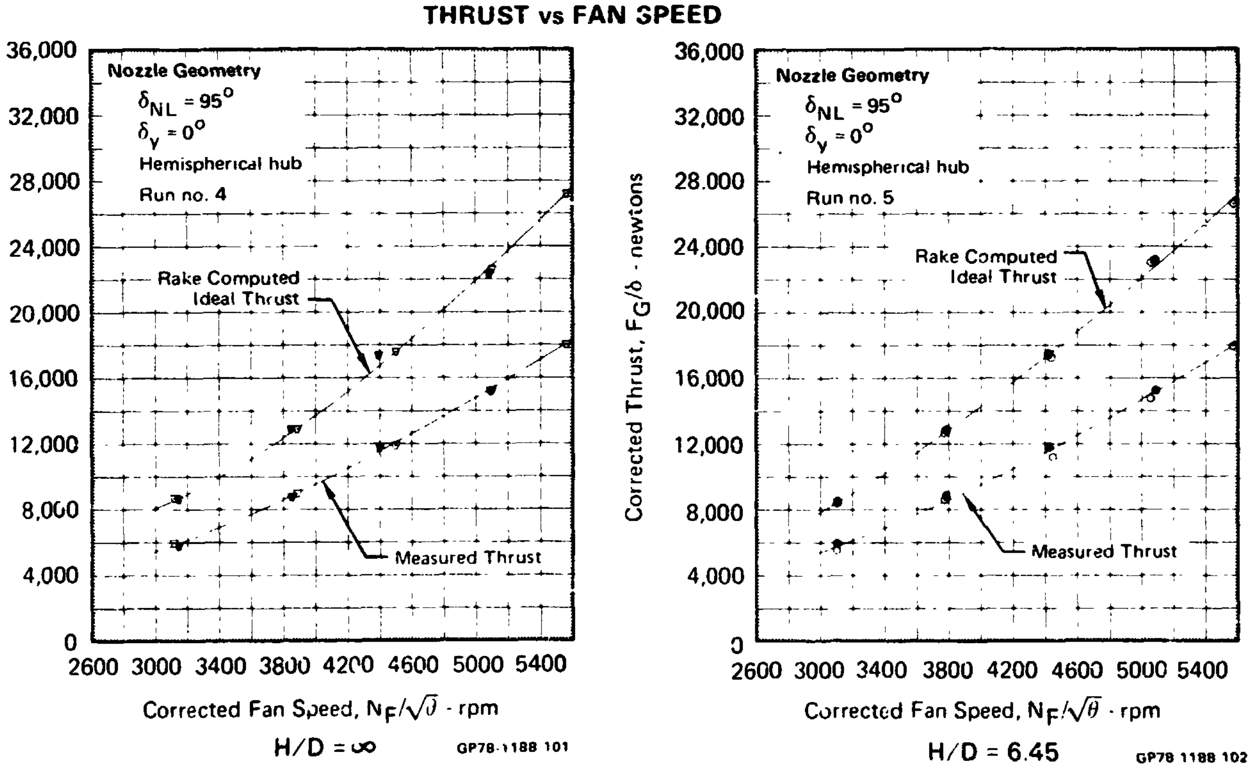

FIGURE 3-57 (Continued)
LF336/J85 NOSE LIFT UNIT PERFORMANCE IN GROUND EFFECT
THRUST vs FAN SPEED

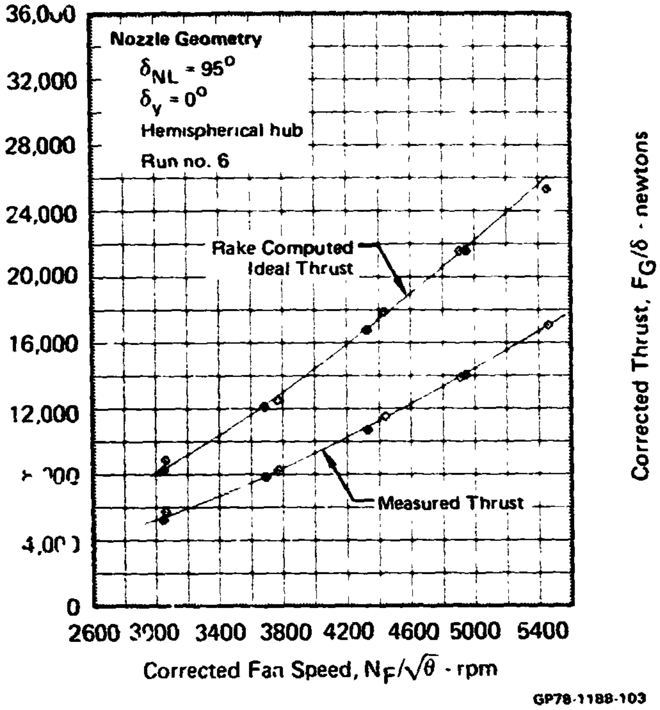

H/D = 2.55

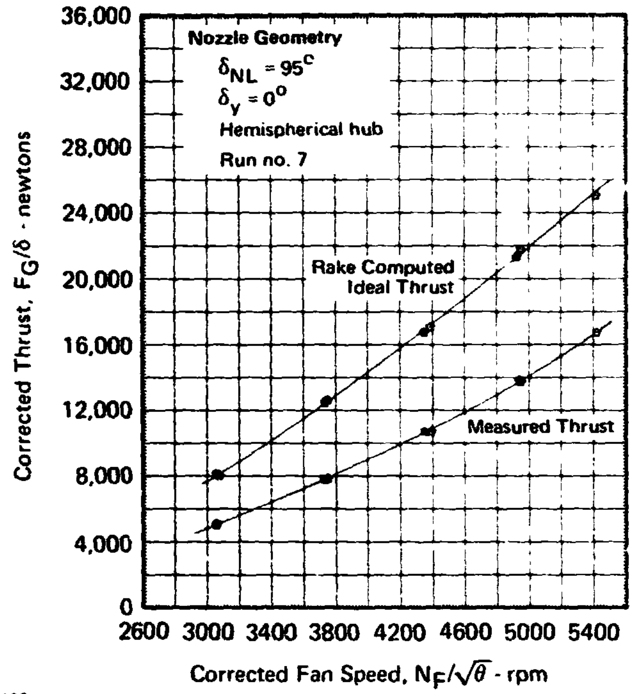

H/D = 1.55

GP78-1188-104

FIGURE 3-58
LF336/J85 NOSE LIFT UNIT
THRUST VECTOR ANGLE AND MOMENT ARM CHARACTERISTICS
H/D = ∞

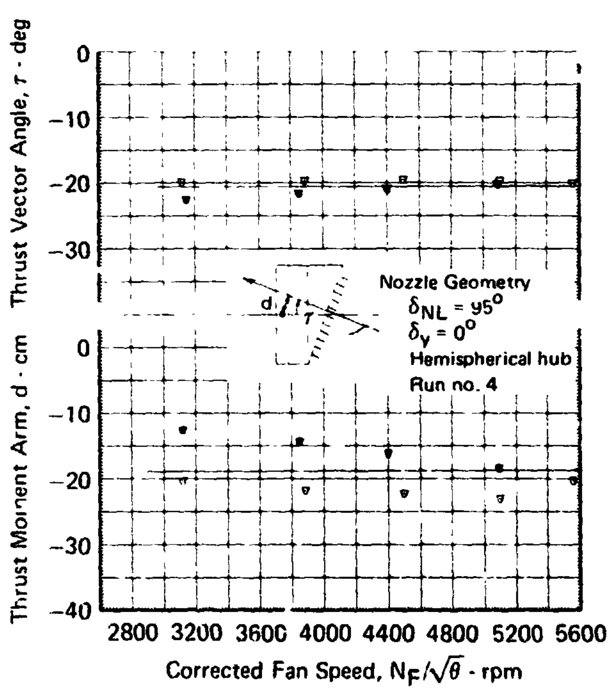

FIGURE 3-59
LF336 J85 FAN PERFORMANCE IN GROUND EFFECT
Louvered Lift Nozzle

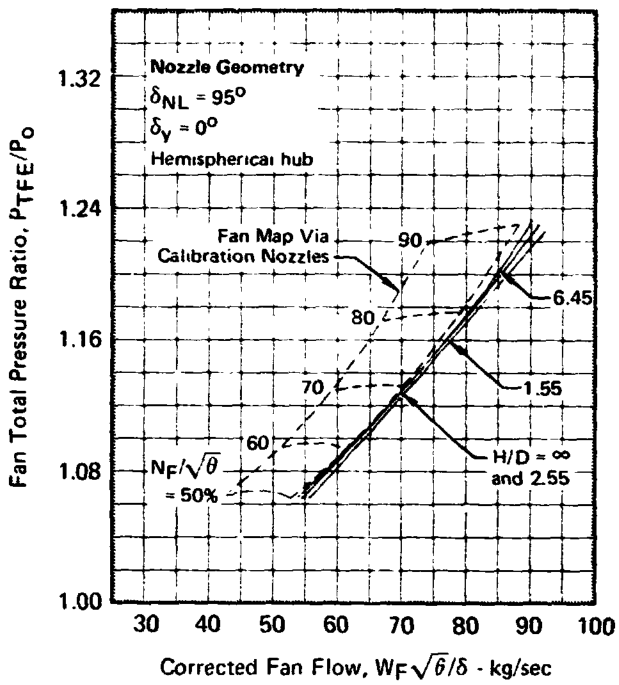

GP78-1188-23

FIGURE 3-60
LF336/J85 NOSE LIFT UNIT EXIT RAKE COEFFICIENTS
δ_{NL} = 95° δ_y = 0° Hemispherical Hub

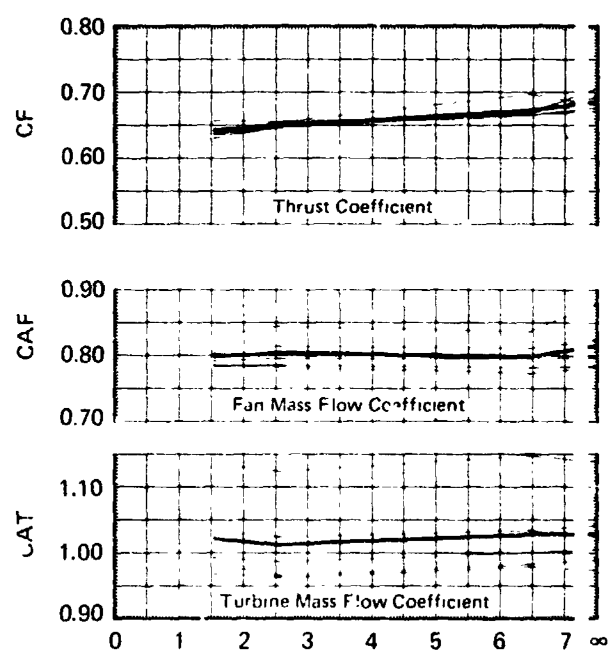

GP78 1188 84

4. CONCLUSIONS

The isolated fan calibration tests were conducted to establish thrust and mass flow performance "in" and "out" of ground effect for the three X376B/T58 turbotip fan thrust vectoring units used in the 70 percent scale, three fan V/STOL model. The effects of a higher fan pressure ratio on the 70 percent model nose louvered lift nozzle were investigated with tests of the LF336/J85 turbotip fan system. The conclusions derived as a result of these tests are presented below:

- The thrust and mass flow performance of the X376B/T58 nose lift unit with a flat plate exit hub installed is essentially constant for H/D variations down to 1.55. At H/D equal to 1.02, back pressurization of the fan nozzle exit occurs and is accompanied by an increase in thrust of 5 percent. Corresponding increases in fan exit hub pressure level were found to produce a change in hub forces which correlated well with measured thrust changes.

- A change in fan exit hub shape from flat plate to hemispherical produces no significant change in louvered lift nozzle performance for height variations from H/D = 1.02 to ∞.

- Operation of the nose lift nozzle at the higher fan pressure ratios generated by the LF336/J85 fan system causes no significant change in ground proximity performance down to an H/D of 1.55, the lowest height tested.

- The thrust and mass flow performance of the left and right X376B/T58 lift/cruise units with 95 degree circular hood deflector nozzles remains unchanged, within ±2 percent, for the range of ground heights from H/D = 1.02 to ∞.

5. REFERENCES

"Wind Tunnel and Ground Static Investigation of a Large Scale Model of a Lift/Cruise Fan V/STOL Aircraft", McDonnell Aircraft Company, NASA CR 137916, August 1976.

Hunt, D., et al, "Wind Tunnel and Ground Static Tests of a 0.94 Scale Powered Model of a Modified T-39 Lift/Cruise Fan V/STOL Research Airplane", Boeing Aerospace Company, NASA CR 151923, January 1977.

Renselaer, D. J., "Low Speed Aerodynamic Characteristics of a Vectored Thrust V/STOL Transport with Two Lift/Cruise Fans", Rockwell International Corporation, NASA CR 152029, July 1977.

Weber, W. B. and Williams, R. W., "Experimental Determination of Propulsion Inducted Ground Effects on Typical Three Fan Type A V/STOL Configurations", AIAA Paper 78-1507, August 1978.

Schuster, E. P. and Flood, J. D., "Important Simulation Parameters for the Experimental Testing of Propulsion Induced LIft Effects", AIAA Paper 78-1078, July 1978.

Schuster, E. P., Carter, E. D. and Esker, D. W., "Investigation of Ground Effects on a Large Scale and Small Scale Model of a 3 Fan V/STOL Aircraft", McDonnell Aircraft Company, NASA CR 152240, July 1979.

Esker, D. W., "Ground Test of the "D" Shaped Vented Thrust Vectoring Nozzle", NASA CR 137959, October 1976.

APPENDIX A

TEST RUN SCHEDULE

The schedule of runs accomplished during the isolated fan tests is shown on Figure A-1. The key to the various parameters found in the run schedule is presented on Figure A-2.

FIGURE A-1
TEST RUN SCHEDULE

RUN NO.	DATE	PO (PSIA)	TO (°F)	FAN	CAL. OR GRD EFF.	NOZZLE	HUB	YAW ANGLE	LOUVER ANGLE	NOZZLE ANGLE	H/D
1	8/18	14.74	-	LF336	CAL.	AN-1	TAPERED CONE	N.A.	N.A.	N.A.	N.A.
2	8/21	14.76	55-60			AN-4					
3			65			AN-3					
4	8/24	14.77	54		GRD EFF.	NOSE	HEMISPHERE	0°	95°		∞
5	8/25	14.78	63-64								6.45
6		14.77	68								2.55
7		14.78	70								1.55
8	9/1	14.65	60-65	X376B L/H L/C		L/H L/C	OGIVE	0°	N.A.	95°	∞
9		14.64	80								6.45
10											2.55
11	9/5	14.65	65-66								1.02
12			66								1.55
13	9/6	14.67	57							0°	∞
14		14.60	63							56°	
15	9/8	14.72	67		CAL.	AN-3	TAPERED CONE	N.A.	N.A.	N.A.	N.A.
16	9/11	14.73	55			AN-2					
17			63			AN-4					
18	9/12	14.65	53			AN-1					
19	9/14	14.66	52	X376B NOSE							
20		14.63	65			AN-2					
21			73			AN-3					
22	9/15	14.73	65			AN-4					
23	9/19	14.81	70		GRD EFF.	NOSE	HEMISPHERE	0°	95°		∞
24	9/20	14.80	49								1.02
25			65								1.55
26											2.55
27			67								6.45
28	9/21	14.74	52								∞
29		14.75	65				FLAT PLATE				
30			76					±12°			
31	9/22		50								1.02
32			60					0°			
33			67								1.55
34	9/25	14.69	63					±12°			
35		14.70	80								2.55
36			77					0°			
37	9/26	14.73	55								6.45
38	9/25	14.76	51	X376B R/H L/C		R/H L/C	OGIVE		N.A.	95°	∞
39			61								1.02
40			67								1.55
41	9/29	14.71	60								1.55
42			63								2.0
43			75								2.55
44											6.45

N.A. - Not Applicable

FIGURE A-2
RUN SCHEDULE KEY

H/D: Height of lift/cruise nozzle exit above ground plane ratioed to nozzle exit diameter: D = .99 m (3.25 ft)

H/D = ∞	H = Ground plane removed
= 6.45	= 6.4 m (21 ft)
= 2.55	= 2.53 (8.3)
= 1.55	= 1.52 (5.0)
= 1.02	= 1.01 (3.3)

Yaw Angle: Position of yaw vanes with respect to vertical

Louver Angle: Position of louvers with respect to vertical

Calibration Nozzle:	AN-1 = 5485 cm^2	(850 in^2)
	-2 = 5935	(920)
	-3 = 6285	(974)
	-4 = 6730	(1043)

Vector Nozzle Angle: Geometric nozzle angle with respect to vertical

APPENDIX B

TEST DATA TABULATION

FGC	-	Corrected Gross Thrust
FGIC	-	Corrected Ideal Gross Thrust
NFC	-	Corrected Fan Speed
PTFE/PO	-	Fan Pressure Ratio
PTTE/PO	-	Turbine Discharge Pressure Ratio
WCBF	-	Corrected Measured Fan Flow Via Bellmouth
WCBG	-	Corrected Measured Gas Generator Flow Via Bellmouth
WC3F	-	Corrected Rake Computed Fan Flow
WC4T	-	Corrected Rake Computed Turbine Flow

NOTE: Speed (NFC) in RPM
Flowrates (WCBF, WCBG, WC3F, WC4T) in KG/SEC
Thrusts (FGC, FGIC) in Newtons

TEST DATA TABULATION

RUN NO.	PT. NO.	NFC	WCBF	WCBG	WC3F	WC4T	FGC	FGIC	PTFE/PO	PTTE/PO
1	2	3037.	42.41	13.15			6166		1.0674	1.0510
	3	3693.	53.07	14.99			9261		1.1024	1.0782
	4	4412.	31.01	16.37			12302		1.1418	1.1102
	5	5037.	70.08	17.38			16092		1.1847	1.1420
	6	5553.	75.30	18.67			19658		1.2274	1.1791
	7	5020.	70.08	17.47			16200		1.1878	1.1427
	8	4384.	59.88	16.23			17178		1.1391	1.1058
	9	3847.	52.39	14.99			9203		1.1021	1.0779
	10	3010.	41.05	13.06			6120		1.0662	1.0503
2	2	3095.	53.07	13.42			6389		1.0688	1.0349
	3	3867.	64.86	15.49			9982		1.1096	1.0553
	4	4457.	73.71	16.79			13147		1.1468	1.0739
	5	5097.	82.56	17.89			16971		1.1966	1.0973
	6	5548.	89.81	18.78			20309		1.2418	1.1224
	7	5048.	82.56	17.78			16971		1.1977	1.0963
	8	4442.	73.71	16.72			13130		1.1469	1.0716
	9	3846.	64.86	15.49			9927		1.1074	1.0506
	10	3106.	53.07	13.50			6595		[illegible]	1.0334
3	2	3052.	50.80	13.40			6379		[illegible]	1.0409
	3	3797.	61.92	15.37			9660		1.1054	1.0633
	4	4371.	69.63	16.59			12743		1.1412	1.0873
	5	4944.	78.93	17.65			16237		1.1824	1.1114
	6	5506.	85.73	19.09			19964		1.2363	1.1464
	7	4967.	78.02	17.76			16316		1.1861	1.1102
	8	4406.	70.76	16.90			13078		1.1483	1.0831
	9	3708.	60.33	15.34			9636		1.1024	1.0610
	10	3101.	50.80	13.65			6425		1.0774	1.0399
4	2	3124.	55.57	13.63	66.64	12.29	6006	8702	1.0710	
	3	3894.	66.91	15.45	81.42	14.96	9041	12972	1.1080	
	4	4502.	75.30	16.76	94.99	16.83	11897	17576	1.1506	
	5	5098.	85.05	17.89	107.37	18.37	15198	22576	1.1989	
	6	5563.	91.85	18.75	118.64	19.28	17982	27178	1.2459	
	7	5085.	84.37	18.03	106.38	18.45	15174	22245	1.1942	
		4395.	73.94	16.82	94.48	16.77	11757	17305	1.1478	
		3861.	65.32	15.51	81.52	14.87	8828	12941	1.1080	
	10	3153.	54.21	13.65	66.42	12.19	5922	8619	1.0708	
5	2	3103.	55.34	13.57	65.47	12.03	5593	8422	1.0690	
	3	3774.	65.55	15.20	80.58	14.77	8318	12629	1.1045	
	4	4435.	74.84	16.69	93.59	16.62	11237	17023	1.1452	
	5	5054.	84.82	17.90	109.31	18.33	14739	22977	1.2025	
	6	5570.	91.63	18.78	117.51	19.08	17893	26521	1.2379	
	7	5078.	85.05	17.79	109.40	18.55	15249	23103	1.2030	
	8	4424.	75.07	16.77	95.35	16.77	11764	17506	1.1494	
	9	3781.	65.32	15.29	81.21	14.96	8861	12856	1.1062	
	10	3099.	54.21	13.62	66.05	12.24	6043	8542	1.0593	
6	2	3061.	55.34	13.64	67.26	12.49	5807	8838	1.0721	
	3	3767.	65.32	15.41	79.79	14.82	8313	12419	1.1026	
	4	4436.	75.30	16.85	97.20	16.82	11540	17809	1.1521	
	5	4914.	82.56	17.51	105.22	18.06	13876	21514	1.1886	
	6	5457.	91.63	18.69	113.92	19.18	16950	25232	1.2225	
	7	4942.	83.24	17.77	105.72	18.10	13981	21587	1.1882	
	8	4327.	73.71	16.73	92.88	16.95	10748	16789	1.1418	
	9	3691.	64.64	15.32	78.83	14.66	7909	12159	1.0996	
	10	3049.	54.43	13.78	65.42	11.89	5323	8238	1.0669	
7	2	3058.	53.07	13.47	64.89	12.14	5200	8138	1.0664	
	3	3754.	66.45	15.39	81.14	14.97	7894	12627	1.1037	
	4	4390.	73.94	16.61	92.24	16.91	10680	17019	1.1436	
	5	4951.	83.92	17.47	106.69	18.30	13709	21757	1.1883	
	6	5419.	90.72	18.72	113.67	19.08	16698	24988	1.2199	
	7	4926.	83.24	17.77	106.06	18.00	13789	21270	1.1850	
	8	4351.	73.71	16.72	93.93	16.60	10742	16772	1.1419	
	9	3730.	63.50	15.46	80.83	14.73	7780	12498	1.1033	
	10	3060.	53.52	13.69	64.16	12.01	5113	8019	1.0643	
8	2	2035.	33.79	3.05	34.48	3.81	1822	2184	[illegible]	
	3	2554.	42.41	3.91	43.20	4.82	2777	3416	1.0277	
	4	2882.	48.08	4.35	50.45	5.46	3748	4633	1.0376	
	5	3250.	53.07	4.89	55.71	5.99	4674	5643	1.0458	
	6	3624.	58.74	5.34	62.58	6.43	5836	7092	1.0585	
	7	3965.	62.60	5.59	66.72	6.72	6696	8122	1.0673	
	8	[illegible]	59.88	5.35	62.96	6.40	5979	7222	1.0597	
	9	3271.	53.52	4.91	56.40	5.92	4911	5779	1.0474	
	10	2890.	46.72	4.35	49.20	5.15	3718	4366	1.0360	
	11	2524.	41.05	3.81	42.71	4.65	2915	3302	1.0269	
	12	2038.	33.11	3.16	34.82	3.80	2035	2197	1.0180	
9	2	1941.	31.98	3.02	34.04	3.62	1660	2023	1.0166	
	3	2520.	41.05	3.83	43.30	4.59	2780	3312	1.0269	
	4	2804.	45.36	4.24	48.28	5.09	3447	4145	1.0338	
	5	3285.	53.52	4.89	57.80	6.01	4738	5947	1.0484	
	6	3669.	58.06	5.30	61.77	6.40	5846	6947	1.0572	
	7	3855.	61.01	5.52	65.81	6.61	6490	7904	1.0658	
	8	3678.	58.06	5.32	62.38	6.19	5910	6945	1.0572	
	9	3248.	52.39	4.85	56.87	5.87	4566	5810	1.0479	
	10	2850.	45.36	4.33	51.13	5.30	3454	4585	1.0371	
	11	2504.	39.69	3.82	43.95	4.61	2584	3399	[illegible]	
	12	2012.	29.94	3.10	-	3.86	1584	2163	[illegible]	

TEST DATA TABULATION (Cont'd)

RUN NO.	PT. NO.	WFC	WCMF	WCBG	WC3F	WCAT	FGC	FGBC	PTFE/PO	PTTE/PO
10	2	1996.	30.04	3.05	33.20	3.61	1615	1993	1.0165	
	3	2510.	39.69	3.85	43.05	4.56	2647	3204	1.0280	
	4	2907.	46.04	4.39	48.89	5.29	3534	4311	1.0352	
	5	3258.	51.71	4.87	57.02	5.87	4432	5907	1.0476	
	6	3649.	56.93	5.27	60.96	6.36	5475	6790	1.0560	
	7	3828.	60.33	5.52	65.70	6.80	6125	7025	1.0640	
	8	3633.	58.06	5.30	60.18	6.46	5499	7351	1.0603	
	9	3258.	51.71	4.84	56.03	5.83	4438	5615	1.0457	
	10	2835.	44.45	4.34	49.65	5.24	3356	4383	1.0355	
	11	2527.	38.10	3.83	42.38	4.66	2579	3204	1.0223	
	12	2022.	30.94	3.12	34.55	3.69	1694	2123	1.0174	
11	2	1991.	33.79	3.07	33.20	3.66	1707	2031	1.0160	
	3	2531.	41.73	3.83	42.49	4.34	2795	3200	1.0270	
	4	2865.	47.17	4.32	48.04	5.20	3613	4265	1.0365	
	5	3256.	54.43	4.95	56.02	5.93	4736	5752	1.0474	
	6	3748.	59.88	5.43	62.72	6.36	5900	7239	1.0600	
	7	3877.	61.24	5.57	65.25	6.62	6409	7025	1.0640	
	8	3672.	59.88	5.40	63.56	6.37	5901	7351	1.0607	
	9	3271.	53.52	4.93	56.96	5.80	4859	5805	1.0484	
	10	2837.	46.04	4.31	48.30	5.14	3400	4412	1.0345	
	11	2407.	39.69	3.82	42.06	4.51	2631	3081	1.0280	
	12	1968.	30.84	3.07	33.31	3.69	1675	1992	1.0062	
12	2	2087.	30.84	3.10	33.96	3.66	1644	2068	1.0171	
	3	2528.	40.14	3.87	42.41	4.53	2682	3194	1.0264	
	4	2809.	45.36	4.36	50.08	5.19	3614	4531	1.0371	
	5	3243.	52.39	4.85	56.14	5.89	4624	5731	1.0467	
	6	3707.	58.06	5.29	62.01	6.30	5764	7085	1.0576	
	7	3874.	61.24	5.58	66.47	6.65	6406	8011	1.0680	
	8	3640.	57.83	5.36	62.18	6.48	5772	7049	1.0580	
	9	3196.	51.71	4.84	55.46	5.95	4406	5593	1.0456	
	10	2804.	45.36	4.25	48.08	5.09	3256	4191	1.0343	
	11	2458.	38.78	3.75	41.60	4.53	2565	3149	1.0257	
	12	1981.	29.94	3.07	33.67	3.68	1599	2057	1.0168	
13	2	2012.	33.79	3.04	37.40	3.62	1707			
	3	2557.	43.09	3.79	47.06	4.56	2722			
	4	2885.	40.44	4.26	53.77	5.07	3615			
	5	3326.	56.93	4.82	61.56	5.79	4758			
	6	3701.	62.60	5.25	68.04	6.37	5911			
	7	4091.	68.27	5.69	74.10	6.77	7060			
	8	3719.	63.50	5.28	68.51	6.43	6042			
	9	3295.	56.93	4.83	61.80	5.89	4819			
	10	2907.	50.12	4.32	54.68	5.17	3748			
	11	2536.	43.09	3.78	47.40	4.50	2756			
	12	2034.	33.11	3.09	37.72	3.71	1818			
14	2	2006.	33.11	3.09	35.72	3.73	1713			
	3	2539.	41.73	3.85	45.06	4.54	2715			
	4	2872.	47.63	4.33	52.07	5.16	3530			
	5	3326.	54.43	4.95	59.49	6.03	4788			
	6	3702.	59.88	5.33	66.42	6.35	5804			
	7	3898.	63.50	5.59	70.43	6.75	6671			
	8	3694.	59.88	5.37	66.51	6.40	5996			
	9	3307.	54.43	4.92	60.85	5.99	4868			
	10	2904.	47.63	4.45	52.37	5.33	3725			
	11	2564.	41.05	3.86	45.14	4.61	2885			
	12	2006.	30.84	3.10	35.84	3.65	1822			
15	2	1990.	31.98	-			1830	2265	1.0173	1.0178
	3	2520.	41.05	-			3006	3766	1.0288	1.0302
	4	2884.	47.17	-			3985	4960	1.0378	1.0417
	5	3274.	54.43	-			5087	6230	1.0469	1.0566
	6	3698.	60.33	-			6521	8020	1.0607	1.0745
	7	4005.	65.32	-			7601	9152	1.0693	1.0862
	8	3705.	61.01	-			6628	8002	1.0605	1.0746
	9	3273.	55.34	-			5432	6377	1.0479	1.0597
	10	2882.	48.31	-			4204	5111	1.0386	1.0447
	11	2521.	41.05	-			3191	3677	1.0279	1.0310
	12	1983.	31.98	-			2060	2292	1.0173	1.0192
16	2	2015.	29.94	-			1880	2183	1.0181	1.0191
	3	2556.	38.78	-			3042	3510	1.0290	1.0324
	4	2938.	46.72	-			4025	4691	1.0385	1.0449
	5	3317.	51.71	-			5033	6035	1.0495	1.0607
	6	3758.	58.06	-			6316	7535	1.0616	1.0794
	7	4050.	51.92	-			7397	8450	1.0686	1.0947
	8	3776.	57.83	-			6431	7402	1.0603	1.0802
	9	3317.	51.71	-			5160	5867	1.0477	1.0620
	10	2891.	46.04	-			3972	4571	1.0375	1.0441
	11	2537.	39.69	-			2992	3444	1.0282	1.0323
	12	2012.	29.94	-			1966	2157	1.0178	1.0199
17	2	2015.	33.79	-			1740	2117	1.0150	1.0149
	3	2521.	43.08	-			2764	3488	1.0250	1.0229
	4	2880.	48.31	-			3634	4620	1.0336	1.0303
	5	3367.	56.25	-			4923	6200	1.0448	1.0448
	6	3705.	62.14	-			6207	8112	1.0591	1.0628
	7	3968.	67.13	-			7203	9293	1.0674	1.0749
	8	3669.	61.24	-			6008	7575	1.0543	1.0610
	9	3343.	56.93	-			5122	6390	1.0463	1.0472
	10	2846.	48.31	-			3804	4708	1.0342	1.0323
	11	2580.	43.77	-			3023	3466	1.0250	1.0234
	12	2010.	33.79	-			1913	2183	1.0154	1.0167

TEST DATA TABULATION (Cont'd)

RUN NO.	PT. NO.	WFC	WCDF	WCDG	WC3F	WCIT	FGC	FGIC	PTFE/PO	PTTE/PO
18	2	2036.	29.94	-			1902	2191	1.0189	1.0216
	3	2569.	38.78	-			3059	3561	1.0307	1.0361
	4	2915.	45.36	-			4122	4779	1.0410	1.0497
	5	3270.	50.80	-			5205	6037	1.0514	1.0669
	6	3737.	57.83	-			6487	7367	1.0623	1.0854
	7	4034.	59.88	-			7503	8210	1.0692	1.1001
	8	3753.	56.47	-			6501	7237	1.0613	1.0848
	9	3334	50.12	-			5252	5890	1.0502	1.0656
	10	2882.	44.46	-			4121	4605	1.0384	1.0484
	11	2545.	38.78	-			3199	3467	1.0296	1.0357
	12	2049.	28.80	-			2078	2164	1.0186	1.0217
19	2	2029.	30.84	2.94			1750	2189	1.0182	1.0194
	3	2548.	38.78	3.65			2874	3514	1.0292	1.0307
	4	2946.	44.45	4.17			3864	4744	1.0397	1.0406
	5	3250.	48.31	4.60			4771	5806	1.0490	1.0518
	6	3734.	56.25	5.12			6214	7620	1.0634	1.0694
	7	4029.	59.88	5.42			7263	8820	1.0738	1.0811
	8	3748.	55.57	5.14			6283	7616	1.0634	1.0690
	9	3301.	48.31	4.59			4859	5779	1.0482	1.0522
	10	2939.	43.77	4.13			3872	4562	1.0383	1.0406
	11	2541.	37.42	3.61			2930	3380	1.0284	1.0304
	12	2031.	29.94	2.95			1931	2180	1.0183	1.0192
20	2	2004.	31.98	2.93			1884	2262	1.0185	1.0185
	3	2580.	40.14	3.71			3066	3620	1.0293	1.0294
	4	2894.	46.04	4.18			4066	4871	1.0386	1.0387
	5	3220.	51.26	4.63			5002	6069	1.0491	1.0486
	6	3747.	57.83	5.14			6426	7780	1.0626	1.0663
	7	3977.	61.01	5.47			7461	9008	1.0729	1.0767
	8	3723.	57.83	5.10			6389	7610	1.0614	1.0665
	9	3273.	51.26	4.61			5089	5918	1.0479	1.0499
	10	2852.	45.36	4.09			4081	4627	1.0375	1.0382
	11	2523.	38.78	3.63			3064	3464	1.0283	1.0288
	12	2007.	30.84	2.96			2015	2195	1.0178	1.0184
21	2	1990.	33.11	2.97			1883	2342	1.0178	1.0170
	3	2499.	42.41	3.70			3025	3594	1.0269	1.0269
	4	2868.	48.08	4.23			4065	5072	1.0381	1.0357
	5	3359.	55.57	4.70			5285	6506	1.0493	1.0474
	6	3660.	59.19	5.06			6257	7726	1.0589	1.0568
	7	4104.	64.86	5.39			7538	9173	1.0698	1.0680
	8	3589.	59.88	5.05			6298	7659	1.0580	1.0580
	9	3292.	55.34	4.74			5352	6635	1.0508	1.0473
	10	2890.	48.08	4.17			4120	4978	1.0382	1.0346
	11	2484.	41.05	3.64			3128	3585	1.0270	1.0264
	12	2011.	31.98	2.96			2040	2338	1.0178	1.0167
22	2	2017.	35.83	2.97			1853	2348	1.0164	1.0140
	3	2535.	44.45	3.67			2921	3719	1.0262	1.0226
	4	2913.	51.26	4.20			3938	5055	1.0359	1.0302
	5	3259.	56.93	4.63			4970	6386	1.0456	1.0393
	6	3688.	63.50	5.12			6275	8108	1.0582	1.0522
	7	4002.	67.59	5.40			7410	9488	1.0689	1.0596
	8	3699.	63.50	5.08			6286	8121	1.0584	1.0512
	9	3263.	56.93	4.61			5030	6337	1.0454	1.0391
	10	2874.	50.12	4.11			3899	4873	1.0349	1.0292
	11	2520.	43.09	3.62			2860	3639	1.0259	1.0220
	12	2003.	33.79	2.91			1829	2277	1.0161	1.0140
23	2	1960.	34.47	2.83	36.2[illegible]	3.15	1587	1973		
	3	2520.	43.09	3.58	46.13	4.08	2606	3351		
	4	2884.	48.08	4.11	53.81	4.55	3444	4370		
	5	3166.	53.52	4.40	59.09	4.90	4176	5338		
	6	3719.	59.88	4.98	67.18	5.56	5677	7100		
	7	3979.	64.1[illegible]	5.3[illegible]	72.56	5.77	6789	8335		
	8	3180.	52.39	4.43	58.47	4.87	4281	5296		
	9	2554.	41.05	3.58	46.76	4.16	2764	3361		
	10	2032.	33.11	2.92	36.77	3.30	1794	2101		
24	2	2064	33.79	3.03	36.64	3.43	1786	2244	1.0176	
	3	2566.	41.73	3.71	45.67	4.19	2835	3495	1.0277	
	4	2957	48.31	4.22	52.71	4.77	3751	4665	1.0371	
	5	3310.	54.43	4.72	59.63	5.27	4885	5996	1.0482	
	6	3798.	60.33	5.17	67.08	5.66	6113	7639	1.0624	
	7	4172.	65.32	5.54	74.19	6.00	7756	9441	1.0782	
	8	3752.	59.88	5.14	66.99	5.64	6191	7639	1.0627	
	9	3321.	54.43	4.71	59.96	5.19	4987	6036	1.0488	
	10	2936.	47.63	4.20	52.45	4.59	3748	4604	1.0371	
	11	2570.	41.73	3.70	45.71	4.25	2908	3516	1.0278	
	12	2054.	33.11	2.99	36.69	3.52	1848	2237	1.0174	
25	2	2000.	33.11	2.94	36.70	3.28	1620	2119	1.0161	
	3	2526.	41.73	3.70	47.06	4.20	2657	3444	1.0260	
	4	2905.	48.31	4.21	54.78	4.69	3602	4693	1.0359	
	5	3292.	54.43	4.69	61.57	5.12	4575	5962	1.0461	
	6	3692.	61.01	5.08	68.73	5.66	5847	7560	1.0589	
	7	4097	65.32	5.50	75.76	5.88	7135	9291	1.0738	
	8	3712	60.33	5.10	69.22	5.62	5850	7653	1.0598	
	9	3304.	54.43	4.69	61.89	5.20	4636	6079	1.0471	
	10	2891.	47.53	4.20	54.63	4.65	3560	4695	1.0361	
	11	2522.	40.14	3.67	46.75	4.05	2629	3410	1.0259	
	12	2020.	29.94	2.97	36.90	3.35	1611	2120	1.0158	

TEST DATA TABULATION (Cont'd)

RUN NO.	PT. NO.	NFC	MCBF	MCBG	MC3F	MC4T	FGC	FGIC	PTFE/PO	PTTE/PO
26	2	2001.	33.11	2.94	36.77	3.25	1608	2104	1.0160	
	3	2494.	42.41	3.67	46.45	4.10	2491	3358	1.0254	
	4	2896.	48.31	4.21	54.23	4.56	[illegible]	4577	1.0352	
	5	3270.	55.34	4.63	61.19	5.04	4400	5859	1.0454	
	6	3658.	60.33	5.08	67.82	5.42	5725	7330	1.0577	
	7	4071.	65.32	5.49	75.07	5.79	7079	9059	1.0718	
	8	3681.	61.01	5.12	68.28	5.55	5906	7463	1.0584	
	9	3286.	55.34	4.66	60.93	5.03	4594	5846	1.0453	
	10	2890.	48.08	4.17	54.48	4.55	3525	4596	1.0352	
	11	2513.	41.05	3.66	46.02	4.06	2597	3409	1.0259	
	12	2014.	31.98	2.97	36.62	3.38	1706	2078	1.0153	
27	2	1981.	31.98	2.91	36.19	3.27	1571	2027	1.0152	
	3	2516.	40.14	3.66	46.58	4.10	2517	3330	1.0250	
	4	2878.	47.17	4.14	[illegible]	4.58	3456	4409	1.0336	
	5	3264.	54.21	4.63	60.64	5.01	4510	5723	1.0438	
	6	3654.	59.88	5.08	67.72	5.52	5693	7244	1.0563	
	7	4102.	64.86	5.51	74.51	5.78	7081	8951	1.0707	
	8	3688.	59.19	5.06	68.16	5.48	5815	7351	1.0574	
	9	3248.	53.52	4.55	60.06	5.08	4568	5654	1.0434	
	10	2875.	47.17	4.11	54.09	4.51	3552	4485	1.0343	
	11	2512.	40.14	3.61	46.10	4.09	2692	3317	1.0250	
	12	2008.	31.98	2.94	36.99	3.30	1741	2065	1.0154	
28	2	2031.	36.29	2.96	37.14	3.41	1620	2174	1.0163	
	3	2565.	44.45	3.68	47.30	4.20	2633	3496	1.0263	
	4	2982.	51.26	4.27	54.98	4.82	3598	4735	1.0358	
	5	3317.	56.47	4.65	61.73	5.20	4574	6003	1.0462	
	6	3741.	62.60	5.15	69.16	5.70	5946	7645	1.0595	
	7	4188.	66.23	5.54	75.76	5.84	7296	9273	1.0736	
	8	3771.	62.14	5.15	68.97	5.70	5881	7677	1.0597	
	9	3337.	56.25	4.68	61.73	5.23	4670	6059	1.0466	
	10	2911.	50.12	4.21	54.46	4.68	3629	4678	1.0356	
	11	2562.	43.77	3.68	46.56	4.15	2648	3431	1.0260	
	12	2058.	34.47	3.00	36.89	3.37	1688	2166	1.0164	
29	3	1979.	31.98	2.95	36.97	3.44	1657	2110	1.0159	
	4	2509.	40.14	3.69	47.09	4.36	2677	3456	1.0261	
	5	2889.	47 17	4.18	54.66	4.80	3564	4659	1.0356	
	6	3310.	54.43	4.75	62.70	5.34	4708	6205	1.0483	
	7	3684.	59.88	5.13	68.43	5.82	5911	7507	1.0587	
	8	4052.	65.32	5 49	75.38	5.98	7097	9219	1.0736	
	9	3702	59.88	5.19	69.23	5.75	5932	7663	1.0603	
	10	3274.	54.21	4.71	62.22	5.28	4832	6140	1.0478	
	11	2885.	47.63	4.21	54.27	4.80	3736	4694	1.0363	
	12	2495.	39.69	3.64	45.89	4.14	2765	3343	1.0256	
	13	2021.	30.84	3.02	37.03	3.40	1855	2184	1.0167	
30	2	1996.	33.11	2 92	36.61	3.36	1730	2100	1.0161	
	3	2527.	42.41	3.69	47.35	4.22	2830	3482	1.0267	
	4	2885.	48.31	4.20	54.75	4.66	3648	4657	1.0361	
	5	3277.	55.34	4.69	61.62	5.22	4758	5981	1.0467	
	6	3661.	61.24	5.13	68.77	5.61	5977	7482	1.0591	
	7	4032.	66.23	5.53	75.16	5.91	7221	9110	1.0732	
	8	3701.	59.88	5.15	68 18	5.55	6071	7444	1.0590	
	9	3242.	54.43	4.69	62.22	5.09	4771	5932	1.0481	
	10	2885.	48.08	4.20	54.28	4.69	3692	4656	1.0364	
	11	2488.	41.05	3.66	46.31	4.06	2715	3370	1.0261	
	12	1998.	31.98	2.96	36.29	3.20	1845	2089	1.0164	
31	2	2083.	36.29	3.04	36.10	3.45	1883	2271	1.0188	
	3	2556.	42.41	3 71	44.44	4.18	2808	3426	1.0283	
	4	3003.	48.31	4.23	52.28	4.85	3818	4753	1.0395	
	5	3776.	55.34	4.72	59.13	5.25	5028	6092	1.0512	
	6	3810.	60.33	5.18	65.93	5.74	6494	7680	1.0653	
	7	4112.	65.32	5.58	72.45	6.11	7777	9293	1.0794	
	8	3695.	59.88	5 14	65.28	5.62	6386	7493	1.0638	
	9	3255.	54.21	4.71	58.53	5.21	5048	6009	1.0506	
	10	2851.	48.08	4.20	51.50	4.69	3900	4634	1.0389	
	11	2547.	41.73	3.68	44.38	4 14	2943	3435	1.0285	
	12	2036.	33.79	3.00	35.27	3.45	1837	2204	1.0181	
32	2	2006.	29.94	2 94	35.25	3.24	1717	2115	1.0175	
	3	2519.	38.78	3 67	44.21	4.14	2752	3352	1.0275	
	4	2926.	46.04	4.21	51.89	4.83	3824	4650	1.0384	
	5	3362.	51 26	4.64	58.75	5.23	4905	5964	1.0499	
	6	3735.	57.83	5.13	66.08	5 61	6289	7593	1.0639	
	7	4176.	62.60	5.52	73.08	5.96	7703	9339	1.0796	
	8	3697.	57 83	5 13	65 98	5.69	6314	7567	1.0638	
	9	[illegible]	51.26	4 69	58.61	5.15	4958	5967	1.0501	
	10	[illegible]	44.45	4 15	50 98	4 78	3761	4535	1.0375	
	11	[illegible]	38.10	3 64	44 31	4 26	2866	3393	1.0277	
	12	2017.	28.80	2 97	34 99	3 36	1852	2115	1.0172	
33	2	2006.	33.11	2 93	35 67	3.30	1520	2006	1.0152	
	3	2493	41.05	3 62	45 34	3 97	2441	3253	1.0252	
	4	2893.	47 63	4.21	53 55	4.72	3439	4624	1.0364	
	5	3315.	55 34	4 69	60 40	5.18	4472	5893	1.0467	
	6	3700	59 88	5 11	67 41	5.50	5616	7427	1.0601	
	7	4083	65.55	5.48	74.68	5.71	6802	9090	1.0740	
	8	3657.	58 06	5.06	66 73	5 54	5346	7284	1.0583	
	9	3286.	54.21	4 68	60 28	5 06	4474	5802	1.0458	
	10	2858.	46 04	4 14	52 75	4 67	3363	4452	1.0345	
	11	2528.	40.14	3 68	46 39	4.14	2606	3455	1.0269	
	12	2016.	30.84	2.98	36 74	3.30	1658	2154	1.0167	

TEST DATA TABULATION (Cont'd)

RUN NO.	PT. NO.	WFC	WCBF	WCBG	WC3F	WC4T	FGC	FGIC	PTFE/PO	PTTE/PO
34	2	2032.	34.47	2.99	36.97	3.48	1604	2163	1.0163	
	3	2509.	43.09	3.65	45.58	4.09	2579	3296	1.0254	
	4	2925.	48.31	4.22	53.32	4.66	3458	4571	1.0353	
	5	3314.	55.57	4.69	60.74	5.13	4544	5924	1.0467	
	6	3694.	60.33	5.11	67.33	5.65	5659	7388	1.0587	
	7	4101.	66.23	5.54	74.10	5.77	7007	8967	1.0728	
	8	3713.	60.33	5.11	67.49	5.55	5699	7421	1.0593	
	9	3282.	55.34	4.67	60.37	5.56	4537	5873	1.0464	
	10	2926.	48.31	4.18	53.76	4.69	3501	4616	1.0360	
	11	2532.	42.41	3.65	46.06	4.17	2647	3396	1.0261	
	12	2032.	33.79	2.97	36.89	3.43	1782	2170	1.0165	
35	2	2014.	31.98	2.98	35.94	3.17	1597	1959	1.0148	
	3	2479.	39.69	3.62	45.79	3.98	2380	3227	1.0246	
	4	2832.	47.17	4.12	53.29	4.55	3176	4403	1.0340	
	5	3181.	53.07	4.55	59.66	5.08	4148	5606	1.0438	
	6	3618.	58.74	5.01	66.97	5.46	5293	7114	1.0563	
	7	4049.	64.86	5.43	74.39	5.74	6756	8898	1.0718	
	8	3652.	59.19	5.05	67.26	5.56	5302	7200	1.0567	
	9	3237.	52.39	4.60	59.78	5.00	4171	5654	1.0444	
	10	2862.	46.72	4.14	53.23	4.58	3182	4461	1.0346	
	11	2468.	39.69	3.62	45.32	3.89	2309	3207	1.0248	
	12	2018.	30.84	2.97	36.08	3.36	1511	2047	1.0155	
36	2	1969.	30.84	2.93	36.33	3.26	1521	1956	1.0159	
	3	2489.	39.69	3.60	45.30	4.08	2407	3240	1.0251	
	4	2877.	46.72	4.13	53.36	4.57	3312	4493	1.0354	
	5	3250.	53.52	4.58	59.24	4.95	4220	5593	1.0445	
	6	3603	58.06	5.05	66.54	5.51	5352	7111	1.0567	
	7	4077.	64.86	5.47	73.71	5.87	6715	8840	1.0714	
	8	3663.	58.74	5.11	67.49	5.59	5524	7304	1.0579	
	9	3230.	53.52	4.64	60.31	5.04	4334	5758	1.0454	
	10	2839.	46.04	4.13	52.65	4.58	3334	4420	1.0347	
	11	2490.	39.69	3.64	45.73	4.05	2569	3313	1.0256	
	12	2025.	30.84	3.02	36.83	3.43	1642	2138	1.0162	
37	2	2070	33.79	3.02	35.98	3.30	1652	2016	1.0151	
	3	2563	41.73	3.69	46.60	4.26	2582	3434	1.0260	
	4	2930.	48.08	4.20	54.03	4.70	3465	4627	1.0357	
	5	3312.	54.21	4.65	60.51	5.14	4456	5861	1.0460	
	6	3722.	60.33	5.12	67.32	5.58	5705	7372	1.0585	
	7	4156.	66.23	5.56	74.82	5.95	7031	9192	1.0738	
	8	3708.	59.88	5.11	67.16	5.57	5701	7322	1.0581	
	9	3321.	54.43	4.67	60.41	5.26	4578	5919	1.0464	
	10	2891.	47.63	4.16	52.78	4.57	3483	4436	1.0344	
	11	2558.	41.05	3.66	45.93	4.11	2676	3389	1.0261	
	12	2044.	33.11	2.98	36.86	3.30	1702	2175	1.0168	
38	2	2041.	29.94	3.01	34.89	3.99	1537	2223		
	3	2564.	38.10	3.72	44.17	4.61	2633	3478		
	4	2891.	44.45	4.21	51.09	5.25	3441	4675		
	5	3344.	52.39	4.75	55.06	5.60	4591	5997		
	6	3772.	57.38	5.17	61.10	5.91	5654	7369		
	7	4166.	62.14	5.55	70.58	6.48	6822	8970		
	8	3774.	57.38	5.13	63.42	5.76	5683	7141		
	9	3327.	51.26	4.64	54.33	5.55	4556	5834		
	10	2944.	45.36	4.17	48.60	4.99	3474	4575		
	11	2557.	38.78	3.63	41.47	4.48	2634	3442		
	12	2033.	29.94	2.92	31.94	3.61	1692	2092		
39	2	1984.	28.80	2.95	32.62	3.67	1494	2076		
	3	2496.	38.10	3.67	41.79	4.49	2478	3407		
	4	2871.	44.45	4.20	48.30	4.89	3443	4526		
	5	3296.	51.26	4.71	55.42	5.59	4466	6017		
	6	3691.	56.93	5.19	61.26	5.88	5660	7376		
	7	4030.	61.01	5.56	65.70	6.37	6694	8697		
	8	3648.	56.47	5.16	60.62	5.87	5512	7232		
	9	3268.	51.26	4.72	55.12	5.58	4559	5941		
	10	2885.	44.45	4.21	48.28	4.83	3537	4553		
	11	2512.	38.10	3.67	42.03	4.48	2494	3443		
	12	1987.	28.80	2.93	33.18	3.67	1531	2113		
40	2	2030.	30.84	3.08	35.17	3.69	1462	2278		
	3	2515.	38.10	3.66	41.69	4.82	2386	3418		
	4	2897.	44.45	4.22	49.31	5.26	3370	4721		
	5	3267	50.80	4.69	56.06	5.61	4251	6055		
	6	3669	56.47	5.18	61.58	5.98	5367	7332		
	7	4007.	61.24	5.54	68.24	6.39	6438	8792		
	8	3667	56.25	5.14	61.69	5.96	5448	7120		
	9	3240.	50.12	4.65	56.30	5.40	4348	5815		
	10	2903.	44.45	4.20	48.99	4.95	3500	4488		
	11	2505.	38.10	3.64	42.64	4.50	2620	3404		
	12	2014.	29.94	2.98	34.63	3.67	1706	2208		
41	2	1985.	30.84	2.93	33.22	3.73	1352	2048		
	3	2557.	40.14	3.70	43.81	4.69	2360	3482		
	4	2934.	46.04	4.23	50.22	5.20	3519	4588		
	5	3346.	52.39	4.76	56.58	5.33	4486	5745		
	6	3724.	57.38	5.25	63.74	5.90	5347	7290		
	7	4036	61.24	5.55	67.43	6.08	6215	8230		
	8	3729.	57.38	5.18	63.87	5.84	5447	7284		
	9	3296	51.26	4.72	56.42	5.46	4394	5757		
	10	2922	46.72	4.24	50.30	4.99	3468	4569		
	11	2528.	38.78	3.67	42.61	4.61	2450	3375		
	12	2004.	30.84	2.94	33.93	3.53	1616	2104		

TEST DATA TABULATION (Cont'd)

RUN NO.	PT. NO.	NFC	WCBF	WCBG	WC3F	WC4T	FGC	FGIC	PTFE/PO	PTTE/PO
42	2	2023.	28.80	2.98	34.09	3.80	1610	2168		
	3	2539.	38.78	3.77	43.88	4.52	2628	3505		
	4	2902.	45.36	4.23	50.34	5.03	3583	4603		
	5	3285.	50.80	4.71	56.99	5.52	4620	5826		
	6	3720.	56.47	5.17	63.84	5.91	5864	7300		
	7	4012.	60.33	5.48	69.30	6.23	6742	8617		
	8	3677.	56.25	5.12	63.29	5.90	5730	7189		
	9	3278.	50.12	4.67	56.62	5.59	4698	5806		
	10	2918.	44.45	4.22	50.54	5.08	3714	4567		
	11	2527.	38.10	3.69	43.05	4.59	2730	3394		
	12	1988.	28.80	2.94	33.59	3.75	1715	2098		
43	2	2014.	28.80	2.92	34.08	3.69	1705	2129		
	3	2522.	37.42	3.67	43.20	4.66	2620	3408		
	4	2871.	43.77	4.18	50.54	4.90	3606	4525		
	5	3273.	50.12	4.68	57.49	5.42	4670	5828		
	6	3691.	56.47	5.14	63.78	5.86	5690	7236		
	7	3909.	59.88	5.42	67.89	6.03	6458	8226		
	8	3651.	55.34	5.08	62.55	5.80	5468	6967		
	9	3246.	50.12	4.62	56.29	5.52	4420	5693		
	10	2834.	43.77	4.12	49.50	5.20	3506	4394		
	11	2516.	38.10	3.65	43.90	4.55	2659	3419		
	12	2022.	28.80	2.93	34.71	3.71	1687	2171		
44	2	1916.	28.80	2.93	33.18	3.52	1676	2033		
	3	2535.	37.42	3.71	43.63	4.49	2650	3361		
	4	2883.	44.45	4.21	50.24	5.22	3483	4504		
	5	3277.	50.12	4.69	58.78	5.50	4554	6033		
	6	3641.	56.47	5.14	63.86	5.95	5548	7239		
	7	3954.	59.19	5.38	67.60	6.13	6485	8220		
	8	3542.	55.34	5.03	61.55	5.91	5353	6792		
	9	3266.	50.12	4.67	57.09	5.49	4553	5798		
	10	2884.	43.77	4.18	51.25	4.96	3619	4663		
	11	2481.	36.29	3.59	42.13	4.23	2617	3147		
	12	2050.	29.94	2.99	35.23	3.82	1745	2243		

APPENDIX C
THRUST, FAN MASSFLOW AND TURBINE MASSFLOW COEFFICIENT DATA

DATA FOR:

FIGURE 3-12

$N_F/\sqrt{\theta}$ (RPM)	H/D	CF	CAF	CAT
2000	∞	.805	.851	.857
	6.45	.789	.912	.875
	2.55	.744	.855	.848
	1.55	.776	.878	.875
	1.02	.827	.853	.875
2400	∞	.803	.862	.857
	6.45	.772	.896	.897
	2.55	.762	.867	.872
	1.55	.745	.891	.872
	1.02	.826	.863	.875
2800	∞	.782	.871	.872
	6.45	.765	.892	.889
	2.55	.748	.875	.867
	1.55	.744	.895	.889
	1.02	.826	.866	.870
3200	∞	.771	.873	.868
	6.45	.769	.887	.882
	2.55	.751	.883	.900
	1.55	.747	.896	.918
	1.02	.826	.872	.882
3600	∞	.778	.872	.895
	6.45	.773	.886	.927
	2.55	.755	.882	.926
	1.55	.748	.895	.926
	1.02	.820	.870	.873
4000	∞	.782	.864	.915
	6.45	.774	.885	.931
	2.55	.757	.882	.931
	1.55	.753	.889	.947
	1.02	.817	.862	.914

AVERAGES

H/D	CF	CAF	CAT
∞	.787	.866	.877
6.45	.774	.893	.900
2.55	.753	.874	.891
1.55	.752	.891	.905
1.02	.824	.864	.882

FIGURE 3-19

$N_F/\sqrt{\theta}$ (RPM)	H/D	CF	CAF	CAT
2000	∞	.782	.961	.853
	6.45	.783	.851	.909
	2.55	.770	.898	.848
	1.55	.773	.818	.848
	1.02	.807	.904	.824
2400	∞	.762	.939	.854
	6.45	.775	.871	.923
	2.55	.746	.898	.846
	1.55	.763	.855	.875
	1.02	.799	.909	.854
2800	∞	.758	.907	.870
	6.45	.772	.831	.911
	2.55	.747	.898	.889
	1.55	.765	.879	.891
	1.02	.804	.912	.870
3200	∞	.762	.918	.882
	6.45	.776	.884	.920
	2.55	.762	.894	.920
	1.55	.770	.888	.902
	1.02	.806	.906	.882
3600	∞	.770	.913	.909
	6.45	.782	.877	.944
	2.55	.773	.892	.944
	1.55	.771	.885	.909
	1.02	.811	.899	.891
4000	∞	.778	.919	.914
	6.45	.786	.864	.931
	2.55	.776	.886	.931
	1.55	.775	.874	.931
	1.02	.813	.892	.914

AVERAGES

H/D	CF	CAF	CAT
∞	.769	.926	.880
6.45	.779	.871	.923
2.55	.762	.894	.896
1.55	.770	.867	.893
1.02	.807	.904	.873

APPENDIX C
THRUST, FAN MASSFLOW AND TURBINE MASSFLOW COEFFICIENT DATA (Cont'd)

DATA FOR:

FIGURE 3-26

$N_F/\sqrt{\theta}$ (RPM)	H/D	CF	CAF	CAT
2000	∞	.851	.889	.879
	2.55	.777	.869	.906
	1.55	.757	.937	.848
	1.02	.841	.948	.848
2400	∞	.804	.890	.875
	2.55	.729	.876	.897
	1.55	.752	.928	.875
	1.02	.839	.945	.850
2800	∞	.793	.884	.870
	2.55	.722	.877	.932
	1.55	.756	.919	.889
	1.02	.837	.935	.870
3200	∞	.795	.883	.902
	2.55	.732	.878	.900
	1.55	.761	.909	.900
	1.02	.837	.922	.822
3600	∞	.808	.882	.927
	2.55	.751	.877	.926
	1.55	.769	.903	.926
	1.02	.839	.918	.891
4000	∞	.809	.881	.915
	2.55	.755	.870	.914
	1.55	.777	.897	.931
	1.02	.826	.907	.915

AVERAGES

H/D	CF	CAF	CAT
∞	.810	.885	.895
2.55	.744	.875	.913
1.55	.762	.916	.895
1.02	.837	.929	.876

FIGURE 3-38

$N_F/\sqrt{\theta}$ (RPM)	H/D	CF	CAF	CAT
2000	∞	.880	.964	.838
	6.45	.759	.898	.816
	2.55	.751	.887	.833
	1.55	.779	.906	.833
	1.02	.817	.929	.827
2400	∞	.857	.957	.815
	6.45	.771	.918	.815
	2.55	.777	.908	.818
	1.55	.777	.922	.852
	1.02	.813	.951	.852
2800	∞	.833	.953	.811
	6.45	.780	.929	.819
	2.55	.775	.917	.817
	1.55	.778	.930	.863
	1.02	.806	.960	.833
3200	∞	.825	.946	.814
	6.45	.801	.931	.828
	2.55	.774	.921	.826
	1.55	.791	.935	.842
	1.02	.808	.951	.835
3600	∞	.829	.942	.820
	6.45	.820	.931	.833
	2.55	.772	.921	.833
	1.55	.797	.932	.841
	1.02	.811	.950	.841
4000	∞	.832	.940	.844
	6.45	.837	.930	.844
	2.55	.772	.919	.844
	1.55	.802	.931	.844
	1.02	.813	.944	.853

AVERAGES

H/D	CF	CAF	CAT
∞	.843	.950	.824
6.45	.795	.923	.826
2.55	.770	.912	.829
1.55	.787	.926	.846
1.02	.811	.951	.840

APPENDIX C

THRUST, FAN MASSFLOW AND TURBINE MASSFLOW COEFFICIENT DATA (Cont'd)

DATA FOR:

FIGURE 3-42

$N_F/\sqrt{\theta}$ (RPM)	δ_{LC}	CF	CAF	CAT
2000	0°	.837	.897	.833
	56	.850	.901	.811
	95	.880	.964	.838
2400	0	.853	.913	.837
	56	.839	.903	.841
	95	.857	.957	.815
2800	0	.858	.921	.804
	56	.826	.907	.827
	95	.833	.953	.811
3200	0	.853	.926	.825
	56	.821	.910	.828
	95	.825	.946	.814
3600	0	.852	.931	.825
	56	.819	.909	.841
	95	.829	.942	.820
4000	0	.857	.932	.836
	56	.814	.910	.838
	95	.832	.940	.844
		AVERAGES		
	0	.852	.920	.827
	56	.828	.907	.831
	90	.843	.950	.824

FIGURE 3-47

$N_F/\sqrt{\theta}$	H/D	CF	CAF	CAT
2000	∞	.780	.869	.763
	6.45	.793	.829	.829
	2.55	.794	.842	.784
	2.0	.756	.852	.784
	1.55	.695	.879	.778
	1.02	.718	.836	.757
2400	∞	.740	.875	.814
	6.45	.755	.850	.837
	2.55	.768	.861	.795
	2.0	.775	.876	.818
	1.55	.728	.890	.795
	1.02	.736	.865	.837
2800	∞	.741	.880	.833
	6.45	.751	.867	.820
	2.55	.770	.875	.820
	2.0	.787	.888	.837
	1.55	.750	.890	.837
	1.02	.754	.879	.854
3200	∞	.757	.879	.849
	6.45	.761	.873	.836
	2.55	.783	.882	.852
	2.0	.793	.889	.852
	1.55	.758	.896	.836
	1.02	.763	.887	.852
3600	∞	.774	.880	.877
	6.45	.775	.883	.864
	2.55	.790	.886	.895
	2.0	.798	.889	.879
	1.55	.759	.894	.864
	1.02	.772	.890	.864
4000	∞	.790	.880	.871
	6.45	.792	.887	.857
	2.55	.800	.888	.902
	2.0	.800	.876	.887
	1.55	.757	.891	.887
	1.02	.777	.884	.859
		AVERAGES		
	∞	.764	.877	.835
	6.45	.771	.865	.841
	2.55	.784	.872	.841
	2.0	.785	.878	.843
	1.55	.741	.890	.833
	1.02	.753	.874	.837

APPENDIX C

THRUST, FAN MASSFLOW AND TURBINE MASSFLOW COEFFICIENT DATA (Cont'd)

DATA FOR:

FIGURE 3-60

$N_F/\sqrt{\theta}$ (RPM)	H/D	CF	CAF	CAT
3000	∞	.679	.889	1.138
	6.45	.696	.835	1.147
	2.55	.654	.844	1.125
	1.55	.636	.829	1.136
3800	∞	.705	.823	1.041
	6.45	.667	.809	1.034
	2.55	.646	.814	1.026
	1.55	.636	.802	1.033
4400	∞	.692	.796	1.006
	6.45	.667	.795	1.000
	2.55	.647	.795	.988
	1.55	.630	.792	.994
5000	∞	.676	.783	.989
	6.45	.665	.780	.983
	2.55	.644	.786	.967
	1.55	.644	.786	.984
5400	∞	.671	.782	.974
	6.45	.665	.771	.979
	2.55	.655	.783	.964
	1.55	.657	.784	.969

AVERAGES

	H/D	CF	CAF	CAT
	∞	.685	.815	1.030
	6.45	.672	.798	1.029
	2.55	.650	.804	1.014
	1.55	.641	.799	1.023